uc3m | Universidad Carlos III de Madrid

Bachelor's Degree in Aerospace Engineering
2016/2017

Bachelor Thesis

Development of a computational tool for turbomachinery Blade Generator

Ionuț Alexandru, Coșuleanu

Tutor
Antonio Antorranz Perales
Escuela Politénica Superior (Leganés)

This page is intentionally left blank.

I would like to thank, firstly, to Jesús Peña Mateos, my family and my tutor Antonio for their support. Also, I'd like to thank to my close friends and colleagues: Bárbara, Andrea, Cvetanka, Alexander, Xu Ke, José Carlos, Alberto, José Medinilla, Silvia, Marina, Kike, Eva, Hasier, Óscar, Nuria, Alba, Eva, Virginia, Esther, Beatriz and Borka; to my beloved XII Board of Local BEST Group Madrid Carlos III: Irene, Laura dB, Laura B, Elena and Santi; and also to BEST Madrid Carlos III. Thank you very much for being there!

Contents

List of Figures

List of tables

List of Symbols and abbreviations

α	Absolute flow angle
β	Relative flow angle
χ	Metal Angle
δ	Deviation Angle
δ^*	Displacement thickness
θ	Camber Angle
θ	Momentum thickness
ξ	Stagger Angle
c	Absolute flow velocity
C_f	Skin friction coeffient
C_p	Pressure Coefficient
H	Boundary layer's shape factor
i	Incidence Angle
l	Chord length
M	Mach Number
m'	Local streamsurface radius
o	Throat
p	Pressure
s	Pitch
w	Relative flow velocity
CFD	Computational Fluid Dynamics
CIRCLE	presCribed suRface Curvature distribution bLade dEsign
LE	Leading Edge

MISES Multiple Blade Interacting Streamtube Euler Solver

NACA National Advisory Committee for Aeronautics

Re Reynolds Number

TE Trailing Edge

Abstract

TURBOMACHINERY BLADE DESIGNER is a tool whose main functionality is to design a turbomachine blade. It provides the ability to interactively construct a 2D smooth blade. There are two modalities of designing depending on the control that user wants to have on final geometry: cascade families - thickness profiles are superimposed over the camber line - and manual design - there is a large set of parameters that has to be filled to obtain the profile. In addition, TURBOMACHINERY BLADE DESIGN performs the flow computation of this blade with MISES. MISES, a quasi 3D CFD (Computational Fluid Dynamics), is a set of different programs that analyse the viscous and boundary layer evolution in a cascade. Along with sample designs which are analysed and several examples, the effect of two geometric parameters are presented in this project.

Keywords: turbomachinery, turbine, compressor, cascade, MISES, blade and Bézier.

Chapter 1

Introduction

1.1 Background

Along this chapter, a brief introduction of turbomachinery is presented. Additionally, related more specifically with this project, the motivation and objectives of this work are specified, together with an explanation of this project's organization.

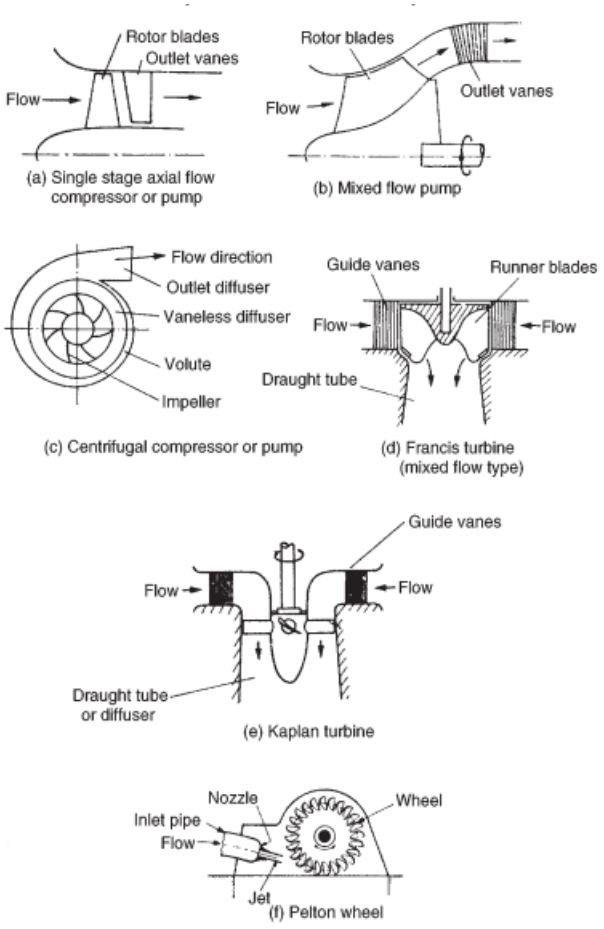

Figure 1.1: Examples of types of turbomachine: a) and e) are axial devices; c) radial; and b) and d) are mixed flow turbomachines; f) is an impulse turbine

Generally, a turbomachine refers to those devices in which there is a flowing fluid and its energy is transferred to a rotating blade row. These devices are also referred as rotordynamic devices. This transfer changes the stagnation enthalpy of the fluid by extracting work from the device or from the fluid. According to this definition, two main types of devices can be encountered:

- Those which *absorb* power to increase the fluid pressure - this is the case of fans, compressors and pumps
- Those which *produce* power by decreasing the fluid pressure - gas turbines, for example.

Apart from that, there is another categorization of turbomachines depending on the flow direction; thus, when the flow is parallel to the axis of rotation, the device is called *axial flow turbomachine*; the flow can be also perpendicular to the axis of rotation and in this case is referred to us as a *radial flow turbomachine*; and the last type is *mixed flow turbomachine*.

Along this project, only axial turbomachines are of importance. And the main of objective of it is creating a software with which the designer is able to design a blade (for a compressor or turbine) and then analysing it with a quasi-3D CFD MISES in order to obtain the performance of the blade.

The program developed in this project can be easily get from GitHub ('ionutalexandru/TurbomachineryBladeDesigner').

1.2 Motivation

Turbines and compressors are turbomachine devices that are used in the aerospace field: aircraft engine. Mainly, the performance of an aircraft depends on the engine (apart on the aerodynamics of the wings and fuselage). So, it may be thought it is fundamental to have a tool which helps students, researchers and engineers to find the blade shapes that offer the performance desired. But not only this, it is also interesting to analyse and understand the effect of the different design parameters. All these applications can result in having more efficient turbomachines and, hence, more efficient engines.

This tool in fact optimizes the time that a student, for example, would have to employ during the design process. The reason behind is that the user uses a user-friendly layout to create the shape and then he or she introduces several inputs to MISES and the results are shown. Moreover, the user has not to learn or use MISES (written in an obsolete language - Fortran) software , which is not provided with an interface. Therefore, all these tasks constitute a big challenge in terms of programming that it is involved in the project.

Last but not least, this project offers a good opportunity to improve and to delve into Turbomachinery field, more specifically, in the Direct Method and the

analysis of the performance of a blade.

1.3 Objectives

The objective of this end of bachelor project is creating a tool that can be used for the design of a blade shape with an user-friendly layout or interface. And, further, to link this tool with MISES, which is a widely used blade-to-blade flow computation in a 2D basis. In order words, to optimize the design process. Another objective is to analyse several cases and find the impact of certain design parameters on blade performance.

1.4 Outline

This report is structured in several chapters. In Chapter 1, an introduction was presented. In the next one (Chapter 2), basic principles and fundamentals of turbomachinery and Bézier curves is explained. Chapter 3 describes the state of the art including an introduction to cascade families, CIRCLE designing method and MISES. In Chapter 4 the design method is covered and in the following one, Chapter 5, how the program works is explained. In this same section, several cases are analysed. Finally, in Chapter 6 conclusions and further work are drawn.

1.5 Socio-economic environment

1.5.1 Budget

In the following figure, it is shown the budget of this project. Basically, three main concepts are considered: licenses, equipment and labour costs. It has to be said that real MISES license price is 10,000 $. The currency employed to obtain the price in € is 0.8367 USD per €. The second comment is about labour costs. They include all the taxes that are need to be paid to the Government and it has been assumed 312 working hours, in accordance with the project planner (Annex A).

Project Budget

Licenses

PRODUCT	DESCRIPTION	COST	
Matlab	Home Edition (MATLAB + Add-On)	154.00 €	
Windows 10	Home Edition	135.00 €	
Ubuntu		- €	
MISES	Commercial License	8,367.49 €	*
	TOTAL	8,656.49 €	

Equipment & other facilities

PRODUCT	DESCRIPTION	COST
Laptop	HP ENVY 15-j100ns	1,098.99 €
Internet Connection	7 months connection	140.00 €
	TOTAL	1,238.99 €

Labour costs

PRODUCT	DESCRIPTION	COST	
Programmer	15€ per programming hour	4,680.00 €	*
	TOTAL	4,680.00 €	

TOTAL PROJECT COST 14,575.48 €

Figure 1.2: Project budget

1.5.2 Socio-economic impact

From the beginning of this document it has been said many times that the performance of a turbomachine is strongly linked with the one of an aircraft. Facilitating the analysis process of a turbomachine is then a must for an engineer. Having higher performance engines affects both, society and economic agents.

Society is affected in the way that people can travel safely and faster. As a consequence, aviation perception in the society will improve. It has not to be forgotten the carbon footprint impact. Less fuel implies a reduction in emissions to the atmosphere. This is a positive impact on the planet and people's health. Nowadays, the emission of pollutants is limited when certifying a vehicle but there are European policies that encourage the research of ways that reduce even more these emissions (Section 1.6).

Regarding the economic impact, the clear consequence of consuming less fuel is then the reduction of total costs and therefore the benefits of an airline increases. Ticket prices may be lower for passengers due to the same idea.

To sum up, the satisfaction and people's perception (about air transport) would be positively affected.

1.6 Regulatory framework

The regulatory framework of this project can be related with the pollutants. Currently, it is applicable Annex 16, Volume II, Part III, Chapter 2 of ICAO (Ref [14]). In this chapter, it is stipulated the maximum allowed Hydrocarbon (HC), Carbon Monoxide (CO) and Oxides of Nitrogen (NOx) in order to have an aircraft certified. It is specified a special unit of measuring pollutant emissions: Dp/Foo (Ref [14] and [13]):

> Dp/Foo: The mass, in grams (Dp), of any pollutant emitted during the reference landing and take-off (LTO) cycle, divided by the rated output (Foo) of the engine.

In these references, it is said that the allowed Dp/Foo for HC is 19.6, for CO 118 and the allowed level of NOx depends on other parameters such as engines number.

Moreover, through the EU framework 'Horizon 2020' (Ref [12]), the entity in charge of research and innovation program, professionals are working to make the European growth more sustainable and smart. It affects all the fields of engineering and science, being therefore Aerospace one of them.

Regarding the Aviation, it is requires a lot of effort in reducing noise and emission, in order words, having a more efficient engine. The improvements that are researched will enter into service in 2025. According to this document (Ref [12]), CO_2 should be reduced 75%, NO_x and particles by 90%. Perceived noise has to be reduced by 65% in 2050. In the same reference, it is mentioned that duration door-to-door within Europe must not exceeds 4 hours. And, in addition, for rides from Europe to Canada it is expected to use electric propulsion in few decades.

Chapter 2

Basic principles and concepts

This chapter is aimed to introduce to the reader few Turbomachinery concepts related with the flow through this kind of devices and cascades. In addition, Bézier theory is also introduced since it is used to construct parametric curves.

2.1 Turbomachinery fundamentals

As already said, in a turbine stage the energy is extracted from the fluid and then it is converted into mechanical energy. In the next figure, Figure 2.1, it can be observed a turbine stage. It is composed by a fixed guided vanes row, nozzles or *stator* and a moving blades row, buckets or *rotor*. This latter component extracts work from the flow.

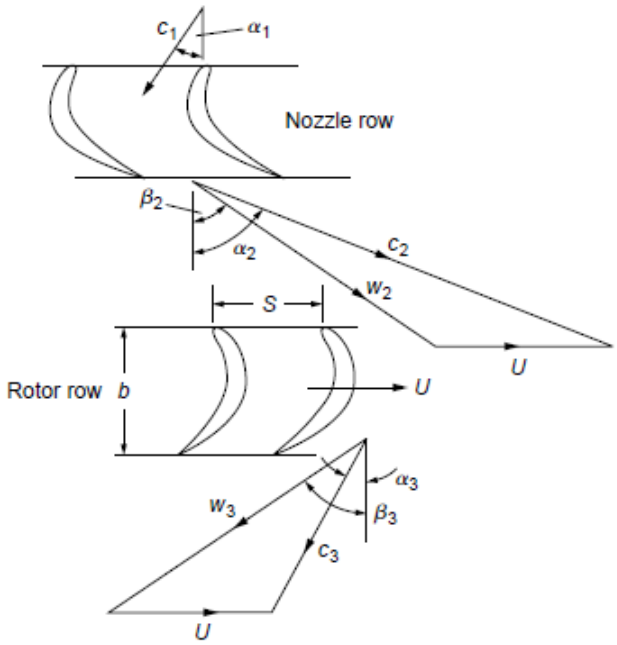

Figure 2.1: Turbine stage

The flow velocity is composed by two component: an axial and tangential

component. The first one is in charge of mass transport while the remaining guarantees the transfer of energy. As it can be depicted from Figure 2.1, the absolute velocities (c) are aligned with the absolute flow angle (α) and relative velocities (w) are aligned with the relative flow angle (β). There is one more velocity component U ($U = \Omega r$, where Ω is the angular velocity of the machine and r is the radial position) that is due to the rotation of the shaft.

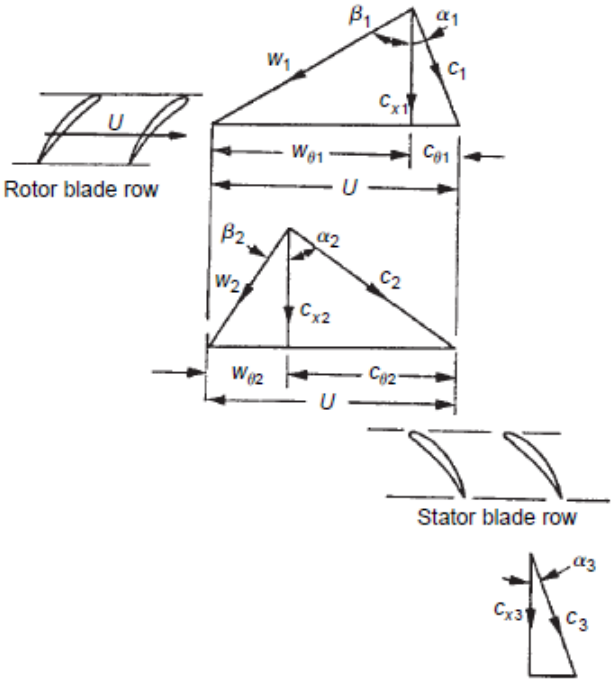

Figure 2.2: Compressor stage

The mechanism of a compressor stage is different than the turbine one. In this case, the fluid becomes more energetic (pressure is raised). It is composed firstly by a rotor blades row and secondly by a stator blades row.

In order to do a preliminary design of a stage, it is useful to take loss mechanisms in turbomachines (Ref [11]) such as viscous friction and flow separation. Empiric correlations from Chapters 3 and 4 of Lewis' book (Ref [1]) can be used to predict loss coefficients.

2.2 Cascade

Axial turbomachines designers have treated the three-dimensional flow of these machines as a superposition of two-dimensional flows. This is better since it is easier to choose a blade design. Let us take the example of a turbomachine whose casing and hub are cylinders. Then, it can be assumed that the stream surfaces remain cylindrical in the turbomachine. To make the design process easier, one can project the blade shapes (for certain radial position r) along the a cylindrical

blade-to-blade section ($x - r\theta$ component[1]). And finally, this can be transformed into a rectangular *cascade* plane. This unwrapping can be seen in the next figure:

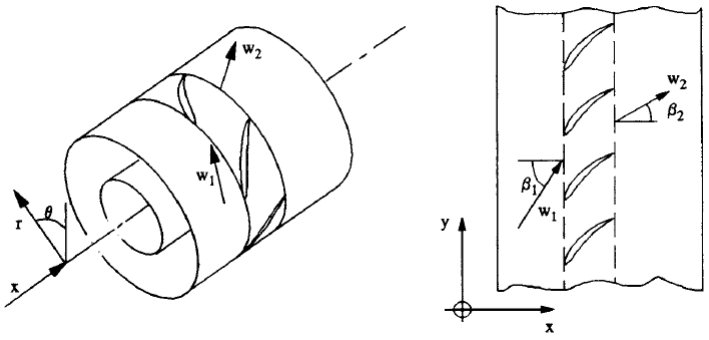

Figure 2.3: Development process of a cylindrical blade-to-blade section into a rectangular cascade plane

The main advantage of this method is that equations are applied for each cascade section independently. In this way, one can find the velocity triangle for that particular blade section. A designer is interested on having certain flow deflection at Trailing Edge (TE) and a smooth inlet flow around the Leading Edge (LE) and these conditions must be fulfilled by the blade profile.

2.3 Mean-line design

Mean-line design is a method that consists on assuming that all flow conditions at the mean radius (named pitchline) is the same for all radial positions. This is true only if the ratio between hub and tip radii is small (about 40%). After applying conservation laws (mass, energy, momentum and entropy), loss and deviation correlations, a preliminary design of the turbomachinery is obtained. Another important application is that the velocity triangle, previously introduced, is sketched in terms of three duty parameters: Reaction degree (R)[2], flow coefficient (ϕ)[3] and stage loading (ϕ)[4]. The outcomes from this theory are the velocity triangles, geometry quantities and also an estimation of the efficiency.

[1]The reference frame of a turbomachine is composed by an axial or x, radial or r and tangential or $r\theta$ coordinates

[2]The ratio between the static enthalpy drop in the rotor over the static enthalpy drop in the stage

[3]This variable is related with the mass flow and the stagger

[4]It is related with the increment of tangential velocity and, therefore, with the turning of the blade

2.4 Blade-to-blade design

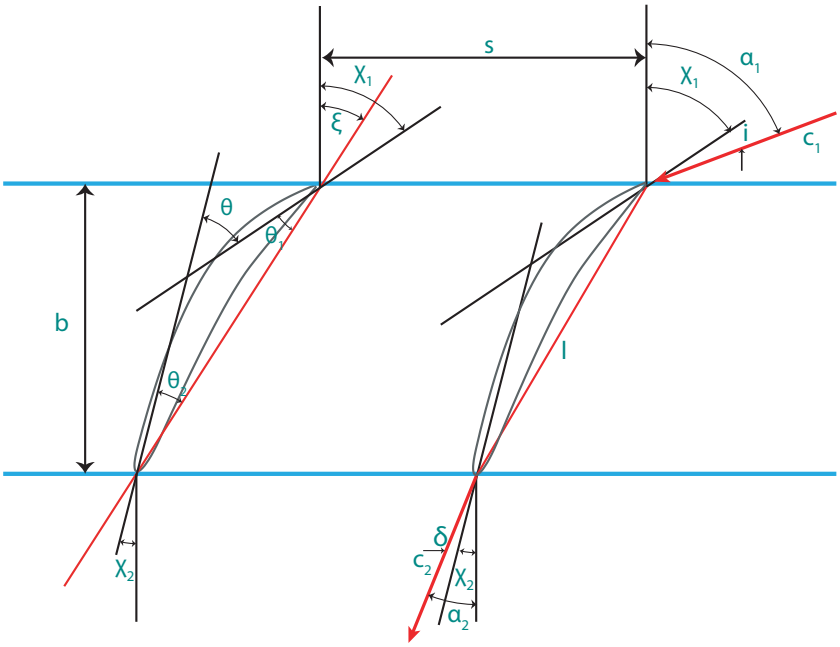

Figure 2.4: Compressor blade

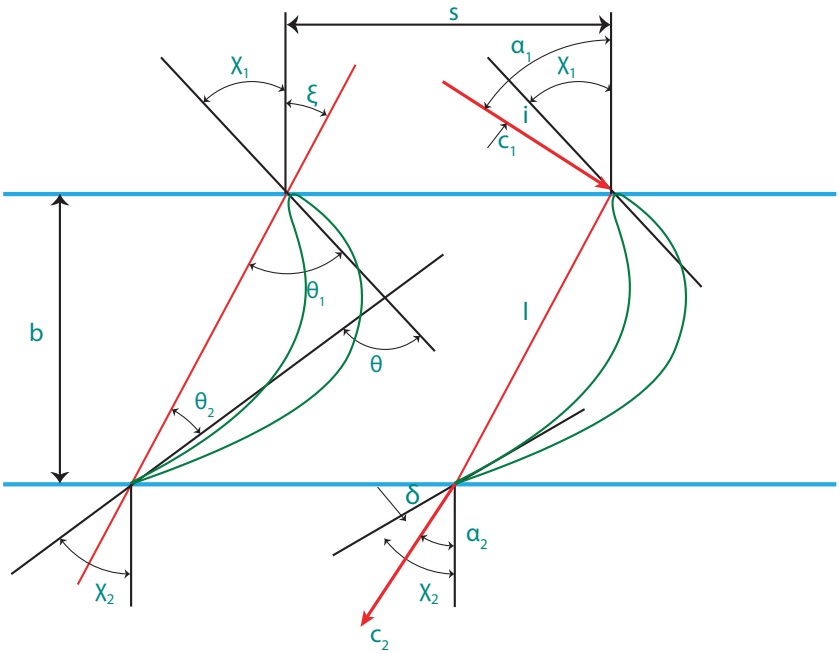

Figure 2.5: Turbine blade

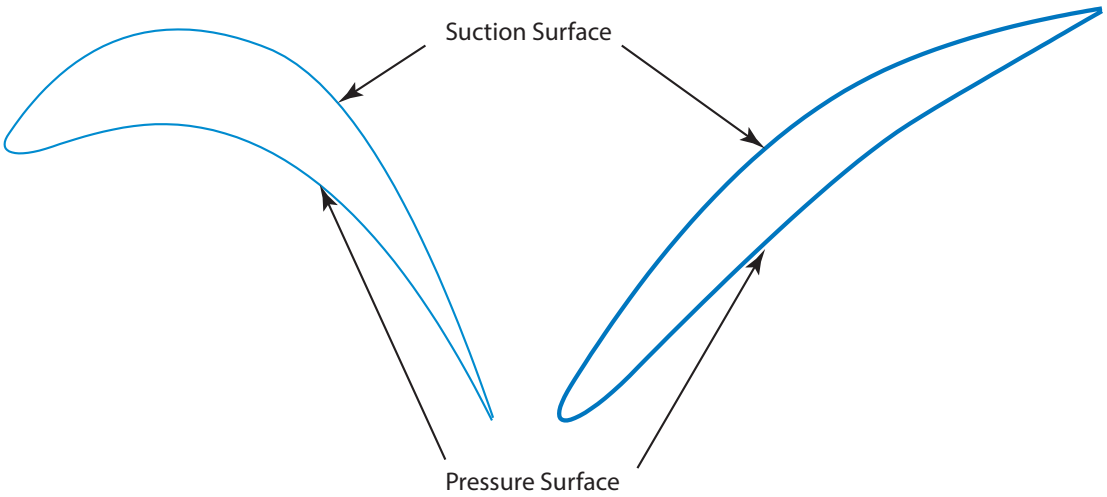

Figure 2.6: Suction and Pressure Surfaces of compressor and turbine blades

To begin with, a blade shape of a cascade is defined by two surfaces: pressure and suction surfaces (Figure 2.6). They are, respectively, lower and upper curves. They receive these names because, generally, the first one has a considerably higher pressure (and hence less velocity) than the second one. In Figures 2.4 and 2.5, there are sketched compressor and turbine stages where sub-index 1 refers to inlet conditions and 2, to outlet conditions. Regarding the geometric parameters, let us define ξ as the *stagger* angle which is the orientation of the camber line with respect to the axial axis; χ is the metal or the blade angle and it is the angle between the axial axis and the camber line at the inlet (χ_1) and at the outlet (χ_2); θ_1 and θ_2 are the camber angle at the inlet and outlet sections, respectively, and, as observed above, it is the inclination between metal and stagger. There are two angles that relate metal and flow angles: incidence i and deviation δ. It is of interesting to investigate how these variables interfere in the performance of a blade.

Finally, the last parameters are the chord l, the pitch s (which is the spacing between two consecutive blade within a cascade, it is measured in meters and it is calculated as $s = \frac{2\pi r}{N}$, where N is the number of blades) and the axial chord (the projection of the chord onto the axial axis - $b = l\cos\xi$). There is one more parameter called throat or o ; it is the distance from the adjacent TE to the point of the suction surface where sonic where the area of the channel is minimum.

From the same figures, there can be found relations between flow and metal angles. In the case of a turbine cascade, $\alpha_1 = \chi_1 + i$ and $\alpha_2 = \chi_2 - \delta$; and for a compressor, $\alpha_1 = \chi_1 + i$ and $\alpha_2 = \chi_2 - \delta$. Moreover, camber curve parameters (θ, ξ and χ) are related in the following way: $\chi_1 = \theta_1 - \xi$ and $\chi_2 = \theta_2 + \xi$ for a turbine; and in a compressor, $\chi_1 = \theta_1 + \xi$ and $\chi_2 = \xi - \theta_2$. There is one remaining parameter that it is called camber angle and it is the addition of inlet and outlet camber angles: $\theta = \theta_1 + \theta_2$.

One important hint that the designer must take into account is that, in order to have a properly designed blade shape, the sign criteria established above must

be fulfilled. So, all the camber angles (θ_1, θ_2 and θ) have to be positive.

2.5 Introduction to parametric curves and Bézier theory

In computer graphics, it is convenient (because of its easiness) to use the so-called "parametric curves". Therefore, a curve is represented like a n grade polynomial that depends on a parameter t:

$$\vec{c}(t) = \vec{a_0} + \vec{a_1}t + \cdots + \vec{a_n}t^n \tag{2.1}$$

where the coefficients $\vec{a}_i$ are points of the plane and t is a parameters that goes from 0 to 1: from the starting point of the curve and the final point.

This way of representing a curve has one important advantage that is its easiness (as said before) although its main drawback is the fact that coefficients behave in a complex way when, for example, one wants to rotate the curve or translate it. Therefore, it is convenient to use another type of representation instead of polynomial curves (but following the same *philosophy*). And one of this type of computational representation of curves are *Bézier curves*.

Bézier curves are very used in computer graphics because they are smooth. In few words, they are constructed by a set of control points, and these points can be displaced in order to modify the plot. As previously mentioned, parametric curves can be transformed (namely, they can be rotated and/or rotated) and in the case of Bézier curves, one has just only to transform the control points properly in order to have these linear transformations.

The degree of a Bézier curve is defined by the set of control points. If $\vec{c}(t)$ is only defined by $\vec{a}_0$ and $\vec{a}_1$, the curve is linear. If it is defined by three points, then it is quadratic. And the degree can be increased up to n. The computational complexity increases with n. In the next figure (Figure 2.7) , one can see these two types of curves in a 2D plane:

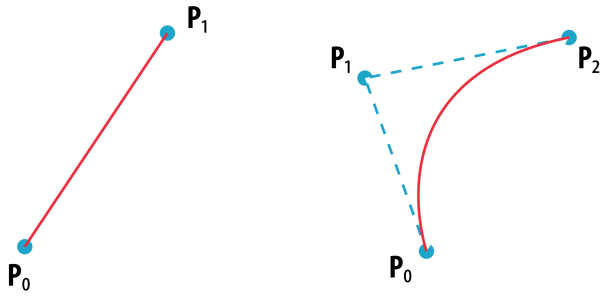

Figure 2.7: Two examples of Bézier curves. Left side - linear cuve; Right side - quadratic curve

Next figure shows how the curve is constructed depending on the value of the parameter t:

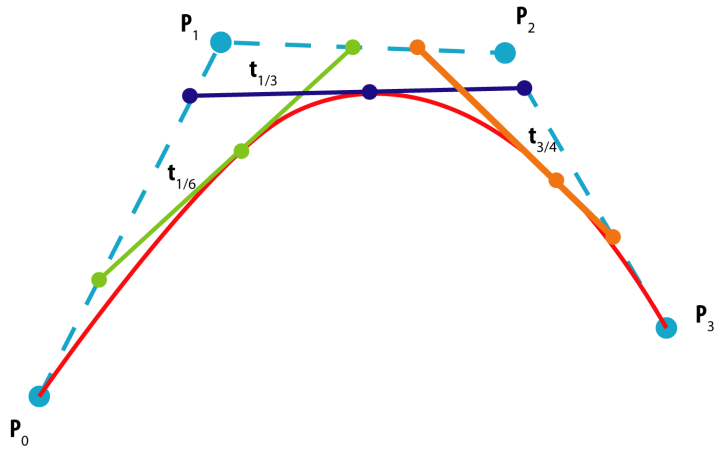

Figure 2.8: Building process of a parametric Bézier graph

For $n = 1$, the curve is expressed as a straight line:

$$\vec{c}(0) = P_0 + t(P_1 - P_0) = (1-t)P_0 + tP_1 \tag{2.2}$$

Let us develop the Bézier curve for a quadratic curve. For this kind of lines, implicitly, the control point P_1 depends on the tangent line of the finishing points.

Making use of Equation 2.1 and defining $\vec{c}(t)$ as a $(x_B(t), y_B(t))$,

$$x_B(t) = a_{0x} + a_{1x}t + a_{2x}t^2$$

$$y_B(t) = a_{0y} + a_{1y}t + a_{2y}t^2$$

or in a matrix form:

$$\vec{c}(t) = \begin{bmatrix} x(t) \\ y(t) \end{bmatrix} = \begin{Bmatrix} t^2 & t & 1 \end{Bmatrix} \begin{bmatrix} a_{2x} & a_{2y} \\ a_{1x} & a_{1y} \\ a_{0x} & a_{0y} \end{bmatrix} = TC_B = TM_BG_B \tag{2.3}$$

From Equation 2.3, T, G_B and M_B are defined as:

- $T = \begin{Bmatrix} t^2 & t & 1 \end{Bmatrix} \rightarrow T' = \begin{Bmatrix} 2t & 1 & 0 \end{Bmatrix}$
- $G = \begin{bmatrix} P_{2x} & P_{2y} \\ P_{1x} & P_{1y} \\ P_{0x} & P_{0y} \end{bmatrix}$
- Matrix M_B is the unknown of the equation and it relates matrices G_B (which depends on the control points) and C_B (which is the coefficients matrix)

In order to determine M_B, let us state the next conditions:

1. $\vec{c}(0) = P_0 = \begin{Bmatrix} 0 & 0 & 1 \end{Bmatrix} M_BG_B$
2. $\vec{c}(1) = P_2 \begin{Bmatrix} 1 & 1 & 1 \end{Bmatrix} M_BG_B$
3. $R_1 = \frac{P_2 - P_1}{t_2 - t_1} = \frac{P_2 - P_1}{1 - 1/2} = 2(P_2 - P_1) = \vec{c}\,'(1) = T'(1)M_BG_B = \begin{Bmatrix} 2 & 1 & 0 \end{Bmatrix} M_BG_B$

R_1 is defined as the tangent at $t = 1$, that is $\frac{d(P(t))}{dt}$. Note that at P_2, $t = 1$ and at P_1, $t = 1/2$. In a matrix form, these conditions are rewritten as follow:

$$G_H = \begin{Bmatrix} P_0 \\ P_2 \\ R_1 \end{Bmatrix} = \begin{bmatrix} 0 & 0 & 1 \\ 1 & 0 & 0 \\ 2 & -2 & 0 \end{bmatrix} G_B = \begin{bmatrix} 0 & 0 & 1 \\ 1 & 1 & 1 \\ 2 & 1 & 0 \end{bmatrix} M_B G_B \tag{2.4}$$

From this last equation, M_B can be calculated and it is equal to:

$$M_B = \begin{bmatrix} 1 & -2 & 1 \\ 0 & 2 & -2 \\ 0 & 0 & 1 \end{bmatrix} \tag{2.5}$$

and since $\vec{c} = TM_BG_B$,

$$\vec{c} = (t-1)^2 P_0 + 2t(t-1)P_1 + t^2 P_2 \tag{2.6}$$

A similar procedure can be followed for a cubic Bézier curve. Apart from the initial and final point conditions, for cubic expression, it may be also note that (as similar for the quadratic form) $R(0) = 3(P_1 - P_0)$ and $R(1) = 3(P_2 - P_1)$. And doing similar computations as before, the Bézier equation is expressed as:

$$\vec{c}(t) = (1-t)^3 P_0 + 3(1-t)^2 t P_1 + 3(1-t)t^2 + t^3 P_3 \tag{2.7}$$

If the process is doing for higher degrees, it can be observed Bézier functions have the shape of *Bernstein basis polynomial*[5] therefore, the explicit equation of order n is:

$$\vec{c}(t) = \sum_{i=0}^{n} \binom{n}{i} (1-t)^{n-1} t^i P_i \tag{2.8}$$

From the practical point of view, only quadratic form of Bézier parametric graphs is the one that it is used for this work.

[5]Bernstein basis polynomial is defined explicitly as $B_n(x) = \sum_{i=0}^{n} \beta_\nu \binom{n}{\nu} x^\nu (1-x)^{n-\nu}$ and few examples of this polynomial basis are $b_{0,0} = 1$, $b_{0,1} = 1 - x$, $b_{1,1} = x$, $b_{0,2} = (1-x)^2$, $b_{1,2} = 2x(1-x)$ and $b_{2,2} = x^2$, and so on

Chapter 3

State of the art

This chapter is divided in various sections that include several methods that are used to obtained a blade shapes: Cascade families, CIRCLE method and MISES.

3.1 Cascade families

This method is proposed in Ref [1] and it consists on making use of thickness families. These families are widely used in the Turbomachinery industry to create blade profiles. In the same reference, it is mentioned a software that a designer can employ to design and analyse a turbomachine cascade called 'CASCADE'. According to the features of the program, a profile thickness is superimposed to a camber line or a mean line. Once it is selected the type of camber line and thickness profile, CASCADE proceeds to do the flow analysis and thereafter tries to predict the outflow angle and the pressure distribution along the blade. It has to be pointed out that this program is not available for a student. Therefore, the theory behind is useful for the purpose of this work.

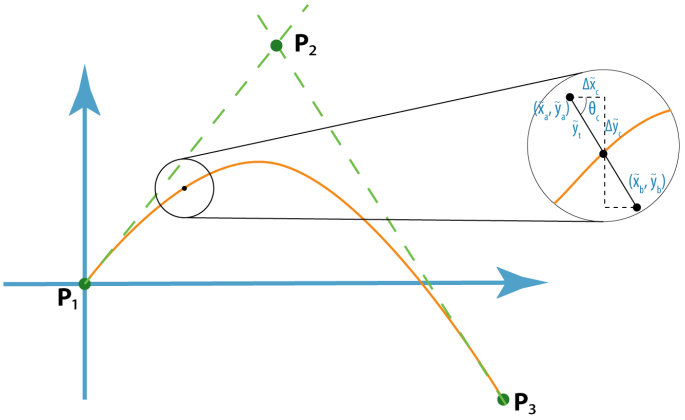

Figure 3.1: Blade shape with a prescribed thickness profile

Thickness profile coordinates, as seen in Figure 3.1, are added perpendicularly with respect to the camber line (in further section it is explained how this line is obtained). Using simple trigonometry relations, the upper blade profile is

determined by this expression:

$$\tilde{x}_a = \tilde{x}_c - \tilde{y}_t \cos\theta_c \qquad \tilde{y}_a = \tilde{y}_c + \tilde{y}_t \sin\theta_c \tag{3.1}$$

and the lower side of the blade by:

$$\tilde{x}_a = \tilde{x}_c + \tilde{y}_t \cos\theta_c \qquad \tilde{y}_a = \tilde{y}_c - \tilde{y}_t \sin\theta_c \tag{3.2}$$

In Equations 3.1 and 3.2, θ_c angle is defined (in concordance with Figure 3.1) as:

$$\tan\theta_c = \frac{\mathrm{d}\tilde{y}_c}{\mathrm{d}\tilde{x}_c} \approx \frac{\Delta\tilde{y}_c}{\Delta\tilde{x}_c} \tag{3.3}$$

Note that, in general, the *resolution* (i.e., number of data points) is low. Then, these coordinates should be interpolated in order to have a proper blade definition.

In 1951, NASA analysed several NACA profiles (Ref [6]), concretely, NACA-65 series. The performance was tested with a low-speed cascade tunnel. These investigations are useful for a designer in the way that it can be observed the blade-section performance as a function of the cascade parameters. Apart from that, the researcher concluded his work this NACA series offers satisfactory results for axial compressors under the flow condition specified in the memorandum.

Along the XX century, NACA 0015 were used in turbines (Wells turbine) whose main application is to utilize the power of the sea (Ref [15]). It has been seen that this profile offers satisfying results in terms of efficiency. Lately, Kaddah et al. improved the performance of the turbine using NACA 0012 and NACA 0021. All these profiles and others suggested in Lewis' book (Appendix II, Ref [1]) and other papers (Ref [16]) are employed in this project (Annex B).

3.2 CIRCLE

This method is based on the one proposed by T. Korakianitis, I.A. Hamakhan, M.A. Rezaienia, A.P.S. Wheeler and E.J. Avital, J.J.R. Williams (Ref [5]) and it is named as CIRCLE which stands for *presCribed suRface Curvature distribution bLade dEsign*. Basically, it consists on a tool that joins the trailing edge and the leading edge circles or ellipses by means of a set of curves that are continuous between these areas.

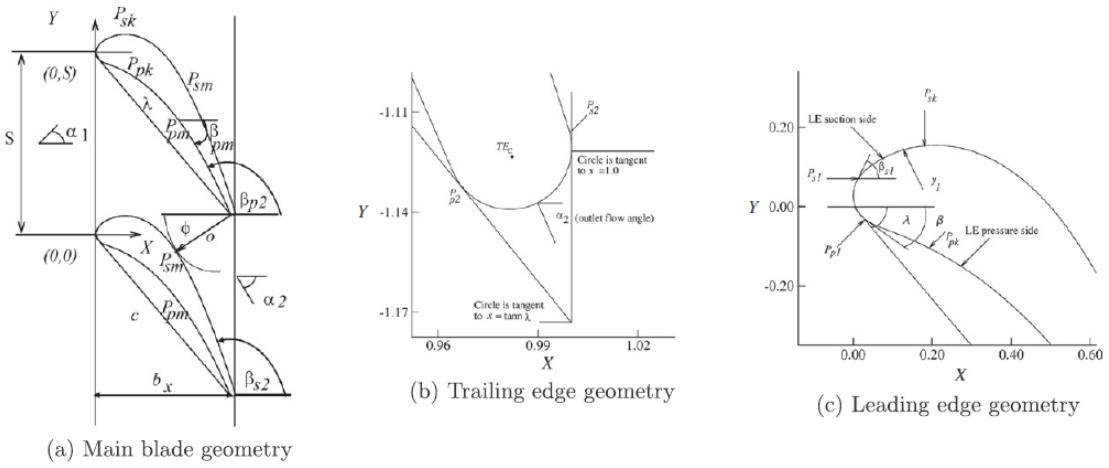

(a) Main blade geometry

(b) Trailing edge geometry

(c) Leading edge geometry

Figure 3.2: CIRCLE blade geometry definition

As it can be seen in Figure 3.2, there are a set of variables that fully define the blade geometry. These parameters are grouped into a) Main blade geometry parameters, b) TE geometry and c) Leading edge geometry. Key variables are the LE and TE radii (in case if they are assumed to be circles) or elliptic geometry parameters; flow angles (or the metal); the stagger; and finally the pitch of the cascade. In order to define the upper surface (and as depicted from this figure), it is needed to take into account the throat o and its angle ϕ. Once this suction surface control point is obtained, user can also define the pressure surface control point. At TE, the blade shape is defined by a circle or an ellipse. The joining points between the mean and TE geometries are P_{s2} and P_{p2}, parameters that are set by the designer (and similarly LE is). Likewise to the tool developed in this project, CIRCLE uses parametric graphics such as Bézier splines or NURBS, which are more advanced methods.

3.3 MISES

MISES (Ref [8]), the acronym for Multiple Blade Interacting Streamtube Euler Solver, is a set of programs non-GUI (Graphical User Interface) created by Mark Drela (from the MIT Aerospace Computational Design Laboratory) with the main purpose of analysing the viscous flow of a cascade in order to optimize the blade shape of a machine. Basically, it is a code that solves the boundary layer equations and different schemes are used to solve it. Euler equations are used to solve the inviscid flow and, to solve the viscous problem, boundary layer equation are utilized in addition. This tool has several advantages in terms of time since it is rapid although it cannot predict losses in the wake region due to Kutta model (applied in the TE), Ref [17].

In the Figure 3.3, one can observe how the software is developed. ISET

program initializes a state file called *idat.xxx*[1] - which contains basic information about the grid and the flow -, *blade.xxx* - file that contains geometry information - and, optionally, *stream.xxx* and *loss.xxx* - stream surface geometry and loss files. Afterwards, ISES uses the state file and the *ises.xxx* files that contains flow conditions. Basically, it solves the Euler Equations capable of solving subsonic and supersonic flows. There is an additional option that is similar to ISES in the way that it performs the same calculation, but in this case it is performed for several parameters. EDP program is used to modify the state file, BLDSET has the functionality of changing files such as *blade.xxx* and, finally, IPLOT plots the flow results. To be noted that blade geometry is defined in the *streamsurface coordinate system*, $m' - \theta$ (Figure 3.3), where m' is the local streamsurface radius $\left(\int \frac{\mathrm{d}m}{r}\right)$ and θ is the circumferential angle.

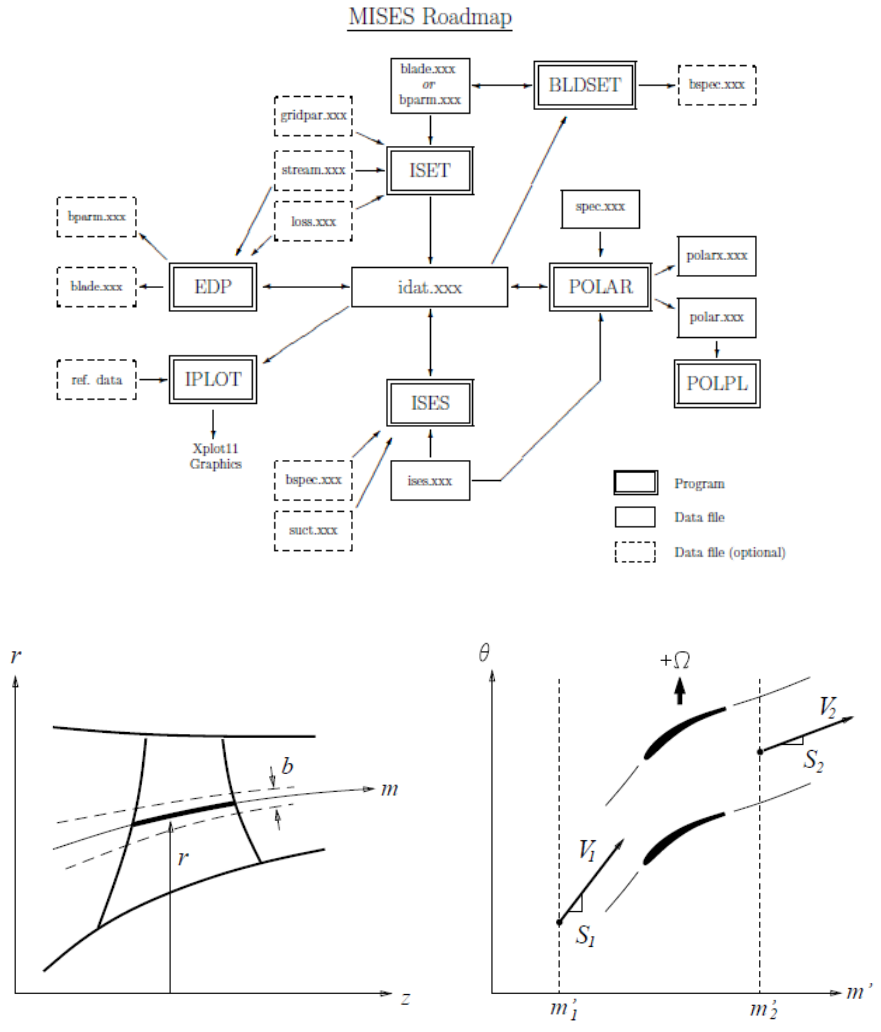

Figure 3.3: MISES Roadmap and streamsurface coordinates definition

Although several files have been mentioned before, only two are of importance: blade and ises files. Blade file is written as follow:

[1] *.xxx* is the extension designated for the case that it is running and it can be any

```
          NAME
          SINL SOUT CHINL CHOUT PITCH
          X(1) Y(1)
          X(2) Y(2)
          . .
          . .
          X(I) Y(I)
```

where:

`Name` is the name of the blade

`SINL` represents the initial value of $S_1 = \tan\beta_1$, where β_1 is the flow angle relative to the axial direction. These value should be close to the final inlet flow angle. Therefore, metal angle can be used as initial value of S_1

`SOUT` Initial value of $S_2 = \tan\beta_2$ and, according to the manual instruction of MISES, it is not used

`PITCH` circumferential pitch of the cascade (previously explained) and it is expressed in radians

`X(I) Y(I)` are the blade geometry coordinates

`CHINL - CHOUT` represent distances and are set by default

On the other hand and as said before, ises file contains information about the flow and boundary condition of the case analysed. In this file, one has to deal with the flow parameters (Mach Number, flow angles and Reynolds Number) but also with a parameter that sets the transition of the laminar flow. Further information related with ises can be found in Annex C.

Chapter 4

Blade profile geometry

In this chapter it is explained how to construct the camber line with Bézier theory and, afterwards, it is presented a similar method to CIRCLE.

4.1 Introduction to Direct Method

There are two ways to design a blade for a compressor and a turbine. These approaches are called:

- *Direct (or analysis) method*: it is basically a geometrical technique. Generated cascades are further analysed by experimental test or theoretical (e.g. MISES software) approaches in order to find the performance.
- *Inverse (or synthesis) method*: this is an advanced method and it is the opposite with respect to the previous one; in this case, the user specifies the velocity and pressure distributions along the surface of the blade and then the profile is generates. These methods are often refereed to as *Prescribed Velocity Distribution* or *PVD* analysis.

It may be thought that inverse method is the one that gives the best results but, in fact, from a practical point of view, direct method is widely used by engineers. And therefore, it is the one that is preferred.

Along this project, there are distinguished two ways:

1. Related Cascade families: already analysed thickness families are used for the construction of blade shapes, which has been detailed in previous sections
2. High parameters design (or *manual*): user has full control on the design by setting a large bunch of parameters, related with CIRCLE method

4.2 Camber line

Camber line is constructed with three inputs angles: metal and stagger angles. Ask the user for the camber line inputs: metal (χ_1 and χ_2) and stagger (ξ) angles. With these inputs, the control points for Bézier theory are obtained in the following way:

1. First point is the initial point of the camber line. For instance, it can be the origin $\mathbf{P}_0 = (0, 0)$

2. Third point is the final point of the camber. This point is easily get using simple trigonometrical expressions (Figure 3.1):

$$\mathbf{P}'_3 = (l\cos\xi, l\sin\xi)$$

Since it is preferred to have a parametric design (with respect to chord length l, for instance), the non-dimensional $\mathbf{P}_3$ is equal to

$$\mathbf{P}_3 = (\cos\xi, \sin\xi)$$

According to the design criterion defined in previous figures, ξ is positive for compressors and negative for turbines. In TURBOMACHINE BLADE DESIGNER all angles (χ_i and ξ) are considered as positive values, then the above expressions are rewritten as:

$$\mathbf{P}_3 = (\cos\xi, \sin\xi) \tag{4.1}$$

for compressors and

$$\mathbf{P}_3 = (\cos\xi, -\sin\xi) \tag{4.2}$$

3. The second control point is obtained with the metal angles and the other two control points:

$$P_{2x} = \frac{P_{3y} + P_{3x}\tan\chi_2}{\tan\chi_1 + \tan\chi_2} \tag{4.3}$$

$$P_{2x} = \frac{P_{3y} - P_{3x}\tan\chi_2}{\tan\chi_1 - \tan\chi_2} \tag{4.4}$$

and the y-coordinate of this control point is simply

$$P_{2y} = P_{2x}\tan\chi_1 \tag{4.5}$$

Once the control points are properly calculated, the camber line is obtained by substituting these coordinates in Equation 2.7. When the curve is obtained, it can be applied the cascade families theory developed in Section 3.1.

In order to have a proper computation in MISES, it may be interesting to approximate the LE elliptically:

$$\tilde{x}_i = a - a\cos\phi \qquad \tilde{y}_i = b\sin\phi \tag{4.6}$$

where a is the semi-major axis (which in this case $\tilde{x}_t(2)$), b is half of the minor axis ($\tilde{y}_t(2)$) and ϕ goes from 0 to $1/2\ \pi$.

As a last remark, for MISES purposes, the final profile should be interpolated but with much less points, 300 for instance because of MISES limitations. It is interesting to use a method in which the interpolation is performed depending on the curvature of the profile. Lewis (Appendix II, Ref [1]) proposed the next one in his book:

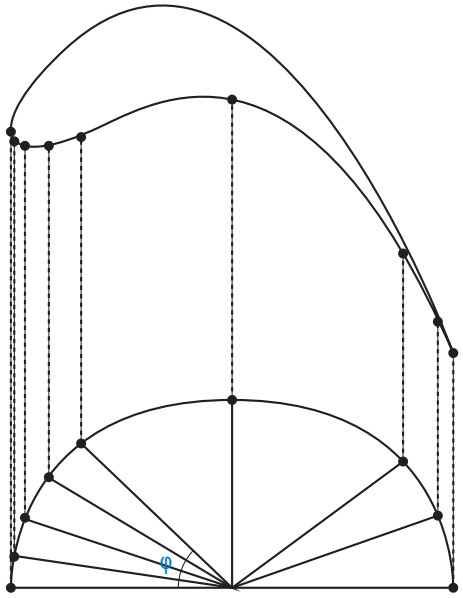

Figure 4.1: Interpolation method depending on the curvature of the profile

As it can be depicted from Figure 4.1, angle ϕ is defined as π/N, where N is an arbitrary number of points ($N = 150$ for example). And, according to this plot, the projection of the $\cos\phi$ over the blade profile is less spaced in the area where the curvature is more pronounced. The interpolation x-coordinates, therefore, is defined as $x_{\text{interpolation}} = l - l\cos\phi$ and the y-coordinates are obtained by using MATLAB functions. This is also applied in the *Higher parameters design* method.

4.3 High parameters design

In this section, a description of the manual design option is given. In this case, there are not any prescribed thickness family. Therefore, more inputs are needed to be asked to the user, apart from the metal angles (χ_1 and χ_2) and the stagger (ξ).

The geometry is defined in three sections: Leading Edge, Trailing Edge and the Main geometry which is based on the Bézier theory and it used to join LE and TE. Firstly, the camber line is obtained as explained in previous sections based on the metal and stagger angles. Moreover, the LE is defined by an ellipse, concretely, by the semi-axes a and b. Later, this ellipse is rotated counter-clockwise (for both, compressor and turbine) at inlet metal angle:

$$\begin{Bmatrix} x_i \\ y_i \end{Bmatrix} = \begin{bmatrix} \cos\chi_1 & -\sin\chi_1 \\ \sin\chi_1 & \cos\chi_1 \end{bmatrix} \begin{Bmatrix} x_j \\ y_j \end{Bmatrix} \tag{4.7}$$

where x_j and y_j are the coordinates with zero metal inlet angle and x_i and y_j are the coordinates after rotating the ellipse, Figure 4.2 - it has to be pointed out that the sketch does not correspond with a real blade design:

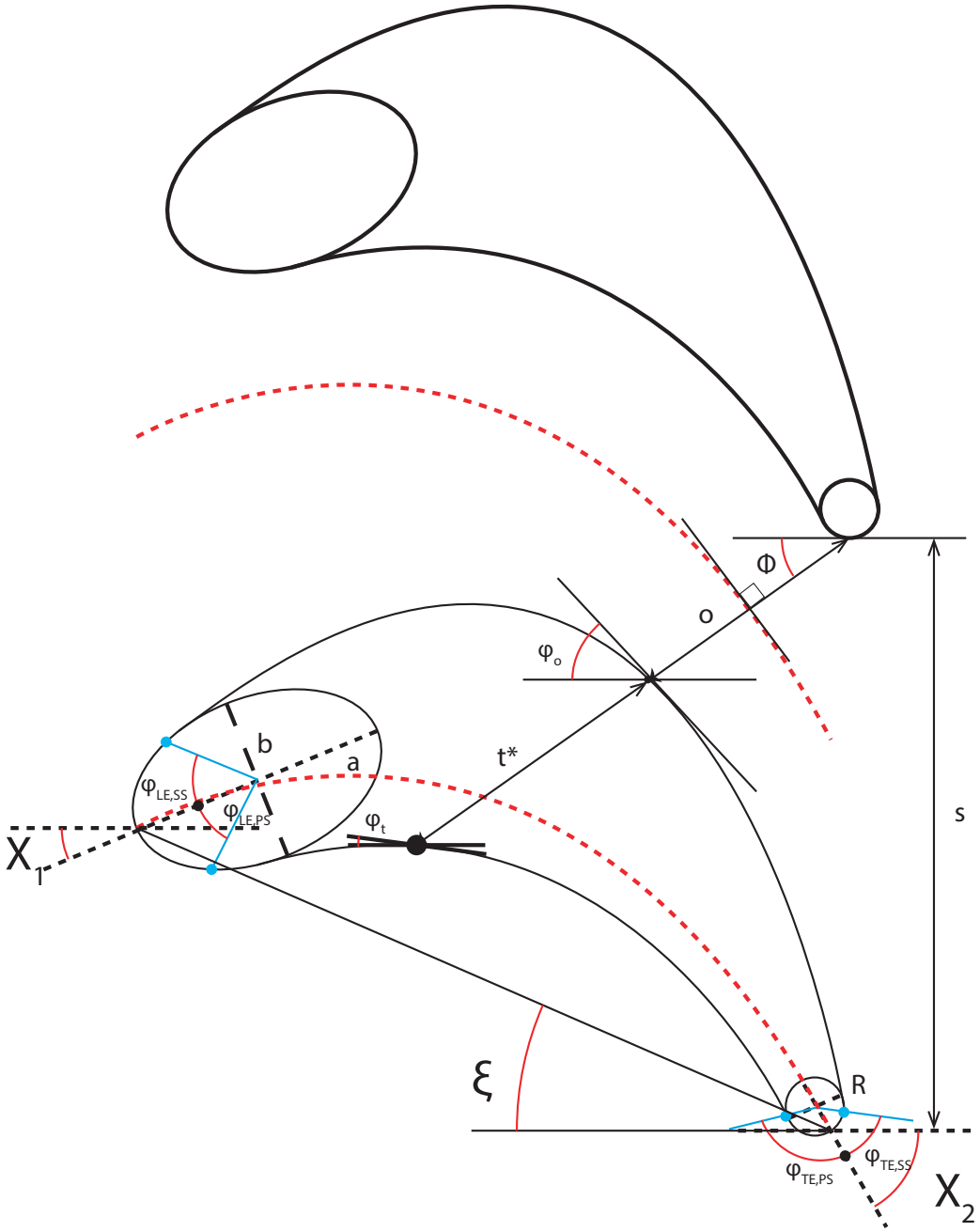

Figure 4.2: High parameters design of a turbine blade

TE is modelled as a circle with radius R. This value, in fact, does not need to be a higher one in order to fulfil Kutta condition.

Likewise to LE, the rotation of TE circle in a turbine blade is clockwise but in a compressor is counter-clockwise. Rotation matrices are

$$R_{\chi_2} \begin{bmatrix} \cos\chi_2 & \sin\chi_2 \\ -\sin\chi_2 & \cos\chi_2 \end{bmatrix}$$

and

$$R_{\chi_2}\begin{bmatrix}\cos\chi_2 & -\sin\chi_2\\ \sin\chi_2 & \cos\chi_2\end{bmatrix}$$

respectively.

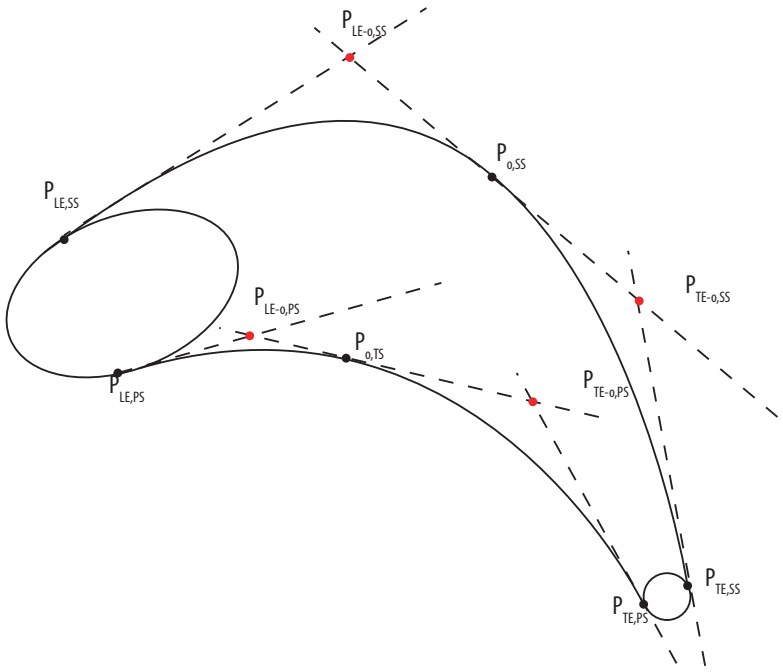

Figure 4.3: Control Points of a turbine blade

About the main blade geometry, firstly, it has to be said that, in order to use parametric graph theory, several control points need to be defined. $P_{LE,SS}$, $P_{TE,SS}$ (for the suction surface), $P_{LE,PS}$ and $P_{TE,PS}$ (for the pressure one) are the four joining points between the main geometry and LE and TE.

Another control point is $P_{o,\mathrm{SS}}$, which is determined by the throat distance o/l, throat angle ϕ and the adjacent TE $(\tilde{x}'_{TE}, \tilde{y}'_{TE})$ of the cascade:

$$(\tilde{x}'_{TE}, \tilde{y}'_{TE}) = (\tilde{x}_{TE}, \tilde{y}_{TE} + s/l) \tag{4.8}$$

The throat angle is a parameter that in CIRCLE paper is set by the designer, but here it is calculated as follow: the camber line is translated $\tilde{s}/2$ above and then ϕ is calculated in such a way that minimizes the distance from the adjacent TE to this line. Let us define the point $P_{\mathrm{d,min}}$ which belongs to the translated camber line and:

$$P_{\mathrm{d,min}} = \min(\tilde{x}'_{TE} - \tilde{x}'_c, \tilde{y}'_{TE} - \tilde{y}'_c) \tag{4.9}$$

Once one has this point determined, ϕ is

$$\tan\phi = \frac{\tilde{y}'_{TE} - P_{\mathrm{d,min,y}}}{\tilde{x}'_{TE} - P_{\mathrm{d,min,x}}} \tag{4.10}$$

and then

$$P_{o,\mathrm{SS}} = (\tilde{x}'_{TE} - \tilde{o}\cos\phi, \tilde{y}'_{TE} - \sin\phi) \tag{4.11}$$

$$P_{o,\mathrm{PS}} = (P_{o,\mathrm{SS,x}} - t^* \cos\phi, P_{o,\mathrm{SS,y}} - t^* \sin\phi) \tag{4.12}$$

All this procedure can be better understood by inspecting Figure 4.2.

Lastly, $P_{\mathrm{LE-o,SS}}$, $P_{\mathrm{TE-o,SS}}$, $P_{\mathrm{LE-o,PS}}$ and $P_{\mathrm{TE-o,PS}}$ need to be determined in order to close the problem, Figure 4.3. They are defined as the intersection between $P_{\mathrm{LE,SS}}$ and $P_{\mathrm{o,SS}}$ tangent lines in the case of $P_{\mathrm{LE-o,SS}}$:

$$P_{\mathrm{LE-o,SS,x}} = \frac{P_{o,SS,y} - P_{LE,SS,y}}{\tan\phi_o + \tan\left(90^\circ - (\phi_{LE,SS} - \chi_1)\right)} \tag{4.13}$$

$$P_{\mathrm{LE-o,SS,y}} = P_{o,SS,y} - \tan\phi_o P_{\mathrm{LE-o,SS,x}} \tag{4.14}$$

The rest of the points are found in a similar way:

$$P_{\mathrm{LE-o,PS,x}} = \frac{P_{o,PS,y} - P_{LE,PS,y}}{\tan\phi_t + \tan\left(90^\circ - (\phi_{LE,PS} + \chi_1)\right)} \tag{4.15}$$

$$P_{\mathrm{LE-o,PS,y}} = P_{o,PS,y} - \tan\phi_t P_{\mathrm{LE-o,PS,x}} \tag{4.16}$$

$$P_{\mathrm{TE-o,SS,x}} = \frac{P_{o,SS,y} - P_{TE,SS,y}}{\tan\phi_o - \tan\left(90^\circ - (\phi_{TE,SS} - \chi_2)\right)} \tag{4.17}$$

$$P_{\mathrm{TE-o,SS,y}} = P_{o,SS,y} - \tan\phi_o P_{\mathrm{TE-o,SS,x}} \tag{4.18}$$

$$P_{\mathrm{TE-o,PS,x}} = \frac{P_{o,PS,y} - P_{TE,PS,y}}{\tan\phi_t - \tan\left((\phi_{TE,PS} + \chi_2) - 90^\circ\right)} \tag{4.19}$$

$$P_{\mathrm{TE-o,PS,y}} = P_{o,PS,y} - \tan\phi_t P_{\mathrm{TE-o,PS,x}} \tag{4.20}$$

In the case of a compressor, the minimum passage area is found near to the LE (not close to TE as in turbines). Therefore, the expressions are slightly different with respect to turbines but the same philosophy is applied (Figure 4.4 - it has to be done the same comment as with the turbine sketch: it does not correspond with a real design):

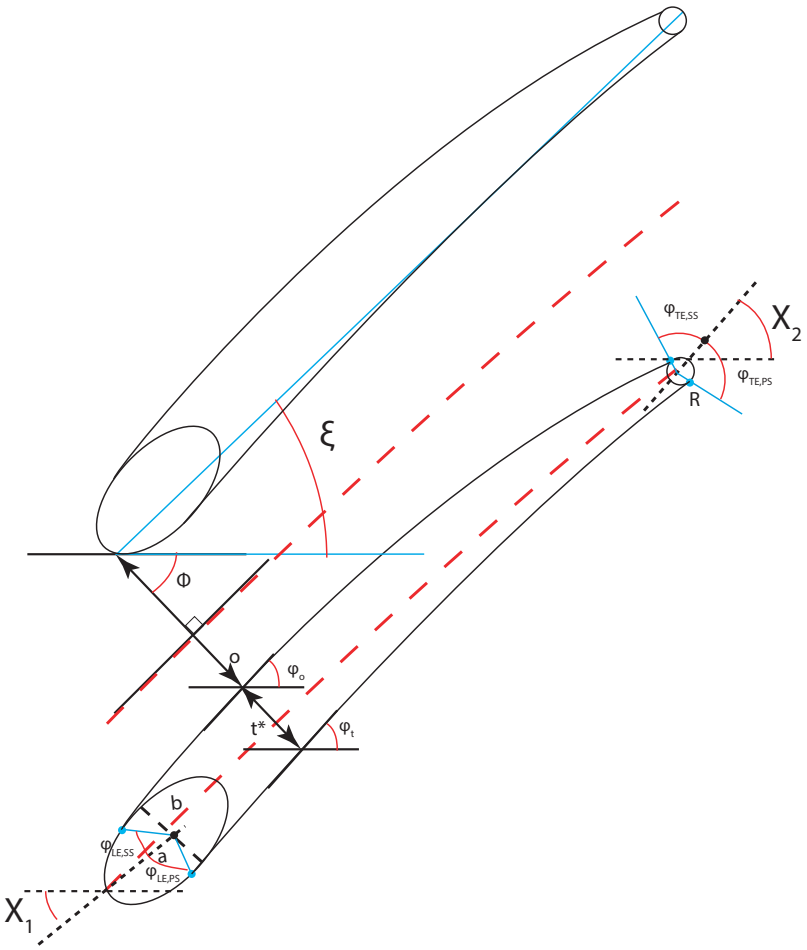

Figure 4.4: High parameters design of a compressor blade

Chapter 5

Results

Along this chapter, the tool Turbomachinery Blade Designer is described. Apart from that, in further sections several cases are analysed.

5.1 Turbomachinery Blade Designer tool

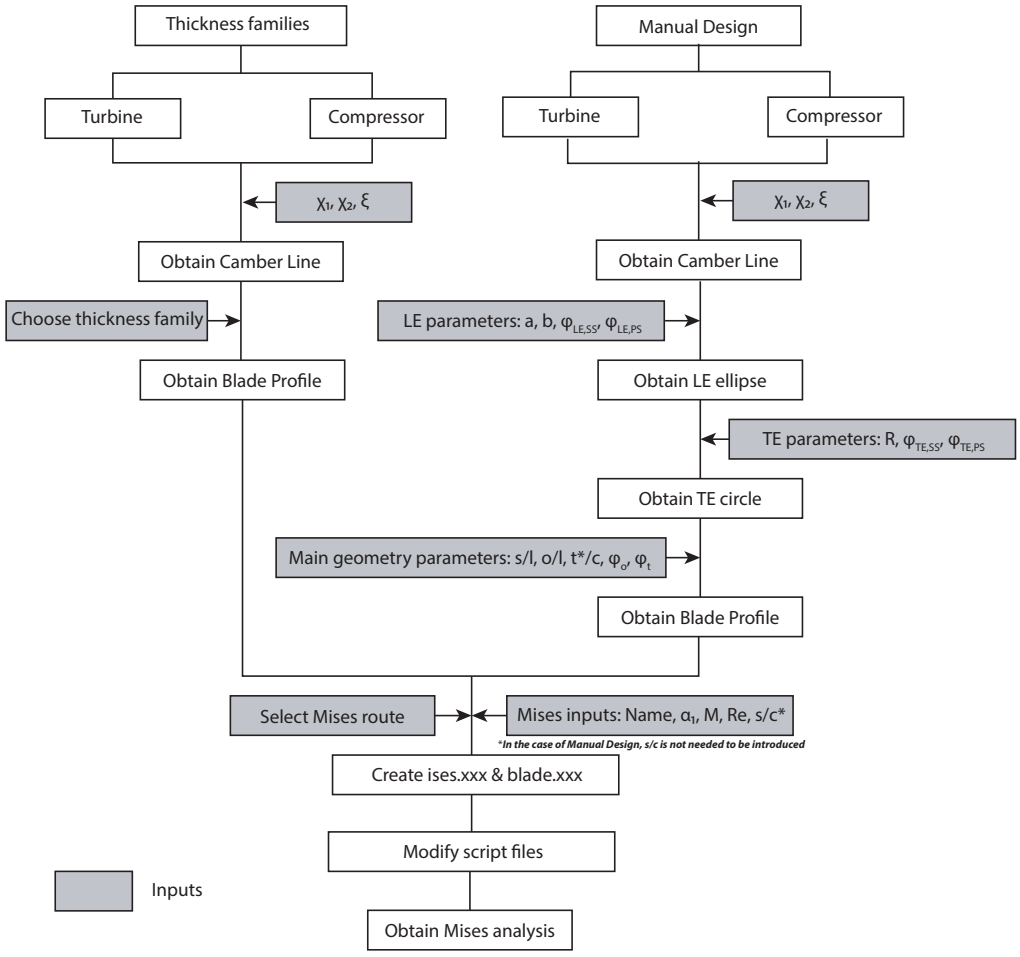

Figure 5.1: Turbomachinery Blade Designer Roadmap

TURBOMACHINERY BLADE DESIGNER is the tool that has been developed in this project. Its main functionalities are:

- Create turbine and compressor blades manually or using a thickness family
- Compute flow evolution with MISES by only introducing several inputs; this means that the user has not to configure the program
- In addition, it has diverse options that help the designer to use TURBOMACHINERY BLADE DESIGNER

The program is run from a UNIX Operating System and through the platform 'App Designer' from MATALB. In the previous scheme (Figure 5.1), one can analyse the roadmap of this tool. As it can be seen, there are there are two main ways of designing: Cascade families (Section 3.1) and a manual way or high parameters design - Section 4.3). Consequently, it is written down the inputs needed to be set by the designer to obtain the different parts of the profile. The last step of the diagram is the introduction of MISES configuration inputs. In this way, two files are created: `ises.xxx` and `blade.xxx`. MISES is run through `meshMISES.scp`, `postMISES.scp`, `resultsMISES.scp` and `runMISES.scp` files. They are in charge of creating the mesh of the problem; run the iteration process and find the flow solution; and to obtain the results.

5.1.1 Turbine layout

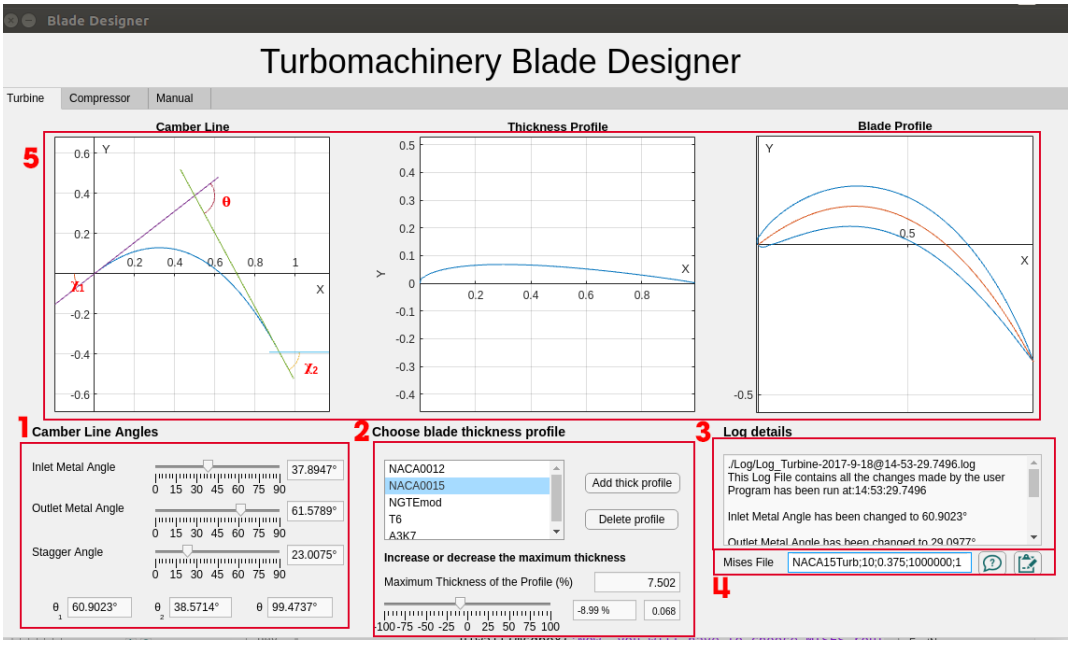

Figure 5.2: Turbine profile design

Turbine layout (Figure 5.2) is composed by five section:

1. In this part, the three inputs of the camber line are chosen; they go from 0° to 90°. In the lower part, camber angles are calculated and displayed, as explained in previous chapters

2. User has to choose, by default, one of the thickness families stated in Annex B. Apart from that, there is the option to delete a profile by pushing 'Delete profile' button; or to add another one with 'Add thick profile' button. Moreover, it is possible to increase the maximum thickness by moving to the left or to the right the slider. There are three boxes: in the upper one it is shown the maximum thickness percent of the chosen profile, in the lower-left side it is written the increment and the new maximum value can be observed in the right side

3. All the changes are shown in this text area and they are saved in a log file

4. In this box, MISES inputs are introduced. In the case of a turbine, it must be introduced the blade or case name, inlet flow angle, outflow Mach Number M, inlet Reynolds Number (Re) and pitch (to the chord ratio)

5. Three graphs are sketched: the first one is the the camber line, the middle is the thickness profile and the final blade shape is represented in the right side of this area

5.1.2 Compressor layout

Compressor layout (Figure 5.3) is equal to the turbine one and it is composed by the same sections. There is only one difference: in the MISES input box, instead of outlet Mach Number, it is introduced the inlet one.

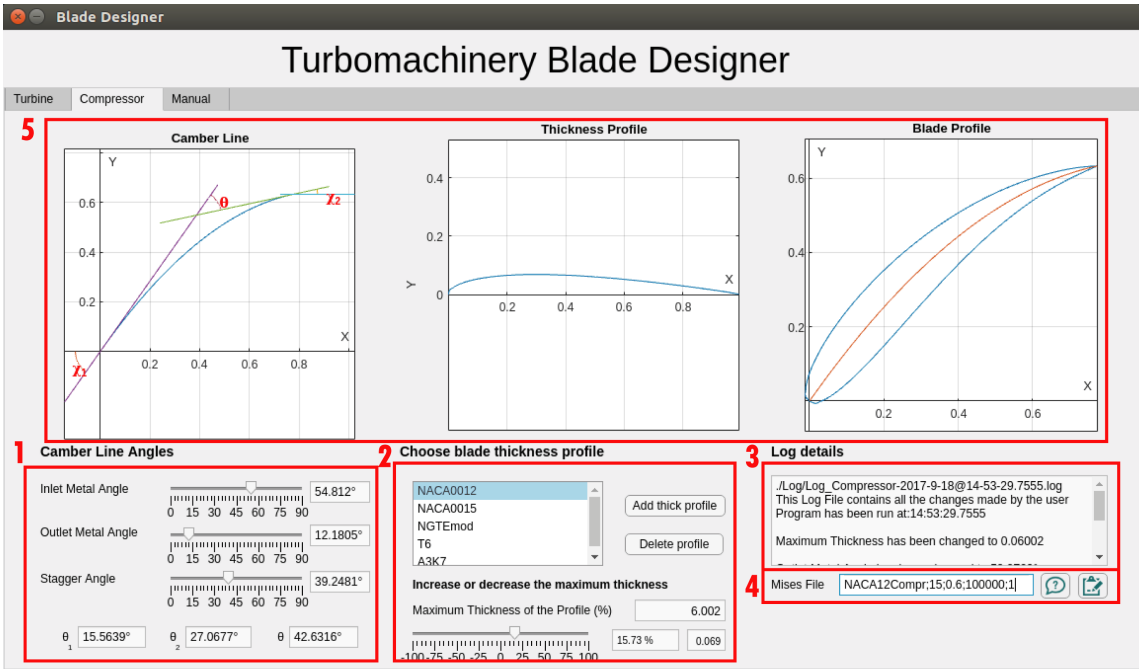

Figure 5.3: Compressor profile design

5.1.3 Manual layout

In this type of design, the following parts are differentiated:

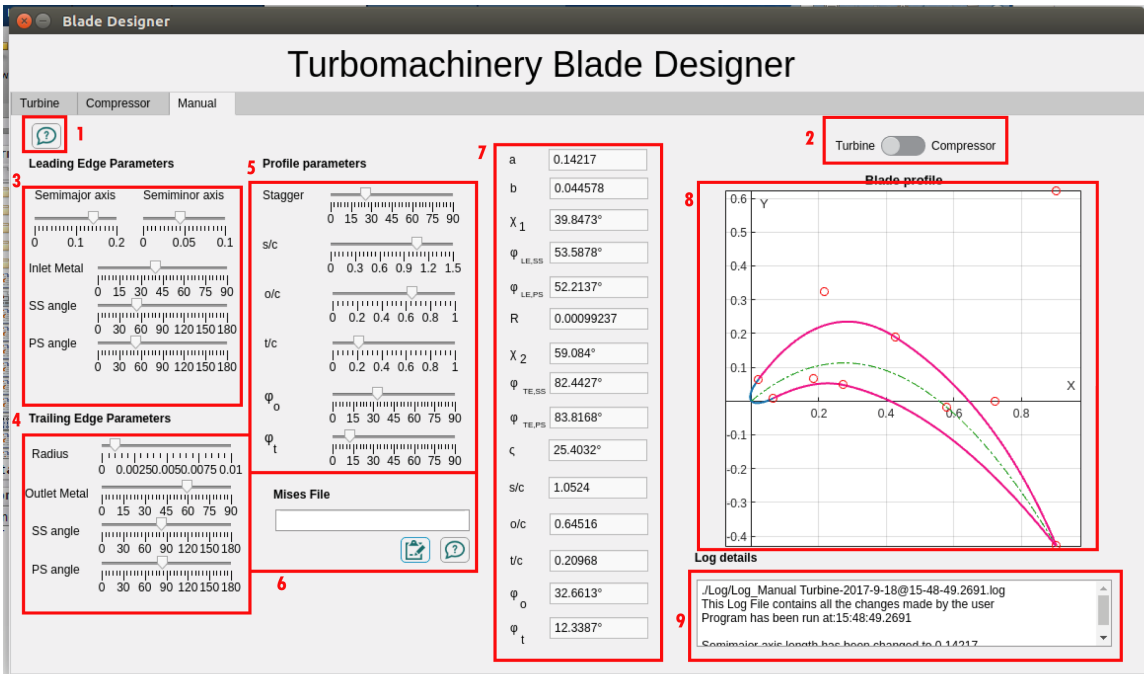

Figure 5.4: Manual profile design

1. This is an information button that, when pushed, it shows Figures 4.2 and 4.4

2. With this switcher, the designer has to choose the type of turbomachine

3. This part of the layout contains the Leading Edge Parameters (semimajor axis a, Semiminor axis b, Inlet Metal χ_1, $\phi_{LE,SS}$ and $\phi_{LE,PS}$). Remember that it is modelled as an ellipse

4. Similar to the previous one, here the parameters of the Trailing Edge are set (R of the circle, χ_2, $\phi_{TE,SS}$ and $\phi_{TE,PS}$)

5. The remaining design parameters are chosen with these sliders (ξ, s/l, t/l, t^*/l, ϕ_o and ϕ_t[1])

6. As the previous types of design, MISES variables are introduced in this box; and the log details are shown in the part of the figure labelled with a 9

7. All the previous values chosen by the designer are shown in this side

8. And the final result can be observed in this place

5.1.4 Other features of the software

Apart from the previous characteristics of the tool, there are more that are mentioned in the next lines. One of them is the possibility to add an extra thickness profile (Figure 5.5)

[1]The character 'c' of Figure 5.4 from s/c, o/c, and t/c refers to the chord length

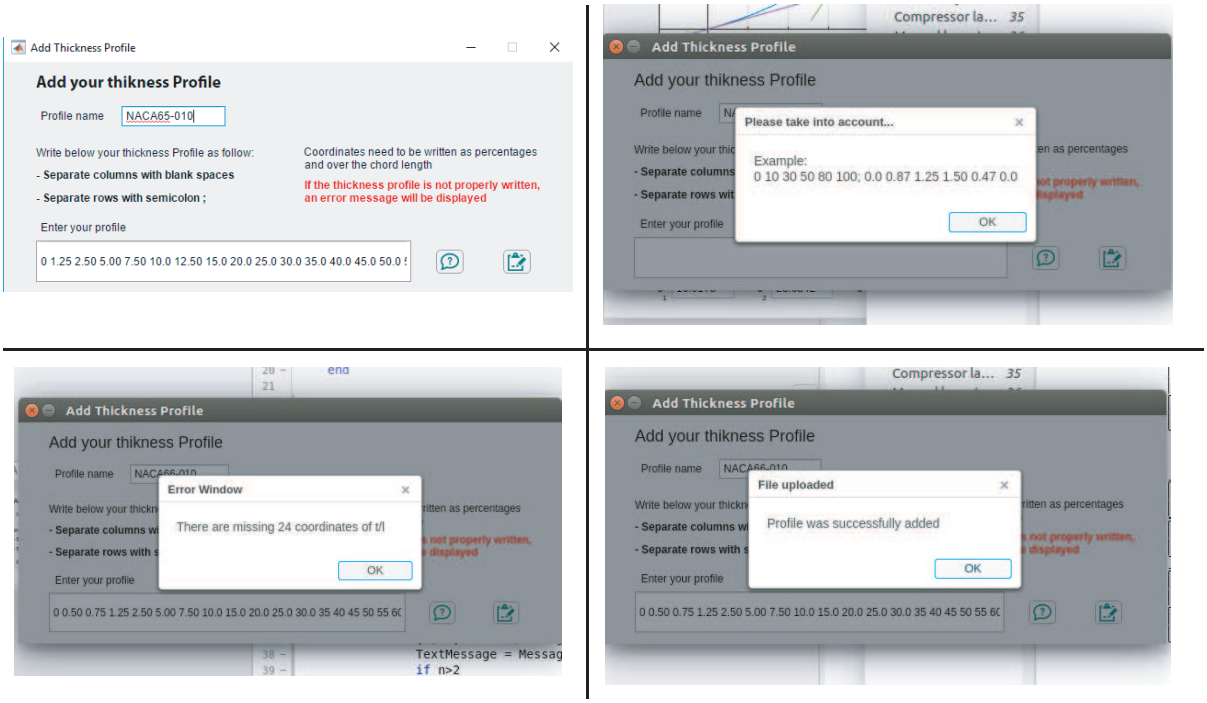

Figure 5.5: 'Add Thickness Profile' layout

As it can be seen in the previous figure, the user can add an extra thickness profile. This option includes, moreover, emergency windows with instructions but also it displays errors when these instructions are not followed. Airfoils databasis are useful in the way that they can be used to add thickness profiles to the tool. It has to be pointed out symmetrical airfoils are useful because of the null mean camber line. Therefore, NACA series 00xx or NACA 6x-0xx may be interesting to analyse their performance in a turbomachine. (Ref [18]).

There are more support windows (instructions and errors) displayed to the design with the purpose of making the process easier. One example is the next one, which shows the variables that are needed to be introduced in order to proceed with the analysis:

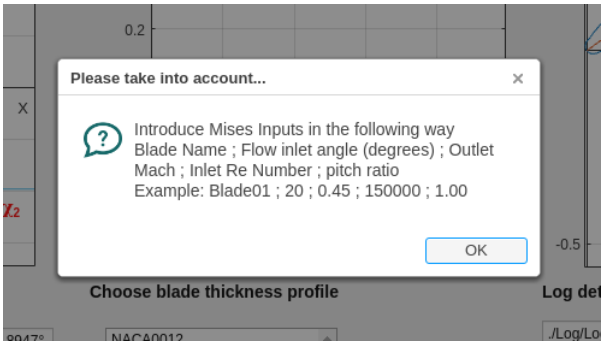

Figure 5.6: Example of a support window

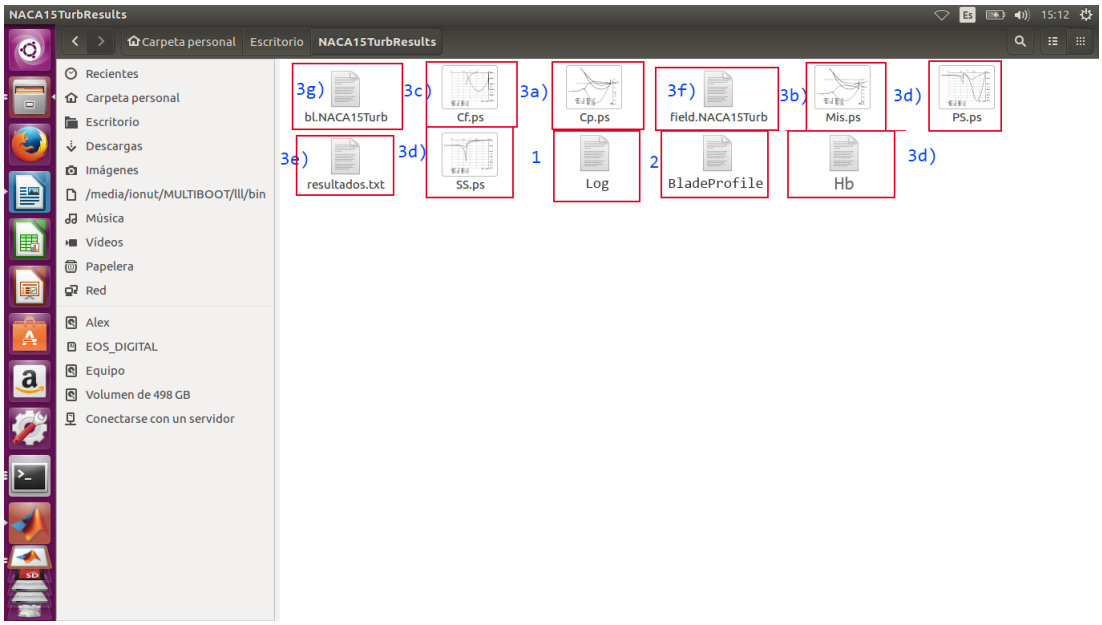

Figure 5.7: MISES Results files

The last feature that is focussed are the results of the tool. Apart from the profile, the output files are:

1. Log file
2. Blade profile coordinates
3. MISES results
   (a) Pressure coefficient C_p versus x/l curve, which undergoes this expression:
   $$C_p = \frac{p - p_1}{\frac{1}{2}\rho_1 V_1^2} \tag{5.1}$$
   where p is pressure, ρ_1, the flow density at inlet station and V_1, the absolute velocity
   (b) Isentropic Mach Number M^{isent} defined with the local static pressure p and radius r, and the inlet pressure p_1 and radius r_1
   (c) Friction Coefficient C_f along x/l
   (d) Boundary layer quantities (momentum θ, displacement δ^* thickness and shape factor $\bar{H}$) for both surfaces, pressure and suction. Shape factor is defined as the ratio between the displacement and momentum thickness:
   $$\bar{H} = \frac{\delta^*}{\theta} \tag{5.2}$$
   (e) Results file: inlet and outlet flow angles, inlet and outlet Mach Numbers, Inlet Reynolds Number, two loss coefficients ($\bar{\omega}$ and ζ), static to total pressure ratios $\frac{p_1}{p_{o1}}$ and $\frac{p_2}{p_{o2}}$, and Velocity ratio `VRat`
   (f) Flowfield file - several flow parameters are printed in a text file
   (g) BL file - in this file, the Boundary Layer quantities are written along the blade shape

5.2 Examples of blade profiles, and MISES analysis and discussion

In this section, several blade profiles are designed. Consequently, they are analysed and their results are discussed.

5.2.1 Cascade families

Turbine example

T6 section is widely used for turbine blade and, as a case example, it is shown the next one. It is defined with the next geometrical parameters: $\chi_1 \approx 30°$, $\chi_2 \approx 59°$ and $\xi \approx 23°$, Figure 5.8:

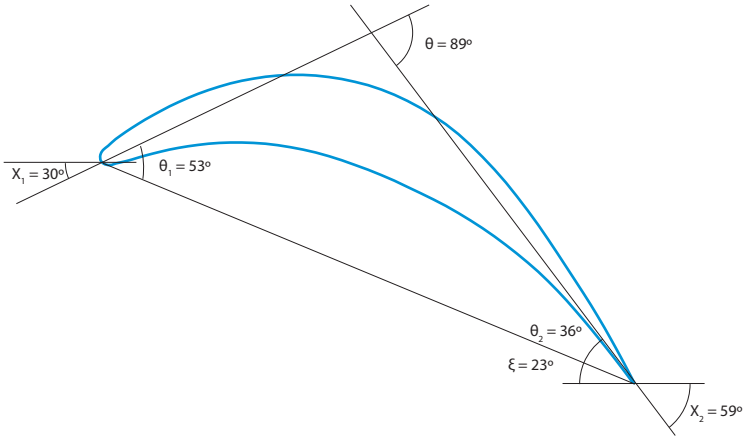

Figure 5.8: Blade shape

As explained in previous sections, TURBOMACHINERY BLADE DESIGNER needs certain flow inputs:

α_1	Re_1	M_2	s/l
15.00°	1,000,000	0.4	1.00

Table 5.1: Flow parameters of a turbine blade

The above values are common ones for a turbine stage. Inlet flow angle must not be large because the turbine stage has to deliver large amount of work and this is achieved with large turning angles ($\epsilon_S = \alpha_2 - \alpha_1$). It is expected then that after the analysis a large α_2. The incidence angle is therefore $i = \alpha_1 - \chi_1 = -15°$. Regarding the Mach Number, a subsonic flow is preferred in order to avoid shock waves and a possible loss in the performance of the blade. The order of magnitude of the Reynolds Number is 100,000 as stated in this example. Finally, about the pitch-to-chord ratio should be in the range of 0.8 to 1.2 in order to maintain an acceptable level of diffusion.

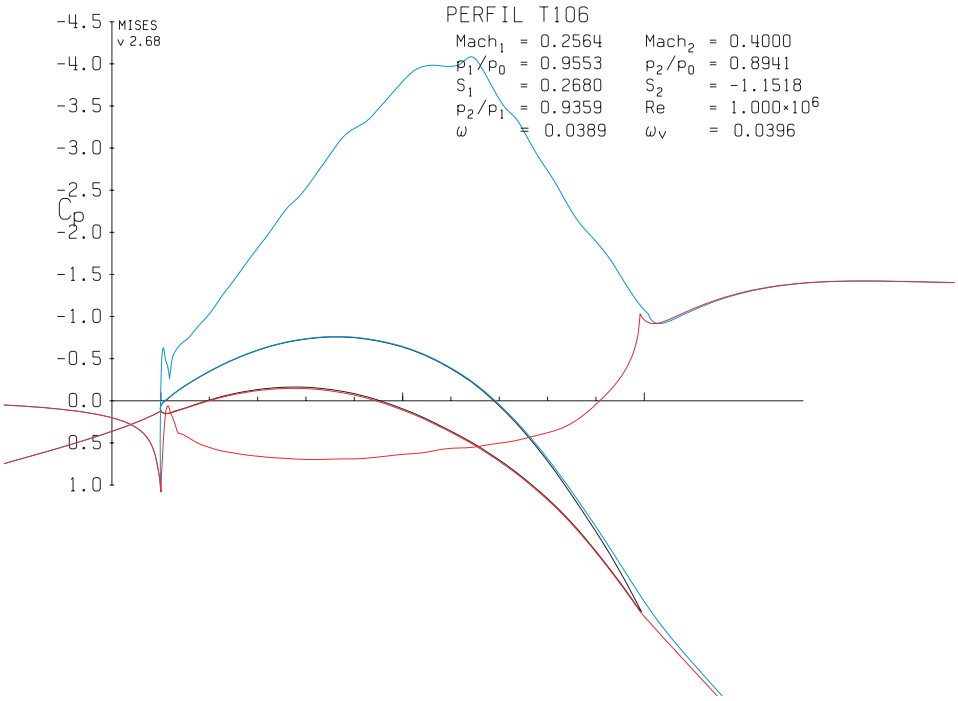

Figure 5.9: Pressure coefficient C_p. In blue - suction surface C_p evolution; In red - pressure surface C_p

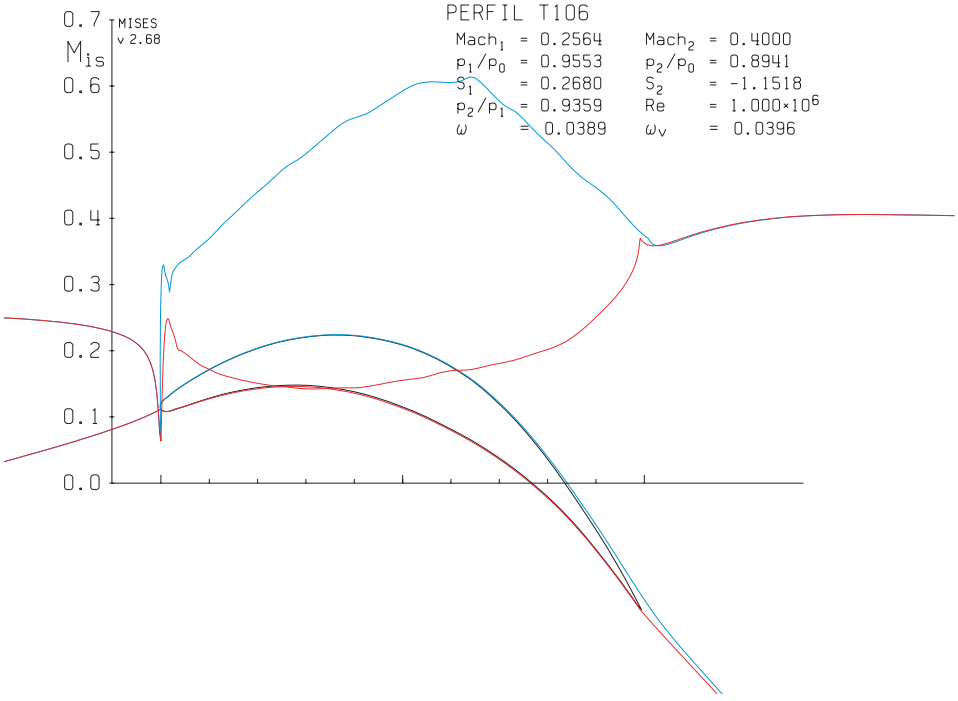

Figure 5.10: Isentropic Mach Number M^{isen}. In blue - suction surface Mach Number evolution; In red - pressure surface Mach Number

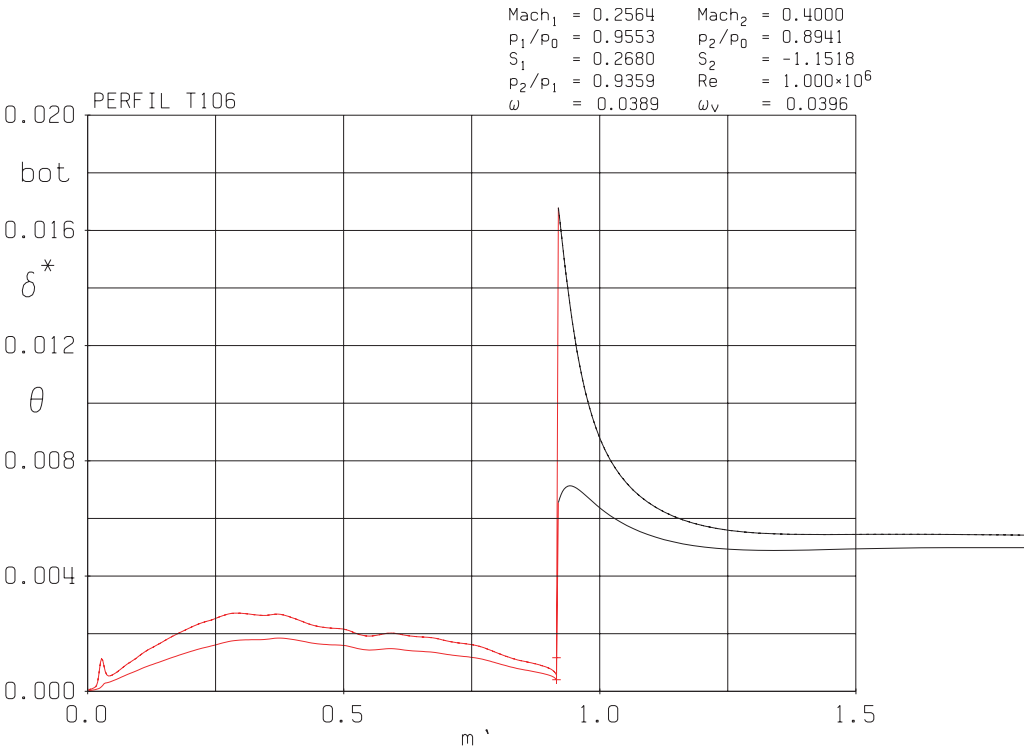

Figure 5.11: Boundary layer evolution (δ^* and θ) of the pressure side. In red - δ^* and θ evolutions along the blade; In black - δ^* and θ evolutions after the TE

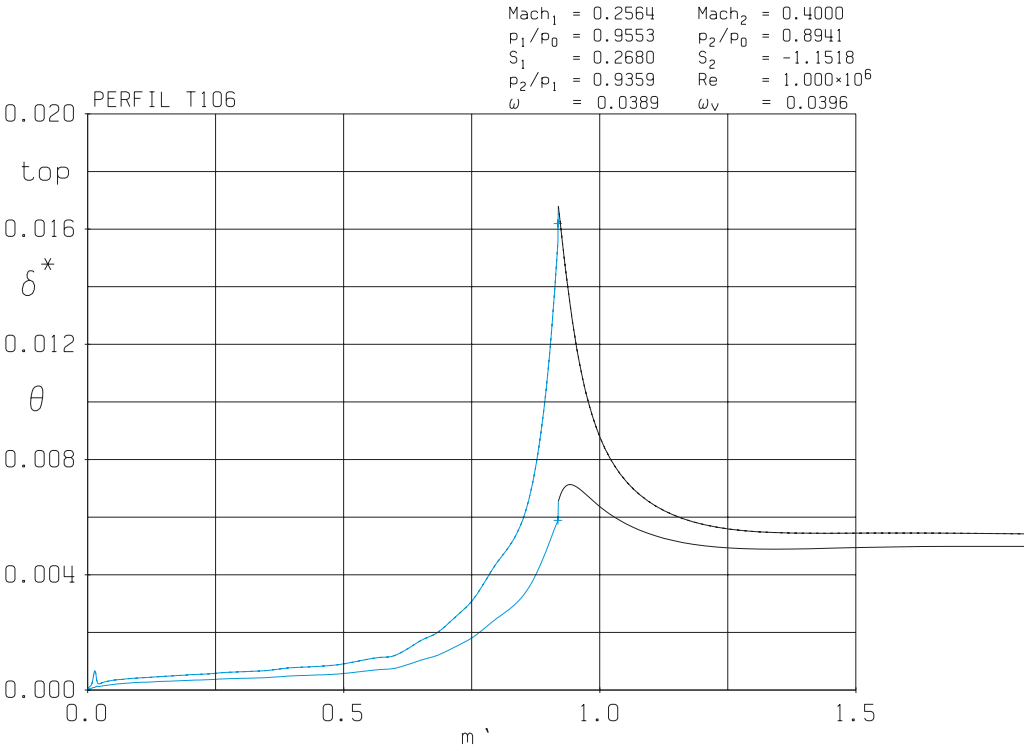

Figure 5.12: Boundary layer evolution (δ^* and θ) of the suction side. In blue - δ^* and θ evolutions along the blade; In black - δ^* and θ evolutions after the TE

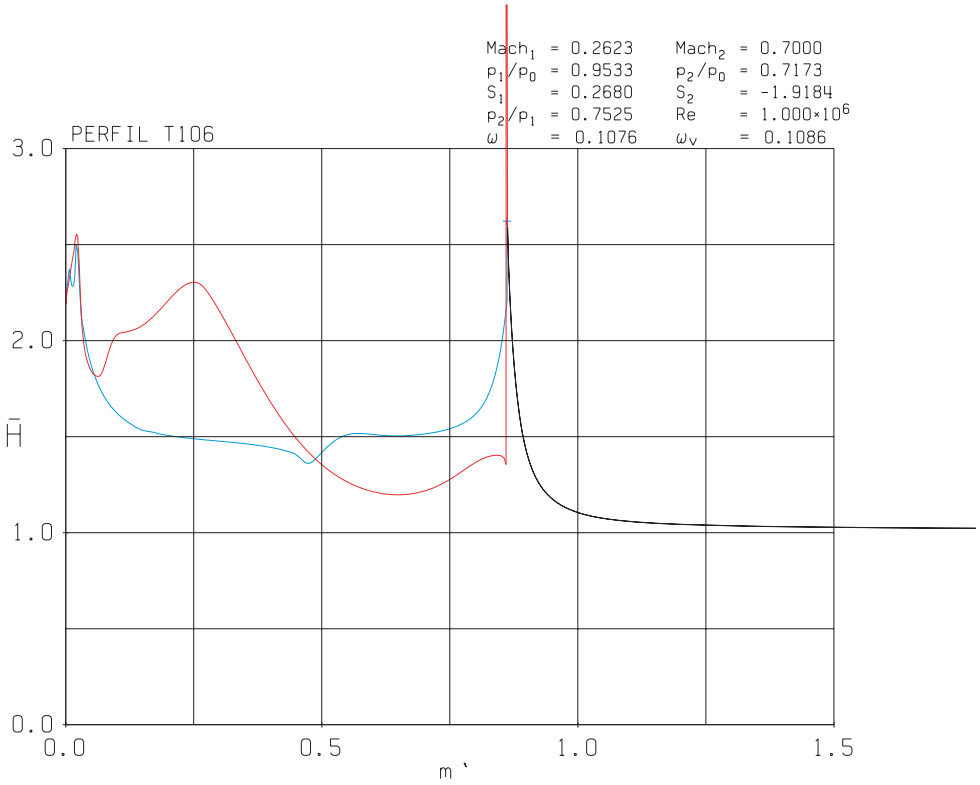

Figure 5.13: Shape factor evolution. In blue - suction surface $\bar{H}$ behaviour; in red - pressure surface $\bar{H}$ In black - $\bar{H}$ evolution after the TE

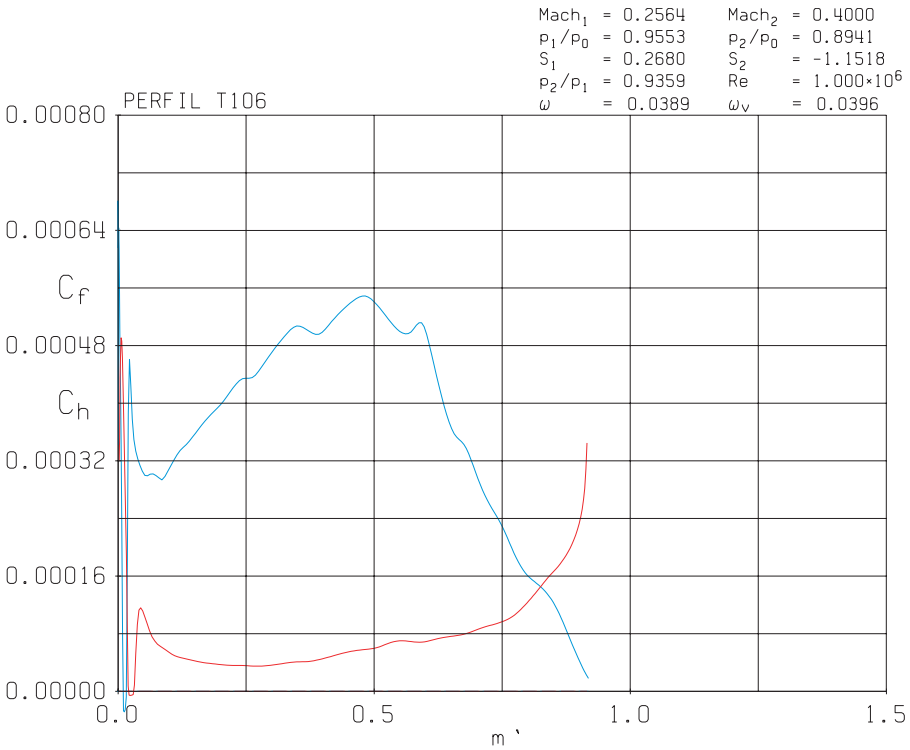

Figure 5.14: Friction coefficients evolution. In blue - suction surface C_f behaviour; in red - pressure surface C_f

α_1	M_1	Re_1	p_1/p_{o1}	Velocity Ratio
15°	0.25621	1,000,000	0.95537 kPa	1.54688
α_2	M_2	p_2/p_{o1}	$\bar{\omega}$	ζ
−49.071°	0.40	0.89398 kPa	0.04098	0.01725

Table 5.2: Flow parameters results

In the Mach Number graph (Figure 5.10), two lines can be seen. Suction side Mach Number increases firstly and then decreases sharply to reach the TE flow condition. In this area of the blade flow starts to separate and a wake is formed. Pressure side Mach Number has an opposite behaviour: firstly it starts to decrease and then it increases because of Kutta condition at TE. The maximum M obtained in the suction surface is $M \approx 0.63$ and the minimum obtained in the pressure side is $M \approx 0.15$. C_p profile (Figure 5.9) has the opposite behaviour as the M since $C_p \propto 1/c^2$. Negatives values are obtained because, remember, the pressure is decreasing through the blade since the energy is extracted from the flow.

Boundary layer is described with four parameters: displacement thickness (δ^*), momentum thickness (θ), boundary layer's shape factor (H) and the skin friction (C_f). The first parameter measures the amount of inviscid flow displaced by the viscid boundary layer. With the second variable one can get the amount of momentum lost due to the viscous boundary layer. As previously said, shape factor is the ratio between these two previous parameters. With respect to m', both displacement and momentum thickness increase. Close to the wall, in the turbulent boundary layer, the momentum thickness and skin friction increase as a result of a higher fluid velocity. During the transition, θ is almost constant but δ^* decrease and as the streamwise increases, both parameters behave evenly (Ref [7]). Shape factor ($\bar{H}$) parameter then can be used to analyse the transition of a laminar to turbulent flow. According to page 454 from Ref [2], when transitioning to turbulent flow, $\bar{H}$ decreases.

In the next two graphs (Figures 5.11 and 5.12), boundary layer evolution for pressure and suction sides are plotted. Before reaching the maximum flow velocity, flow separation is not so intense as after this point ($m' \approx 0.67$). After this point, the boundary layer becomes thicker and when the flow reaches the TE, a peak can be observed. Comparing top and bottom graphs it is seen that the boundary layer is thicker in the suction side in the area close to the TE. Another interesting fact is that the fluid is not really attached to the blade wall.

Boundary layer's shape factor behaves as expected. It takes larger values in the area where the flow is laminar and then there is seen a sudden decrease where the flow starts to separate and lastly it is nearly constant.

In Figure 5.14, skin friction coefficient increase with wall velocity, as said before. That may be one of the reasons that explain the fact that C_f is higher for the suction surface than for the pressure one. Near to the separation point, skin friction is higher and the pressure surface is more affected by the skin friction

where the flow is turbulent. This last fact may be caused by the increment of the flow velocity.

Finally, in Table 5.2, certain flow results are tabulated. It is seen that the turning angle is $\epsilon_S = -64.071°$[2], which is an acceptable results. Normally, a designer does want a turning that exceed 90°. The pressure ratio takes a value of $p_2/p_1 = 0.93574$. It is also seen that mixed-out loss coefficients are small. When designing a turbine blade, $\bar{\omega}$ is of importance since $\zeta < \bar{\omega}$.

Compressor

As done with the turbine, in Figure 5.15 there is an example of a compressor blade. The chosen design parameters are $\chi_1 \approx 48°$, $\chi_2 \approx 8.8°$ and $\xi \approx 20.3°$. In a compressor, a raise of pressure is desired and thus the kinetic energy of the flow must decrease. This is obtained by turning the flow toward its axis (Figure 2.2). The amount of turning in a compressor station is not very large because of the stability of the blade may be compromised (large deflection leads to stall effects and rapid diffusion). In the next table (Table 5.3) it is written down the input flow parameters of a stator blade:

α_1	Re_1	M_1	s/l
45.00°	250,000	0.3	1.00

Table 5.3: Flow parameters of a compressor blade

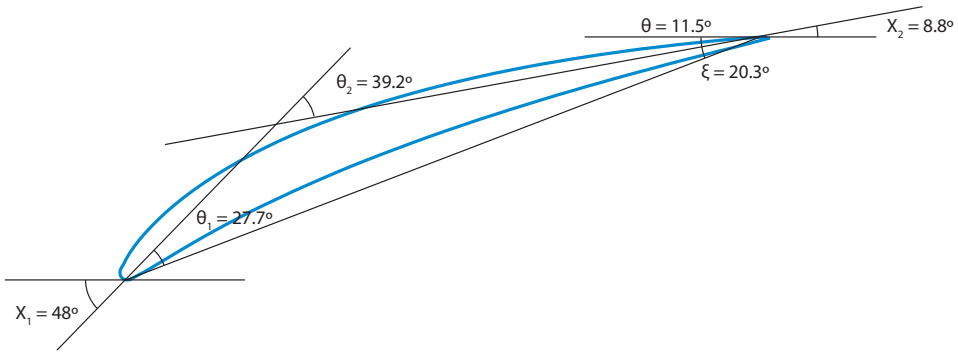

Figure 5.15: Blade shape

[2]According to the sign criteria defined in previous figures, counter-clockwise angles are positive and clockwise, negatives

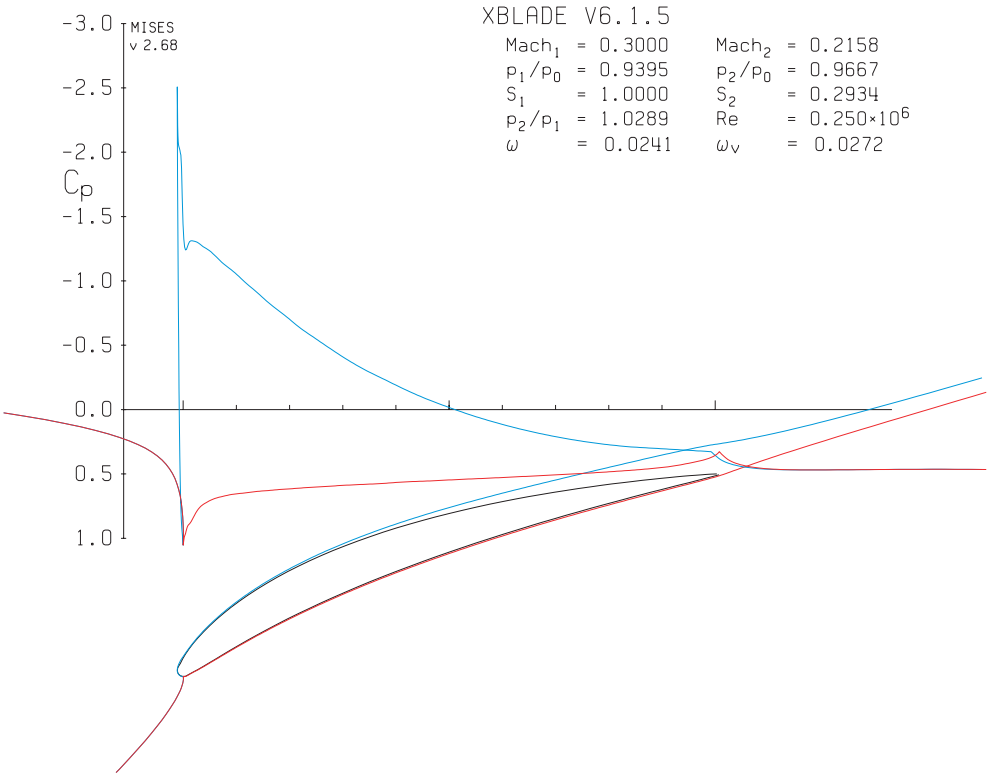

Figure 5.16: Pressure coefficient C_p. In blue - suction surface C_p evolution; In red - pressure surface C_p

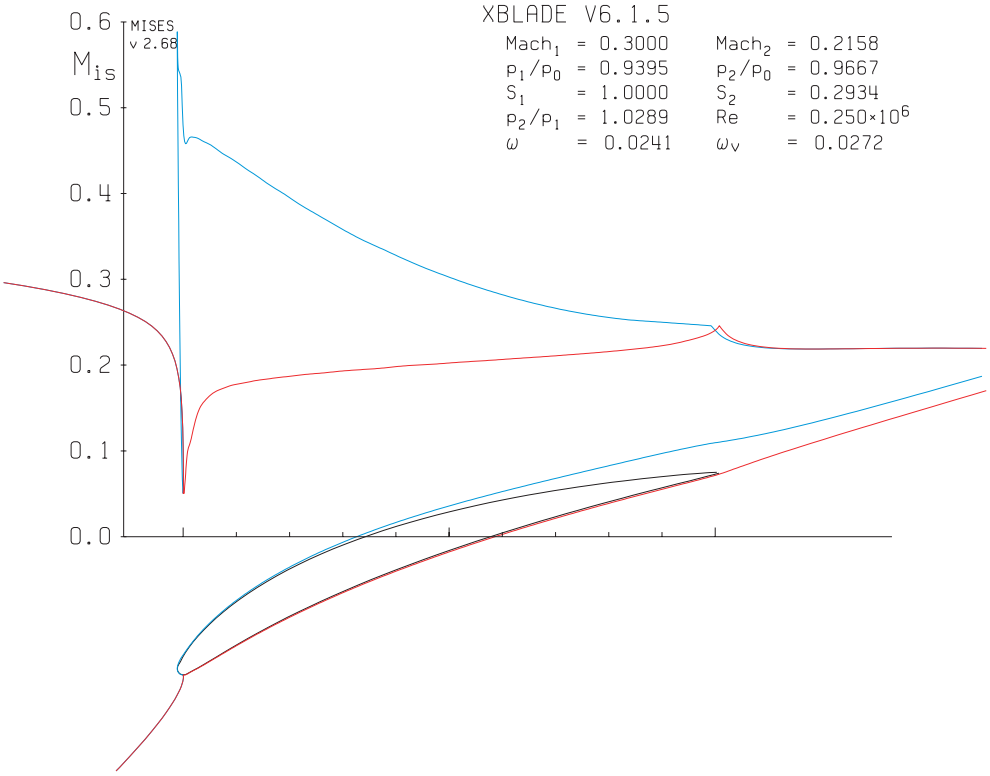

Figure 5.17: Isentropic Mach Number M^{isen}. In blue - suction surface Mach Number evolution; In red - pressure surface Mach Number

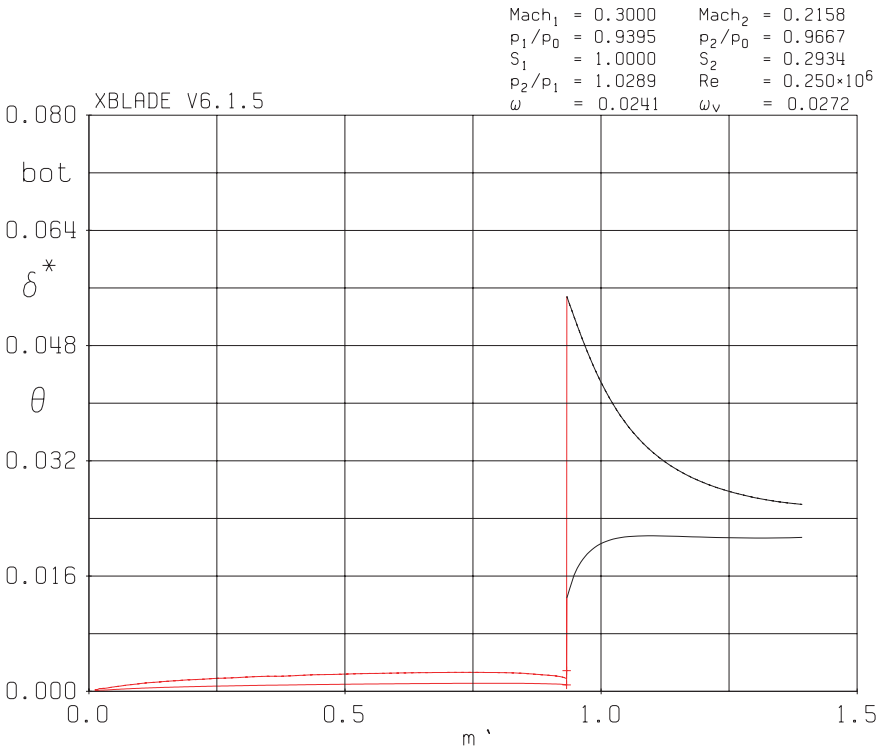

Figure 5.18: Boundary layer evolution (δ^* and θ) of the pressure side. In red - δ^* and θ evolutions along the blade; In black - δ^* and θ evolutions after the TE

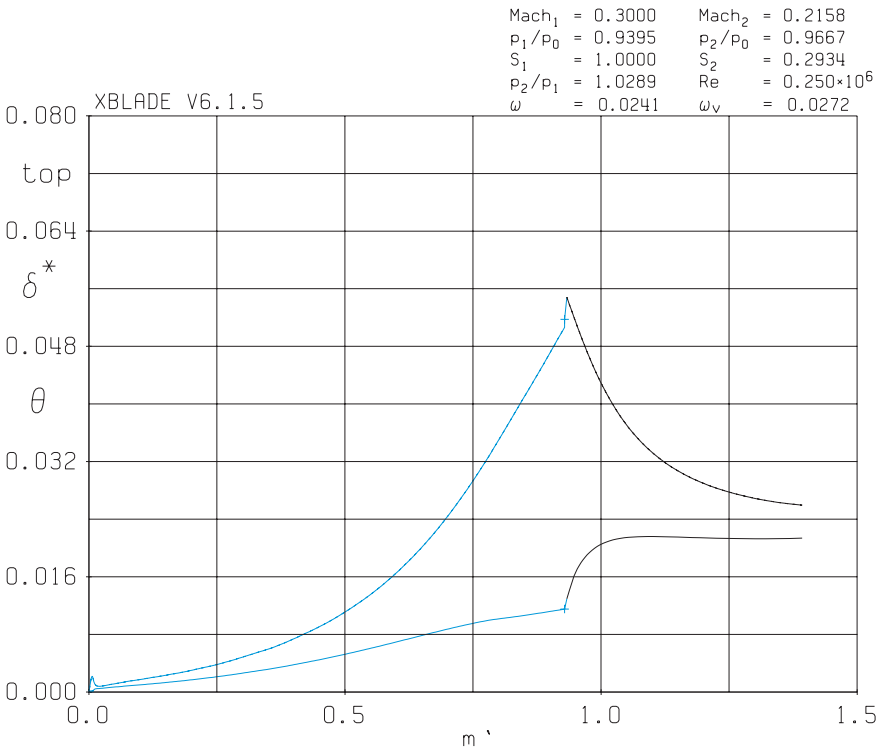

Figure 5.19: Boundary layer evolution (δ^* and θ) of the suction side. In blue - δ^* and θ evolutions along the blade; In black - δ^* and θ evolutions after the TE

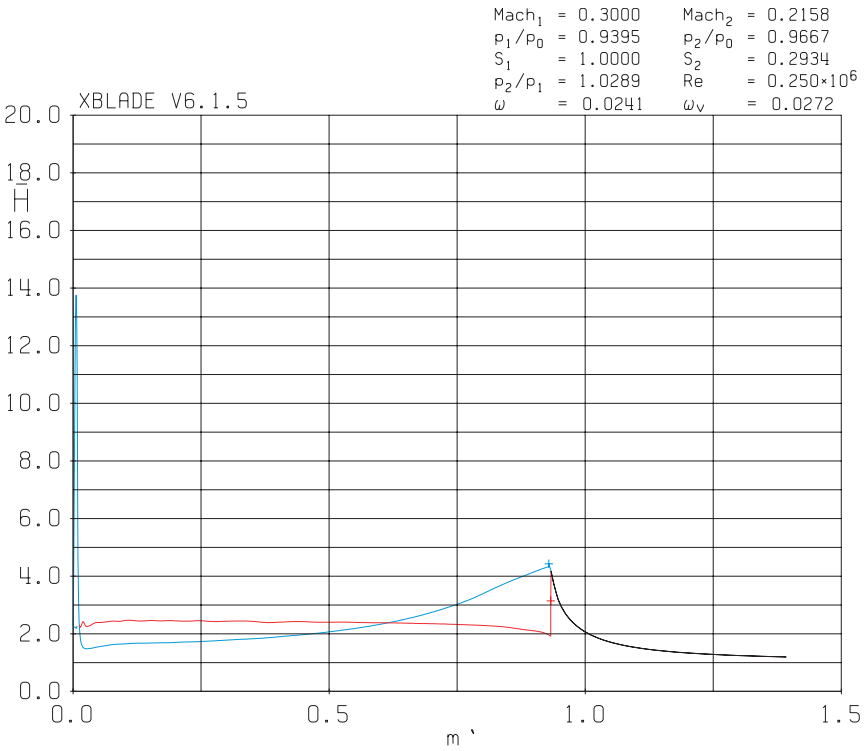

Figure 5.20: Shape factor evolution. In blue - suction surface $\bar{H}$ behaviour; in red - pressure surface $\bar{H}$ In black - $\bar{H}$ evolution after the TE

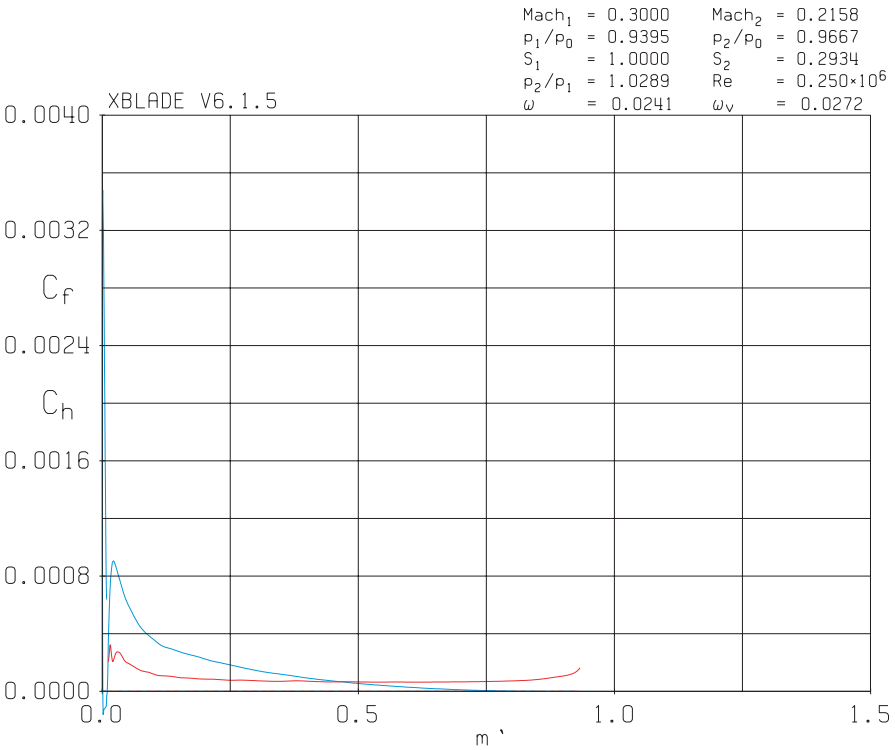

Figure 5.21: Friction coefficients evolution. In blue - suction surface C_f behaviour; in red - pressure surface C_f

α_1	M_1	Re_1	p_1/p_{o1}	Velocity Ratio
45.00°	0.30	250,000	0.93947 kPa	0.72235
α_2	M_2	p_2/p_{o1}	$\bar{\omega}$	ζ
16.35°	0.21578	0.96666 kPa	0.02415	0.04385

Table 5.4: Flow parameters results

As said before, in order to obtain larger pressure (or larger C_p - Figure 5.16), the flow velocity along the blade (or the Mach Number - Figure 5.17) must decrease. Then, the ratio velocity (Table 5.4) is lower than unity and pressure ratio is greater than unity. Respectively, they are equal to $c_2/c_1 = 0.722$ and $p_2/p_1 = 1.029$. It is observed also that the M and pressure coefficient is almost constant in the pressure side of the blade.

About the boundary layer it can be said that in both surfaces the flow is not attached to the wall. Both parameters are nearly constant as m' increases and there is flow separation (as expected) in the TE (Figure 5.19). On the pressure side (Figure 5.18), the flow is close to the wall and therefore there is no separation. By inspecting the shape factor, it is seen that the flow is laminar; there is not turbulent regime. Since the boundary layer thickness is practically constant for the pressure side, C_f is small and constant.

As a last comment, the mixed-out loss coefficients ($\bar{\omega}$ and ζ) are not high; it is seen that $\zeta > \bar{\omega}$, therefore the designer should pay attention to the evolution of this coefficient when designing a compressor blade.

5.2.2 Manual design

Turbine

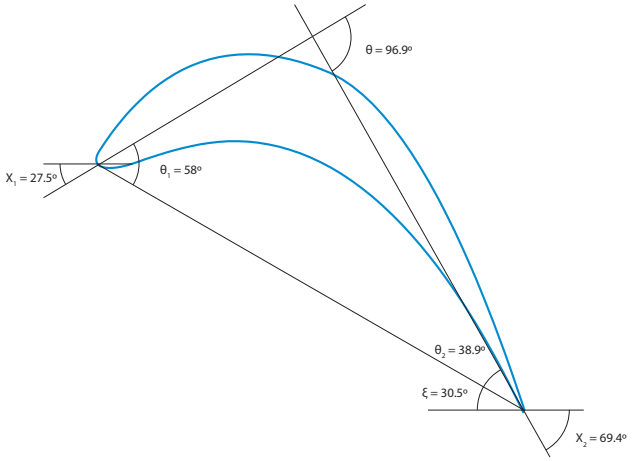

Figure 5.22: Blade shape of a turbine section using the 'Manual design' option

Main design parameters are sketched in the previous figure. For this case, $\chi_1 \approx 27.5°$, $\chi_2 \approx 69.4°$ and $\xi \approx 30.5°$ and this results in a camber angle $\theta \approx 96.9°$. In the analysis, the Mach Number is incremented up to $M_2 = 0.7$ (Table 5.5):

α_1	Re_1	M_2	s/l
15.00°	1,000,000	0.7	0.99

Table 5.5: Flow parameters of a turbine blade

The remaining geometric parameters are presented in the next table:

a	b	χ_1	$\phi_{LE,SS}$	$\phi_{LE,PS}$
0.116	0.039	27.48°	30.23°	68.70°
R	χ_2	$\phi_{TE,SS}$	$\phi_{TE,PS}$	ξ
$1.489 \cdot 10^{-3}$	69.39°	87.94°	86.57°	30.48°
s/l	o/l	t^*/l	ϕ_o	ϕ_t
0.992	0.500	0.234	22.500°	0.000°

Table 5.6: Geometric parameters of a turbine blade

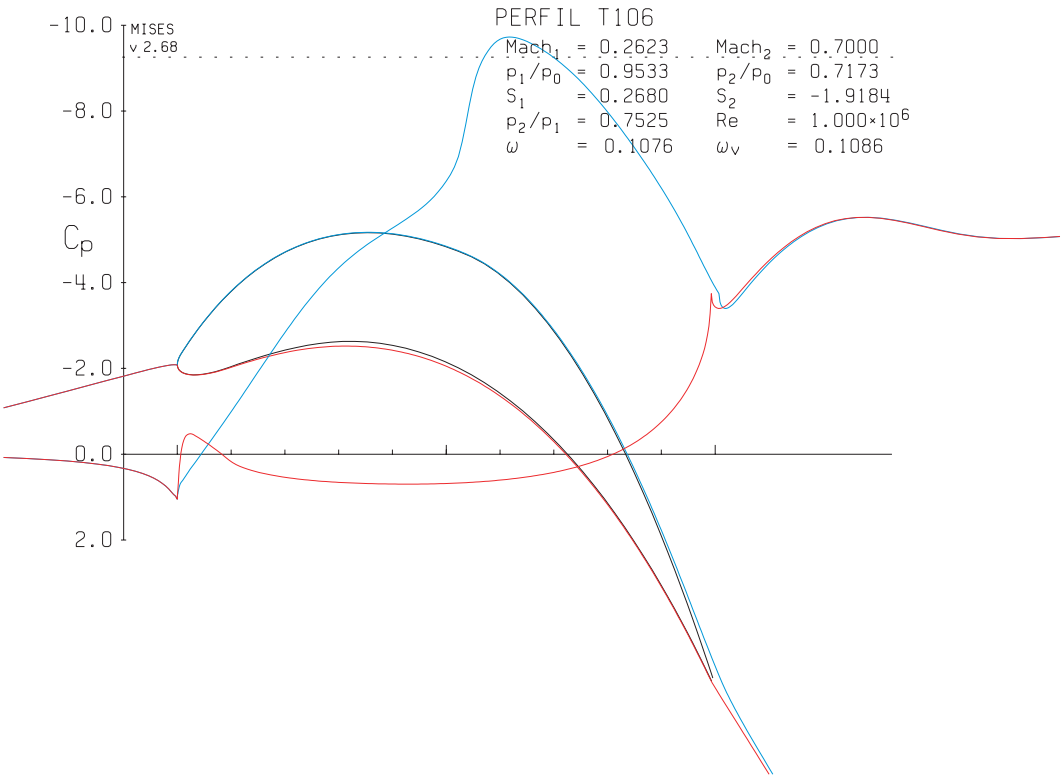

Figure 5.23: Pressure coefficient C_p. In blue - suction surface C_p evolution; In red - pressure surface C_p

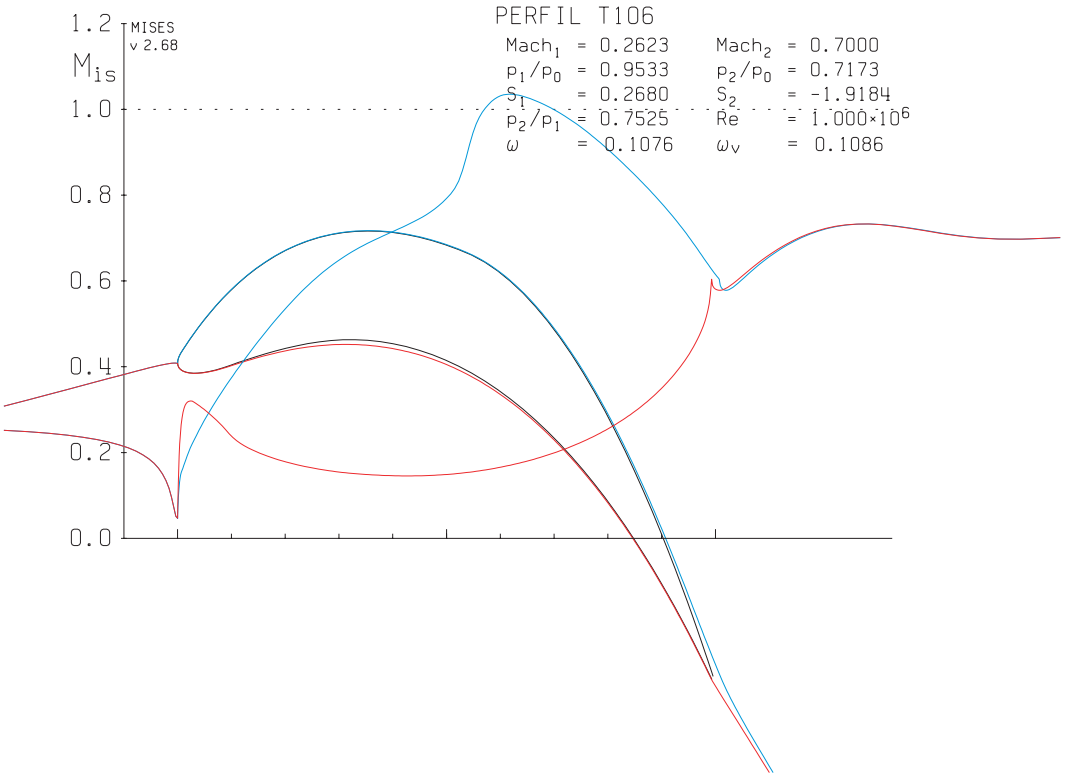

Figure 5.24: Isentropic Mach Number M^{isen}. In blue - suction surface Mach Number evolution; In red - pressure surface Mach Number

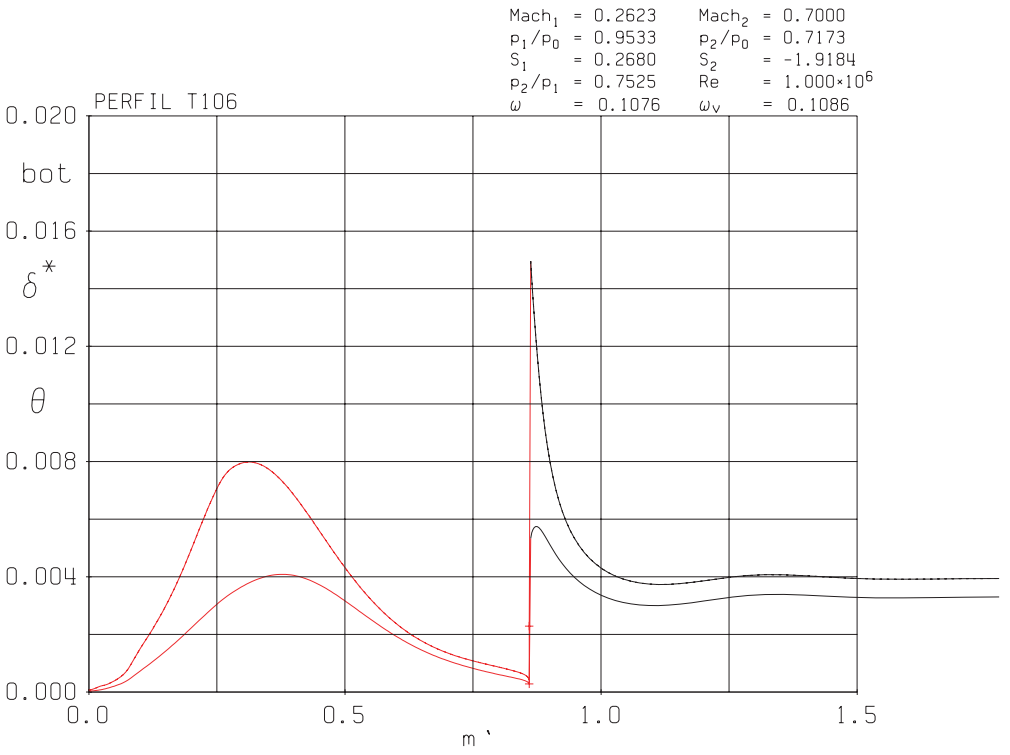

Figure 5.25: Boundary layer evolution (δ^* and θ) of the pressure side. In red - δ^* and θ evolutions along the blade; In black - δ^* and θ evolutions after the TE

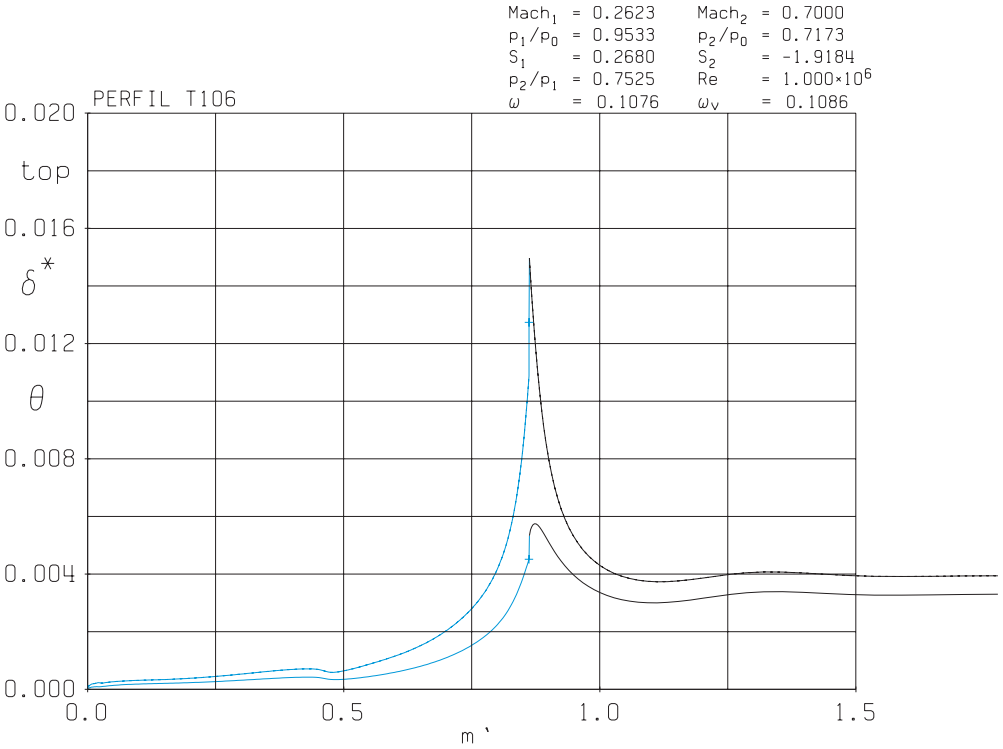

Figure 5.26: Boundary layer evolution (δ^* and θ) of the suction side. In blue - δ^* and θ evolutions along the blade; In black - δ^* and θ evolutions after the TE

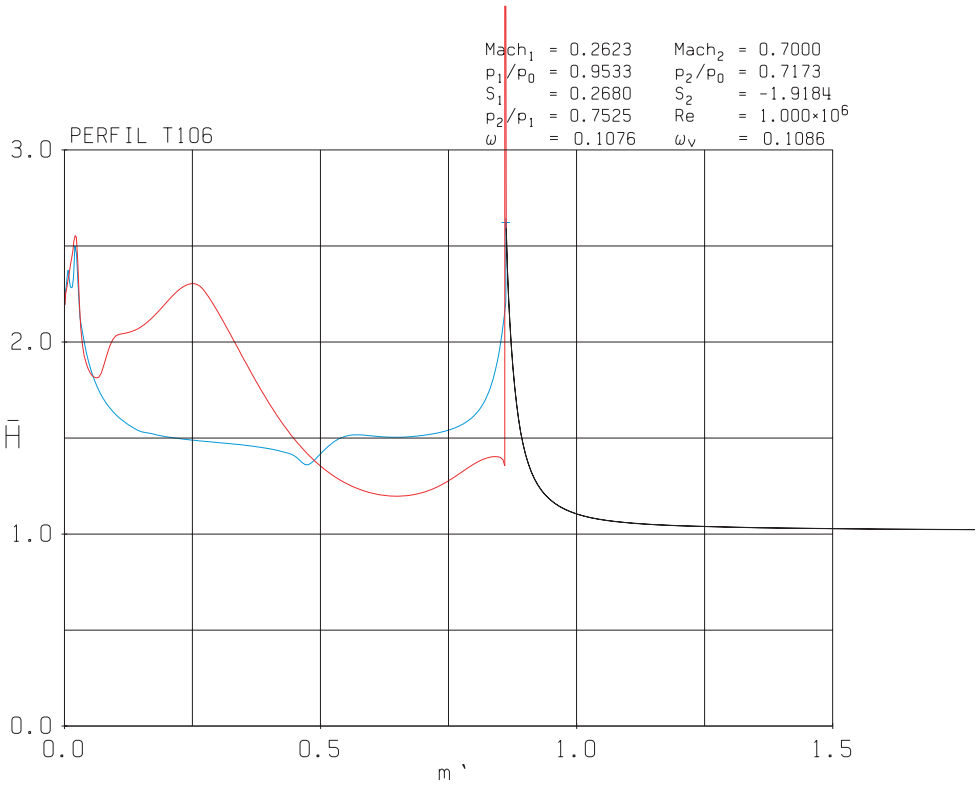

Figure 5.27: Shape factor evolution. In blue - suction surface $\bar{H}$ behaviour; in red - pressure surface $\bar{H}$ In black - $\bar{H}$ evolution after the TE

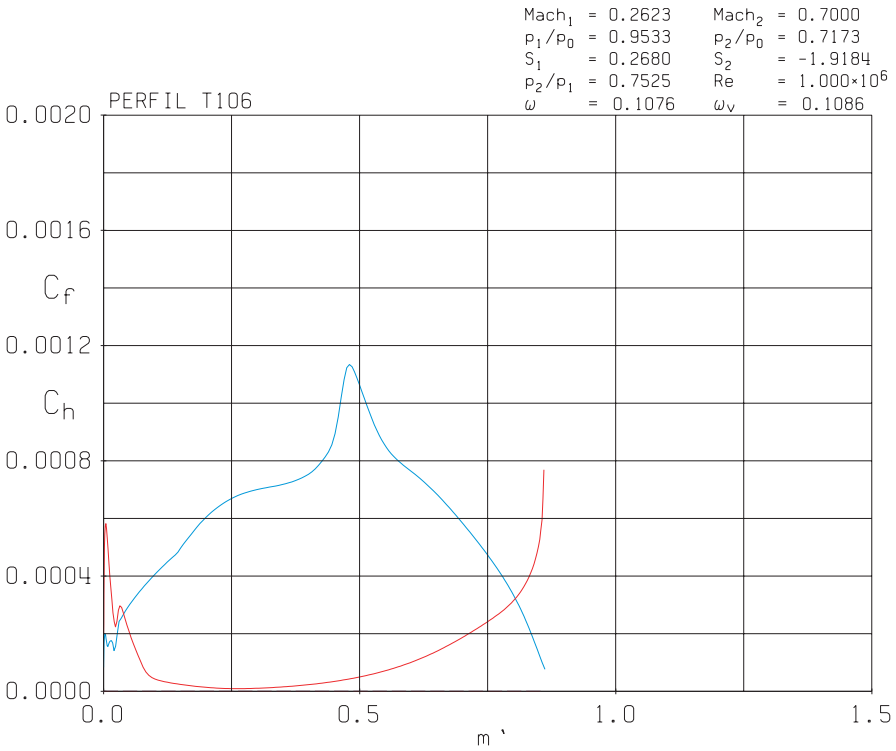

Figure 5.28: Friction coefficients evolution. In blue - suction surface C_f behaviour; in red - pressure surface C_f

α_1	M_1	Re_1	p_1/p_{o1}	Velocity Ratio
15.00°	0.26232	1,000,000	0.95329 kPa	2.56409
α_2	M_2	p_2/p_{o1}	$\bar{\omega}$	ζ
−62.468°	0.70000	0.71730 kPa	0.10763	0.01778

Table 5.7: Flow parameters results

In the previous plots, flow results are shown. It is observed that there is a region along the blade where supersonic condition is achieved (Figure 5.23). And these high velocities make the boundary layer to grow. It can be said that in the top surface the boundary layer is practically turbulent (or at least there is a transition phase from laminar to turbulent regime) according to Figure 5.27. On the contrary, the boundary layer is laminar in the bottom side at the beginning (until reaching $m' \approx 0.45$) and afterwards it becomes turbulent, and this leads to an increment in the skin friction (Figure 5.28). The pressure ratio is equal to $p_2/p_1 = 0.7524$; that means more power is extracted from the fluid and this results from a higher turning angle ($\epsilon_S = -77.47°$). In comparison with the previous turbine blade example, the mixed out loss coefficients are penalized since they are larger than the previous case. Possible sources of loss of efficiency are the higher flow velocities and greater skin friction along the blade.

Compressor

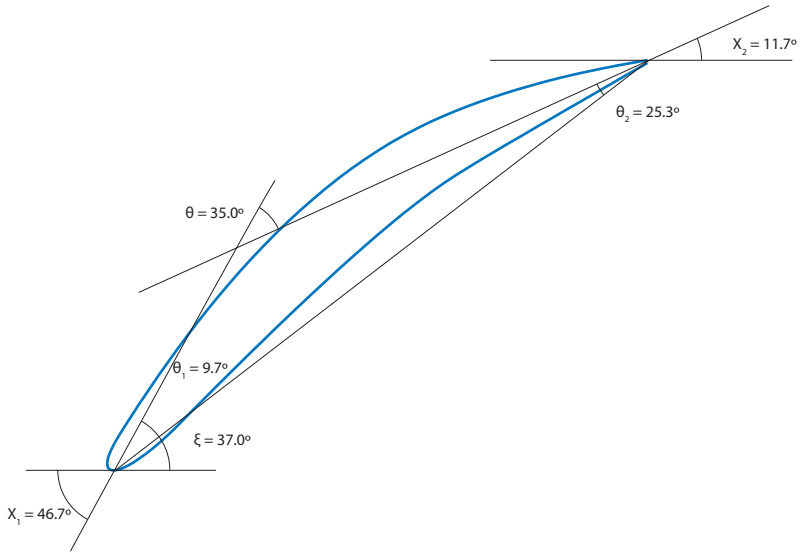

Figure 5.29: Blade shape of a compressor section using the 'Manual design' option

In the case of this compressor blade example, $\chi_1 \approx 46.7°$, $\chi_2 \approx 11.7°$ and $\xi \approx 37°$ and this results in a camber angle $\theta \approx 35.0°$. In this analysis example, the inlet Mach Number is slightly increased up to $M_1 = 0.4$ (Table 5.8):

α_1	Re_1	M_1	s/l
45.00°	250,000	0.4	0.99

Table 5.8: Flow parameters of a compressor blade

The remaining geometric parameters are presented in the next table:

a	b	χ_1	$\phi_{LE,SS}$	$\phi_{LE,PS}$
0.130	0.030	46.72°	49.47°	85.19°
R	χ_2	$\phi_{TE,SS}$	$\phi_{TE,PS}$	ξ
$2.213 \cdot 10^{-3}$	11.68°	87.94°	72.82°	37.02°
s/l	o/l	t^*/l	ϕ_o	ϕ_t
1.028	0.702	0.089	24.68°	27.58°

Table 5.9: Geometric parameters of a compressor blade

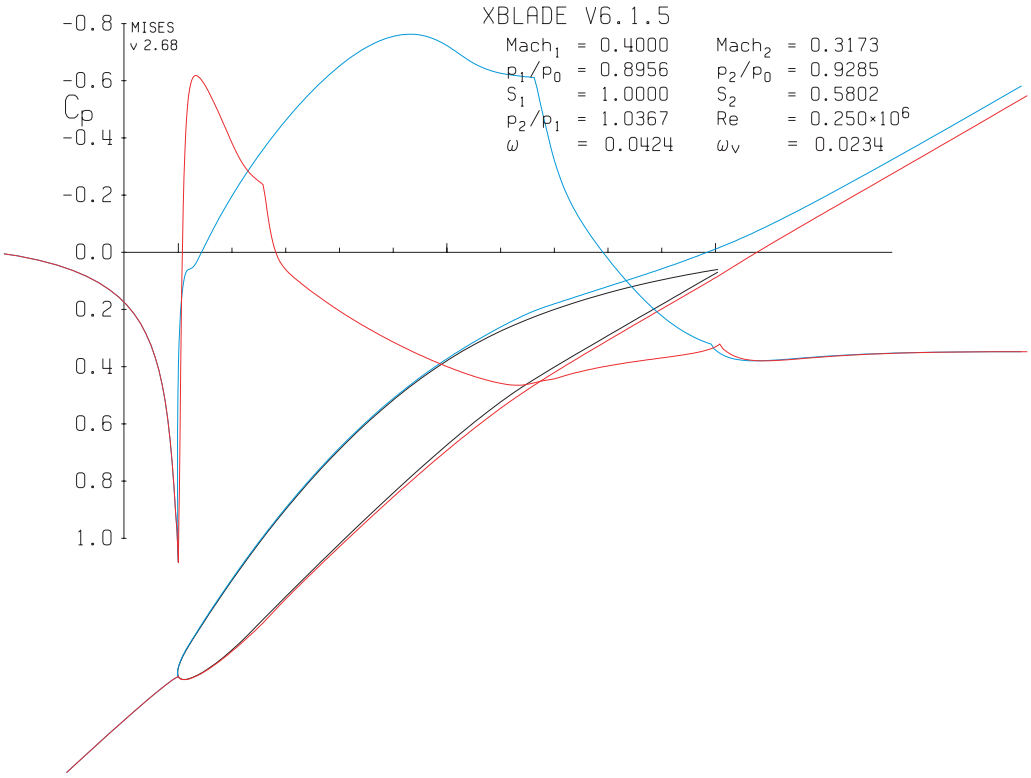

Figure 5.30: Pressure coefficient C_p. In blue - suction surface C_p evolution; In red - pressure surface C_p

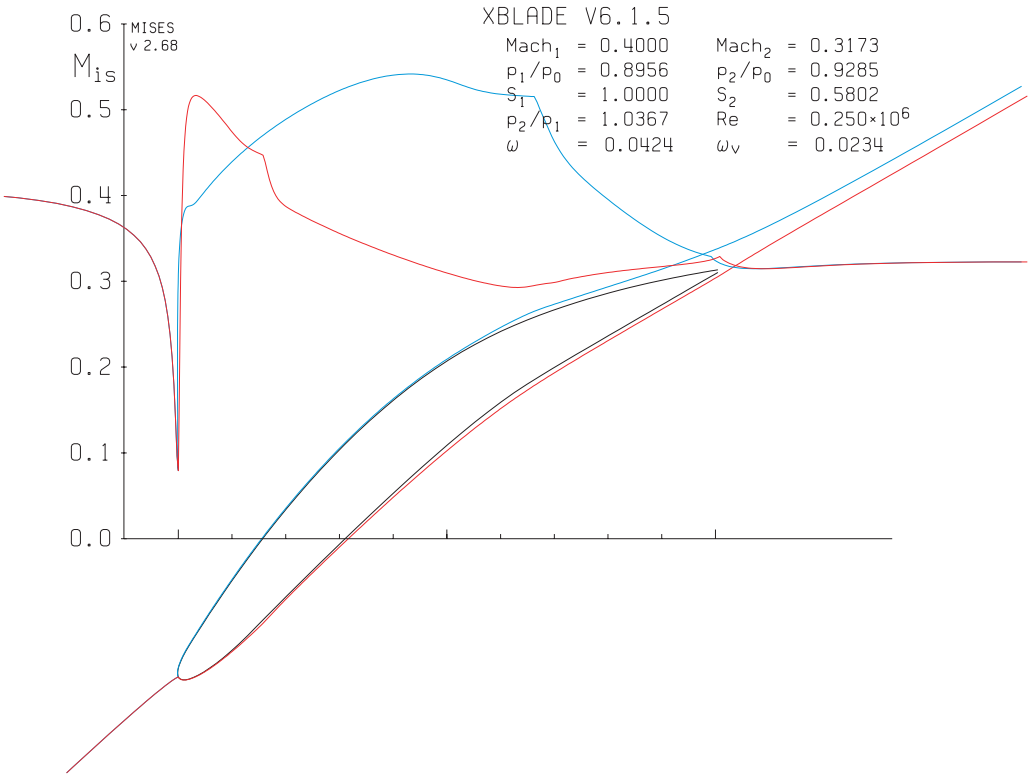

Figure 5.31: Isentropic Mach Number M^{isen}. In blue - suction surface Mach Number evolution; In red - pressure surface Mach Number

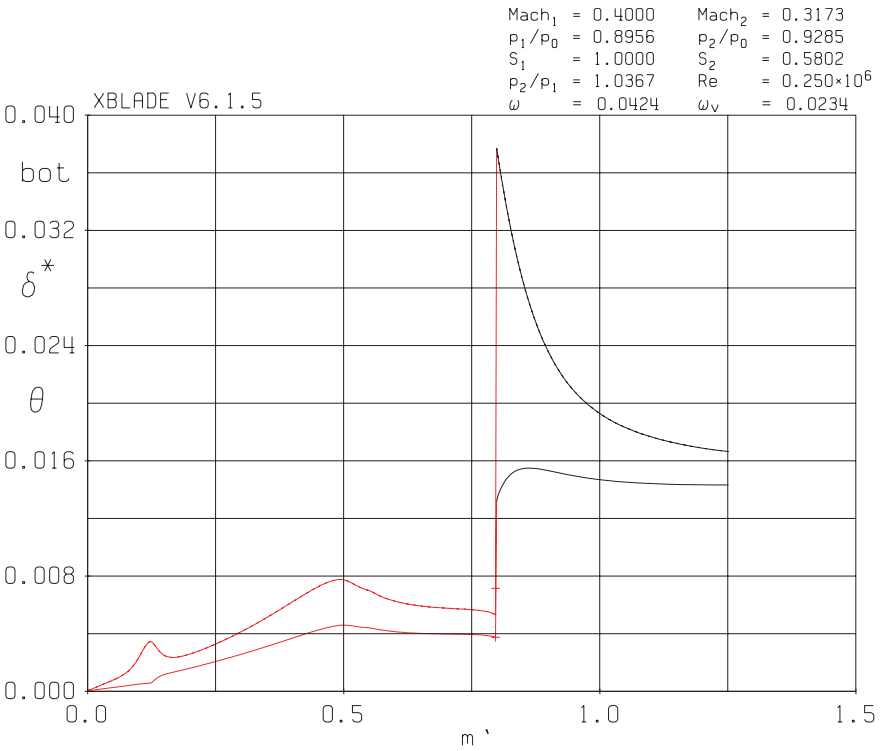

Figure 5.32: Boundary layer evolution (δ^* and θ) of the pressure side. In red - δ^* and θ evolutions along the blade; In black - δ^* and θ evolutions after the TE

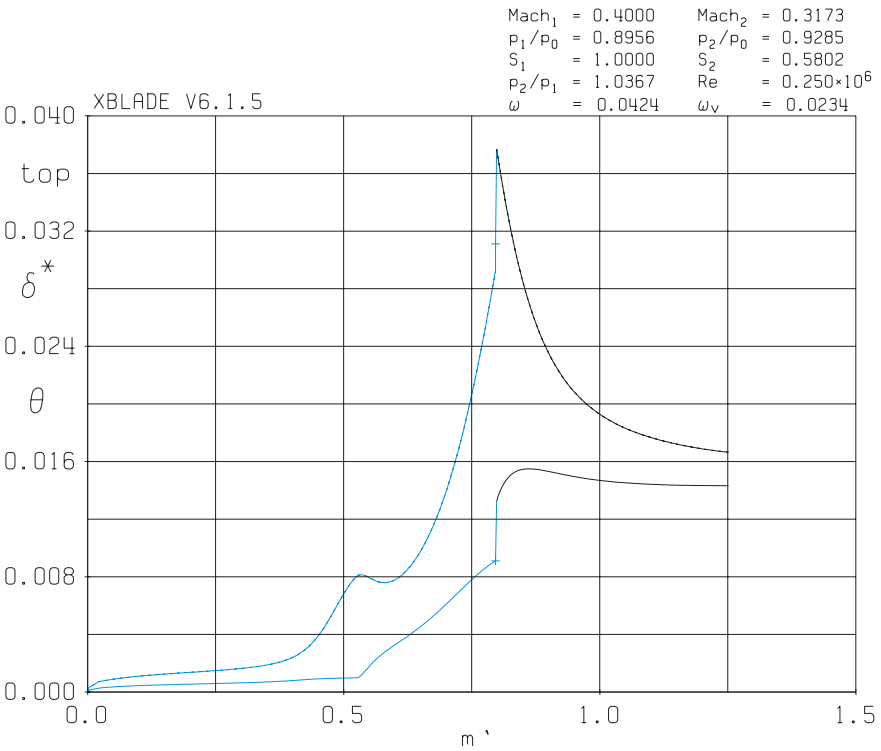

Figure 5.33: Boundary layer evolution (δ^* and θ) of the suction side. In blue - δ^* and θ evolutions along the blade; In black - δ^* and θ evolutions after the TE

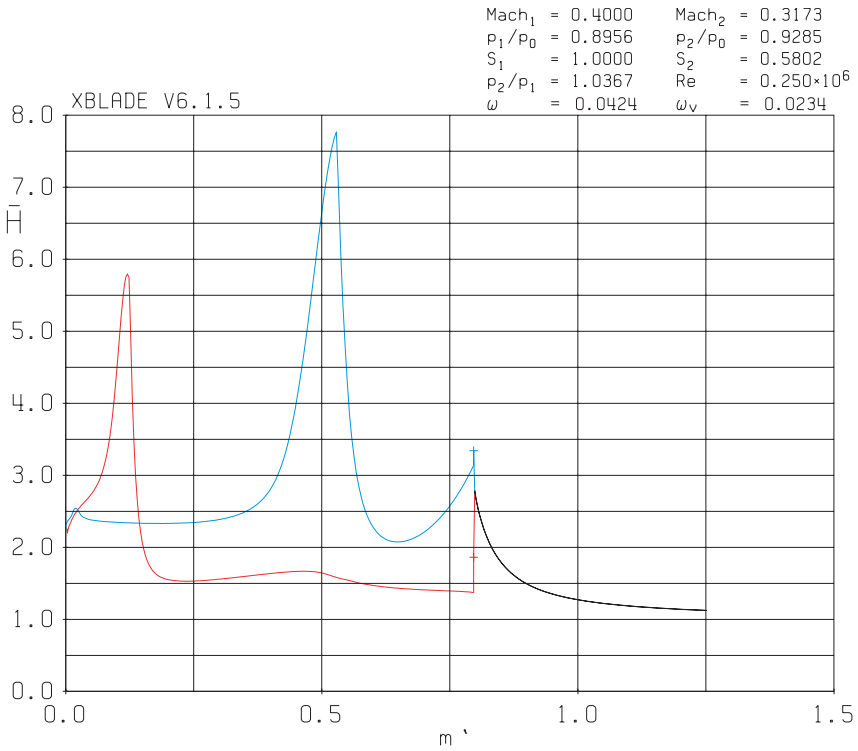

Figure 5.34: Shape factor evolution. In blue - suction surface $\bar{H}$ behaviour; in red - pressure surface $\bar{H}$ In black - $\bar{H}$ evolution after the TE

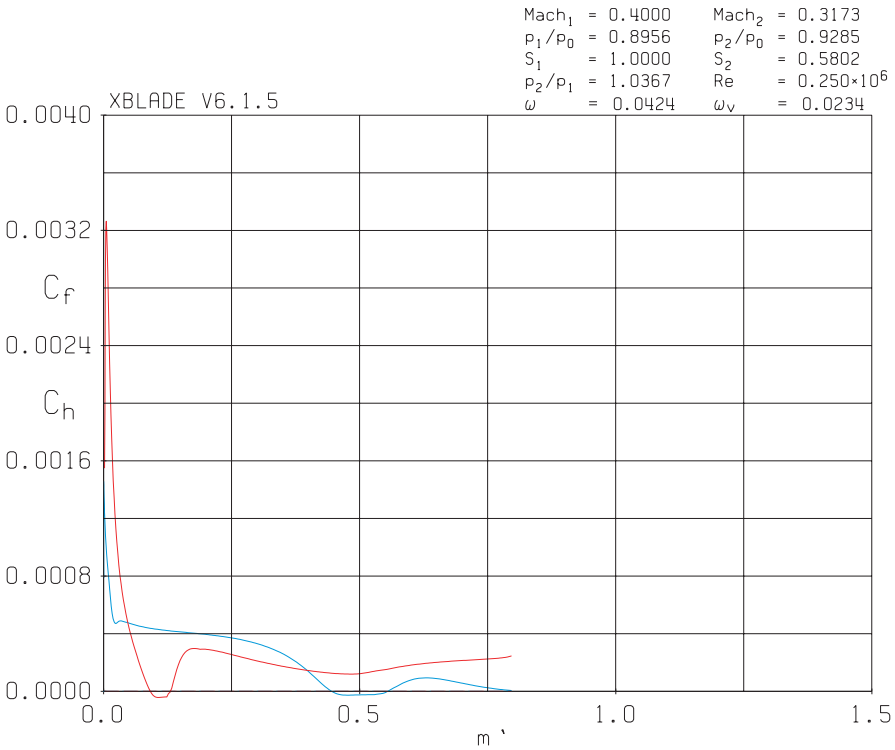

Figure 5.35: Friction coefficients evolution. In blue - suction surface C_f behaviour; in red - pressure surface C_f

α_1	M_1	Re_1	p_1/p_{o1}	Velocity Ratio
45.00°	0.4000	250,000	0.89561 kPa	0.79774
α_2	M_2	p_2/p_{o1}	$\bar{\omega}$	ζ
30.123°	0.31726	0.92849 kPa	0.04243	0.06194

Table 5.10: Flow parameters results

The flow along the suction side of the compressor blade is mainly attached to the wall and it starts to separate at a $m' \approx 0.55$. It is also characterized by being laminar. The flow in the pressure side starts to separate earlier (at $m' \approx 0.17$) but in this case the boundary layer is becoming turbulent. $\bar{\omega}$ and ζ is not very compromised (they increase slightly) in this example in comparison with the previous compressor example.

5.3 Effect of ξ on a turbine blade

In this section, it is analysed the impact of increasing the Stagger angle ξ over the performance of a turbine blade. A NACA 0015 thickness profile is employed and the metal angles are $\chi_1 =$ and $\chi_2 =$. Twelve analyses are performed under the next flow conditions: $\alpha_1 = 15$, $M_2 = 0.40$, Re = 500,000 and $s/l = 1.00$.

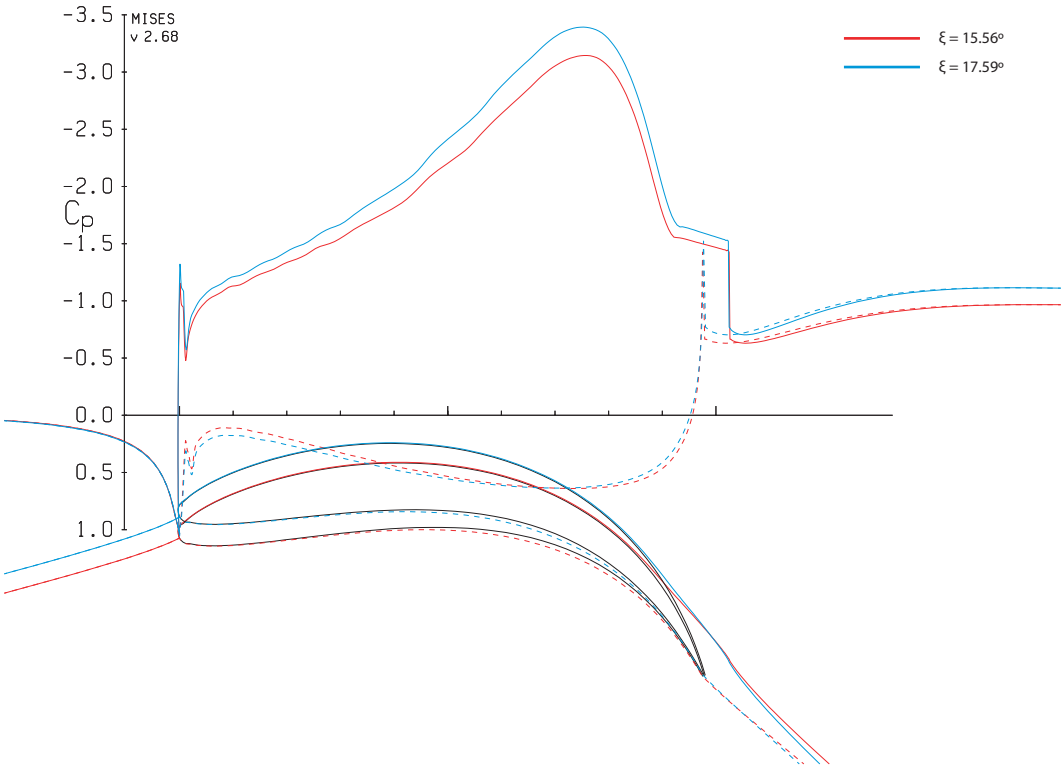

Figure 5.36: C_p evolution at $\xi = 15.56°$ and $\xi = 17.59°$. Dash line represents the pressure surface

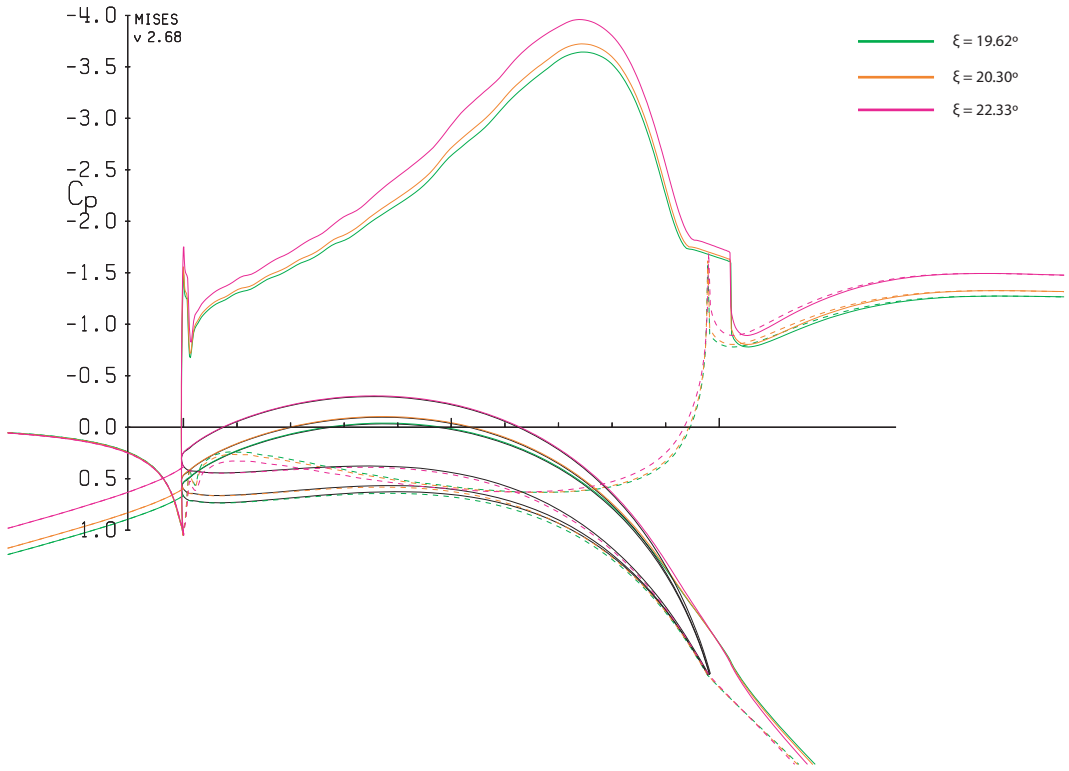

Figure 5.37: C_p evolution at $\xi = 19.62°$, $\xi = 20.30°$ and $\xi = 22.33°$. Dash line represents the pressure surface

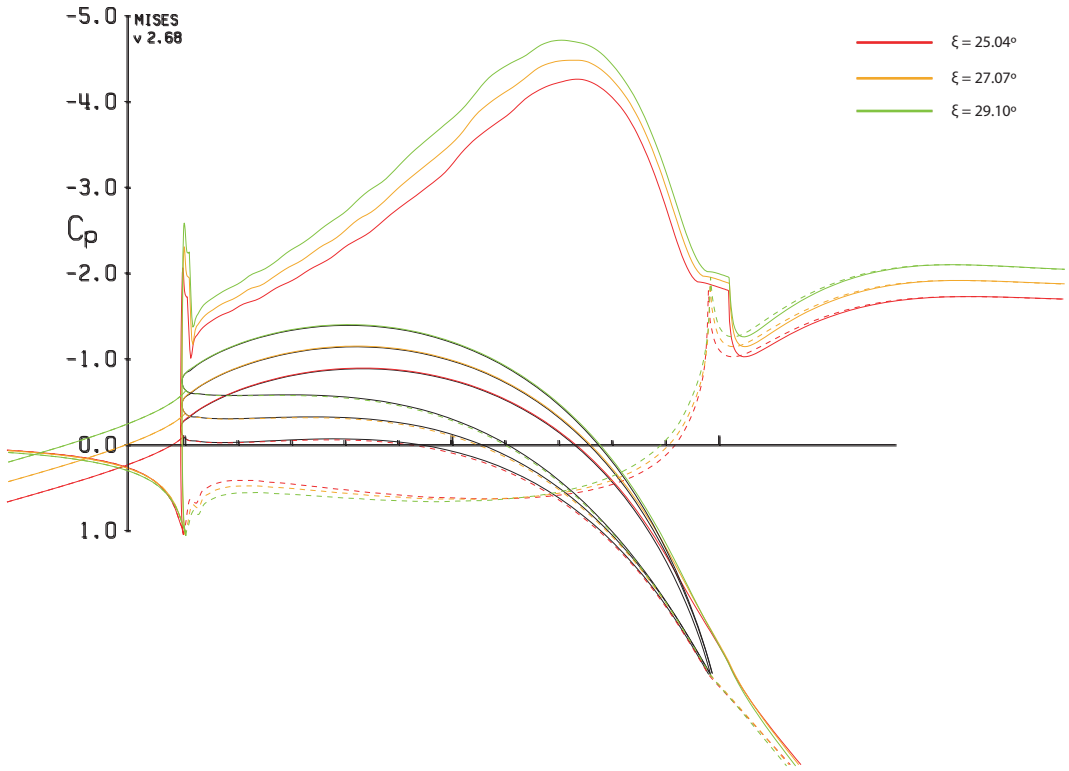

Figure 5.38: C_p evolution at $\xi = 25.04°$, $\xi = 27.07°$ and $\xi = 29.10°$. Dash line represents the pressure surface

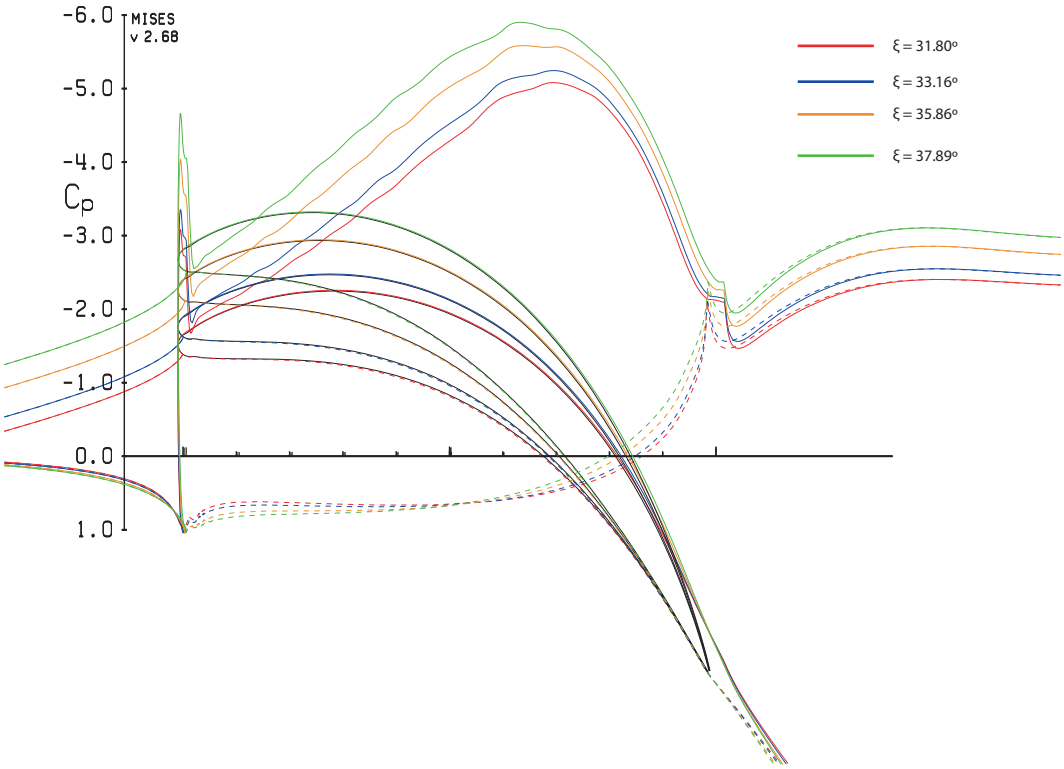

Figure 5.39: C_p evolution at $\xi = 31.80°$, $\xi = 33.16°$, $\xi = 35.86°$ and $\xi = 37.89°$. Dash line represents the pressure surface

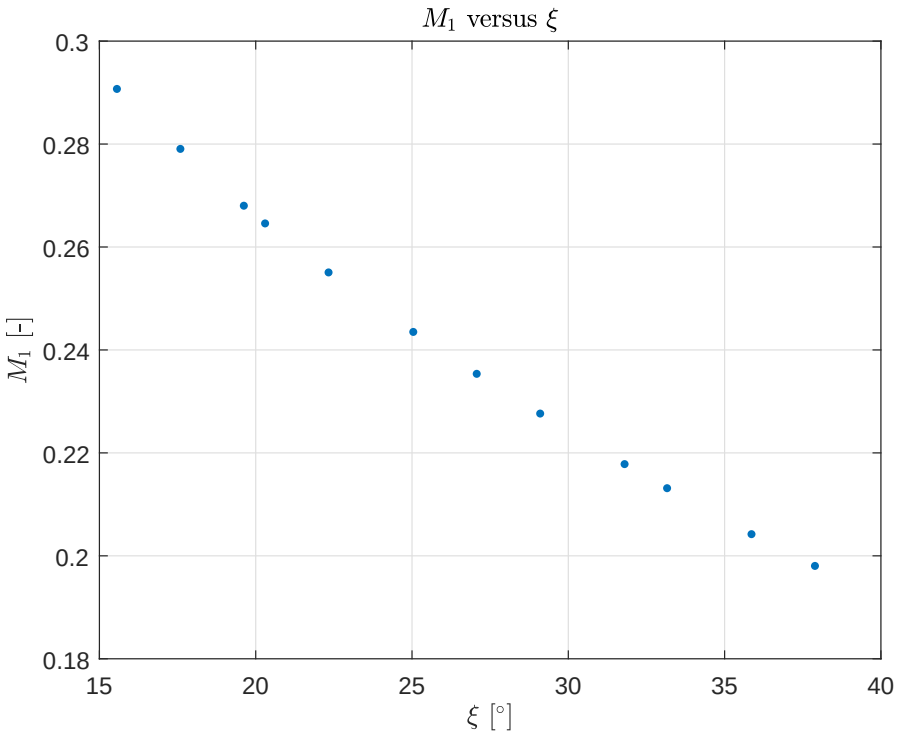

Figure 5.40: Inlet Mach Number as a function of ξ

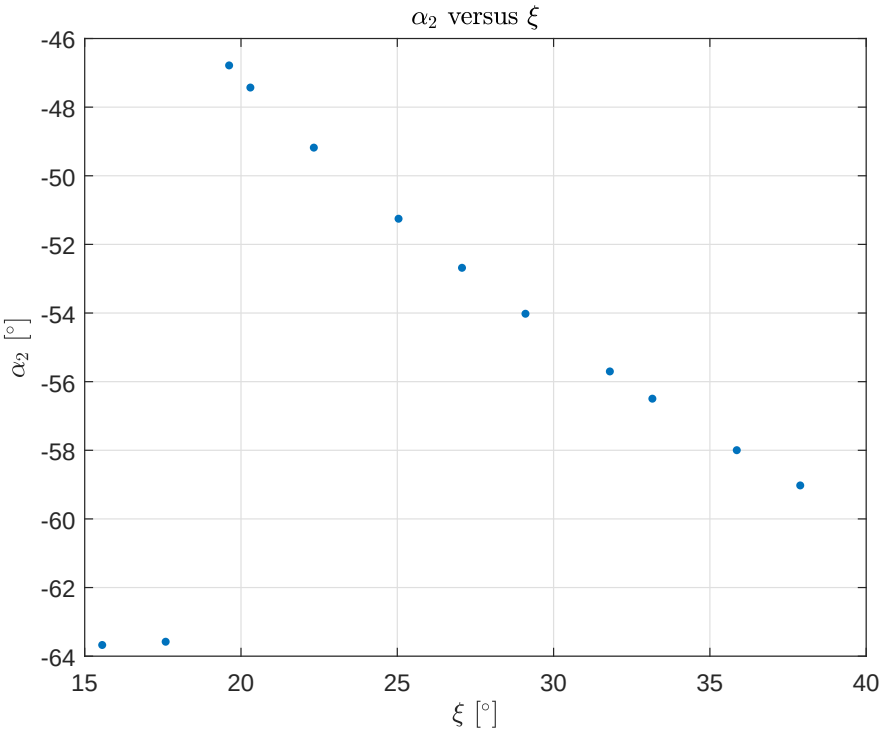

Figure 5.41: Outlet flow angle as a function of ξ

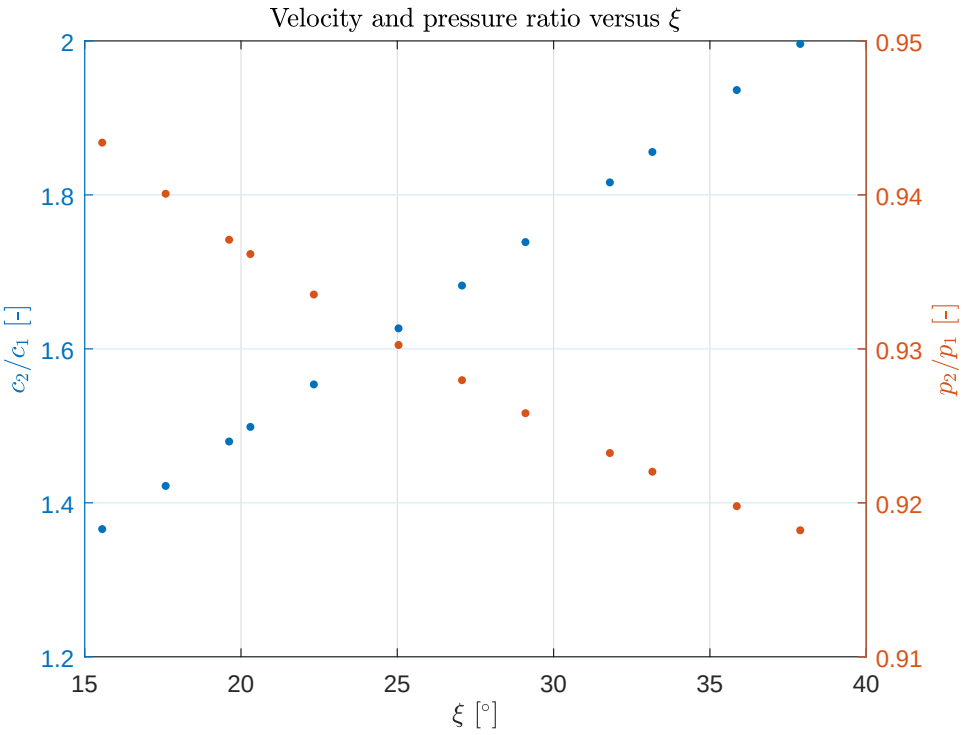

Figure 5.42: Velocity and pressure ratios as a function of ξ

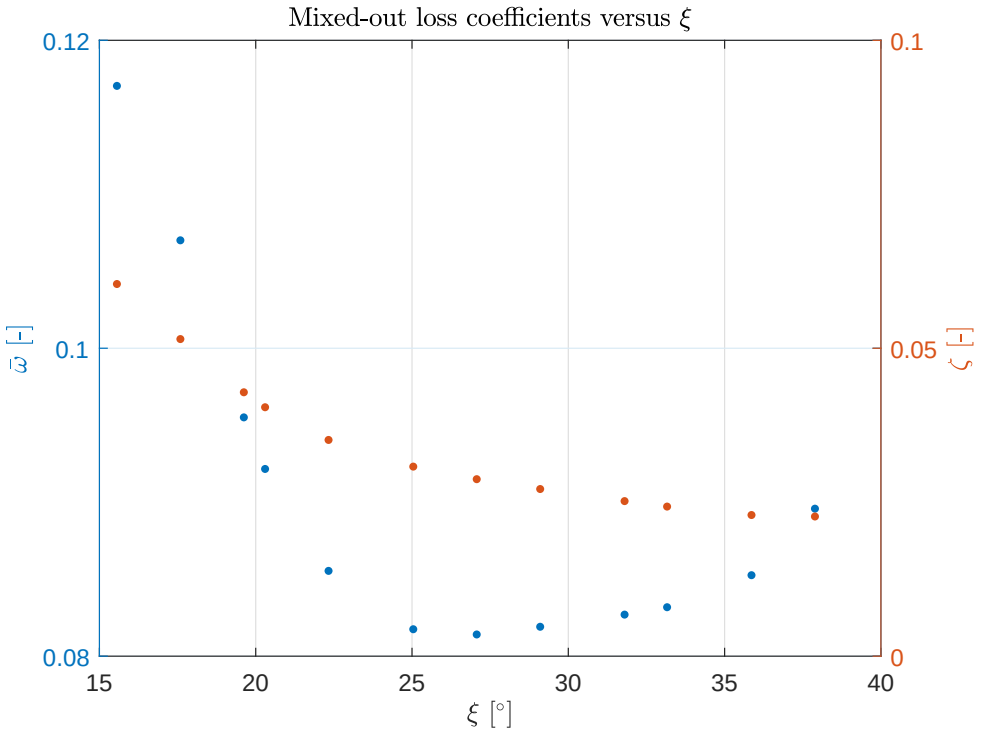

Figure 5.43: Mixed-out loss coefficients as a function of ξ

In the first four graphs, it is plotted the pressure coefficient over the axial chord of the blade. It is seen that as ξ increases, the curve is moved upwards. That means more pressure is extracted through the turbine. It may be seen as a positive consequence. This is also proved in the Figure 5.42. This outlet pressure decrement is because of higher turning angles are obtained as ξ increases ($\epsilon_S = \alpha_2 - \alpha_1$ - Figure 5.41) - note that inlet flow angle is kept constant. The behaviour of these parameters is almost linear with respect to the Stagger angle. In addition, it is possible to say greater ξ improves the performance of a turbine. However, it has not been taken into account the impact of ξ over $\bar{\omega}$ and ζ. Up to $\xi \approx 27°$, $\bar{\omega}$ decrease and after this point, it grows (ζ is decreasing). Therefore, for this flow conditions and this geometry, the designer must have in mind that for certain ranges of ξ loss coefficients grow.

5.4 Effect of ϕ_o on a turbine blade

A turbine blade is designed manually similar with the last blade example. In the next table below, the parameters are shown. About the flow, a inlet angle of 20° has been chosen, an outlet Mach equal to 0.5 and a Reynolds Number of 500,000.

a	b	χ_1	$\phi_{LE,SS}$	$\phi_{LE,PS}$
0.118	0.037	28.17°	32.98°	67.33°
R	χ_2	$\phi_{TE,SS}$	$\phi_{TE,PS}$	ξ
$1.412 \cdot 10^{-3}$	70.76°	85.19°	87.94°	30.48°
s/l	o/l	t^*/l	ϕ_o	ϕ_t
1.04	0.500	0.274	-	0.000°

Table 5.11: Geometric parameters of the analysed turbine blade

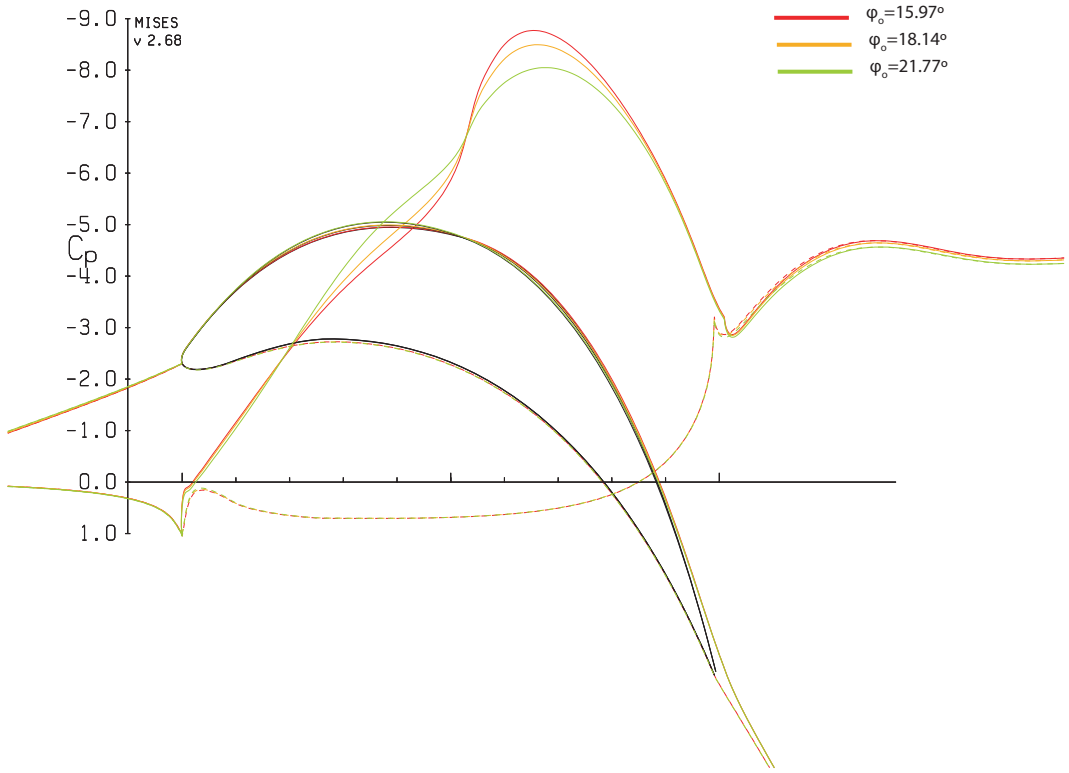

Figure 5.44: C_p evolution at $\phi_o = 15.97°$, $\phi_o = 18.14°$ and $\phi_o = 21.72°$. Dash line represents the pressure surface

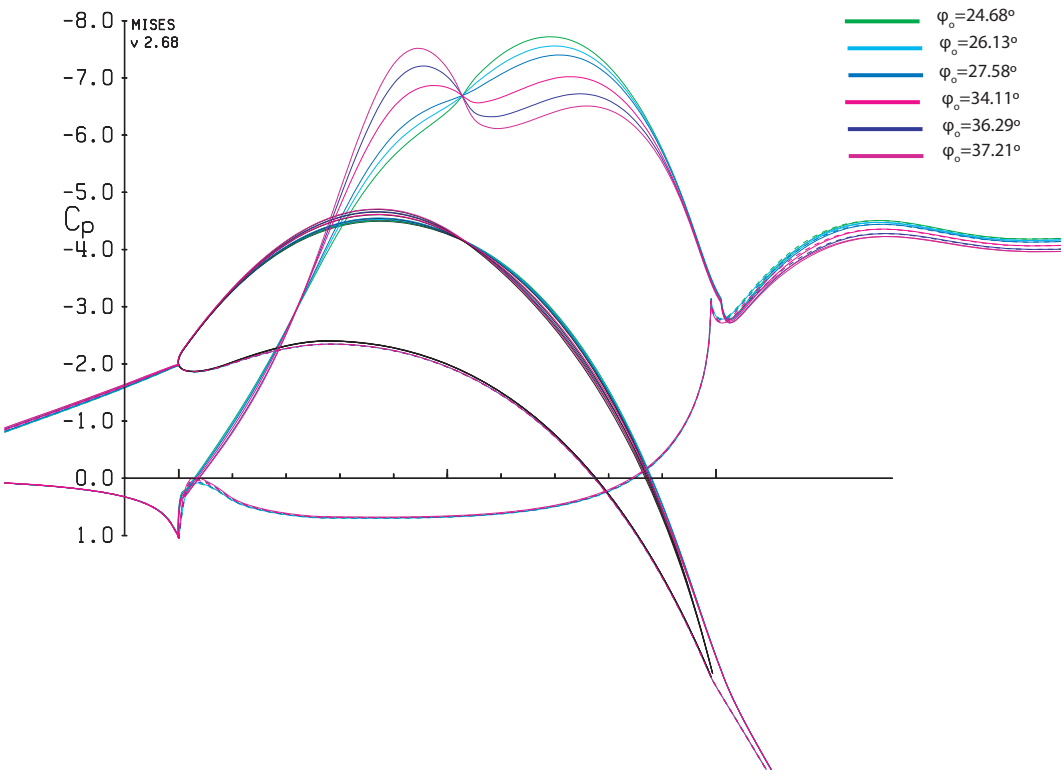

Figure 5.45: C_p evolution at $\phi_o = 24.68°$, $\phi_o = 26.13°$, $\phi_o = 27.58°$, $\phi_o = 34.11°$, $\phi_o = 36.29°$ and $\phi_o = 37.21°$. Dash line represents the pressure surface

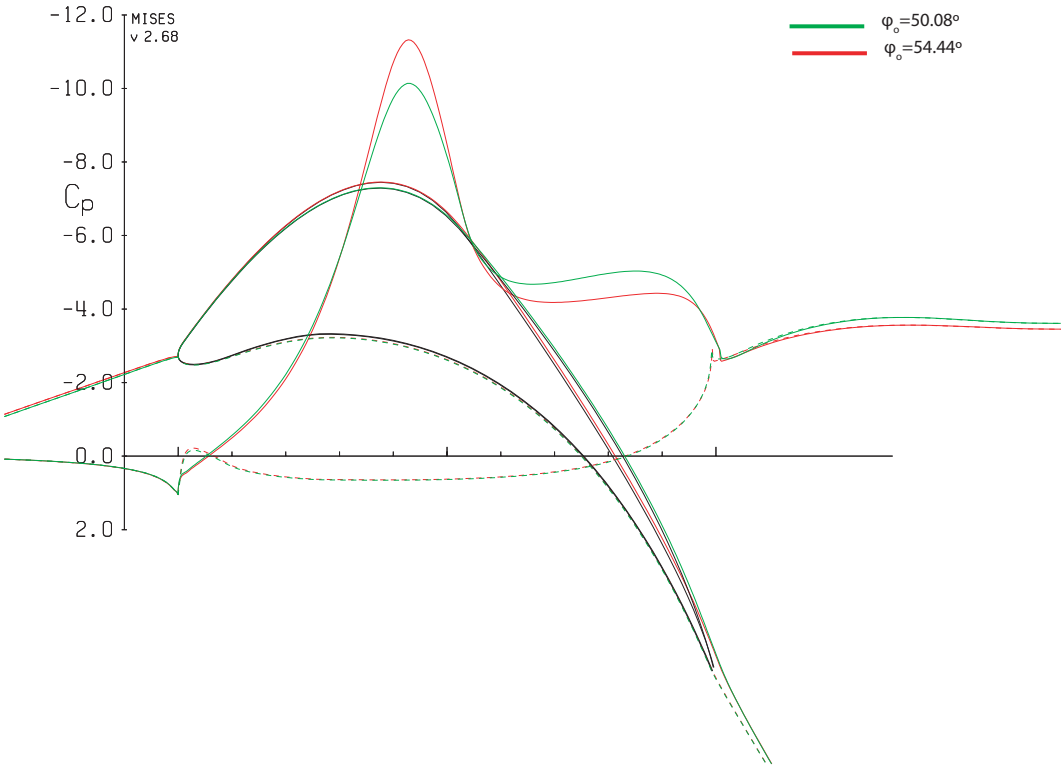

Figure 5.46: C_p evolution at $\phi_o = 50.08°$ and $\phi_o = 24.44°$. Dash line represents the pressure surface

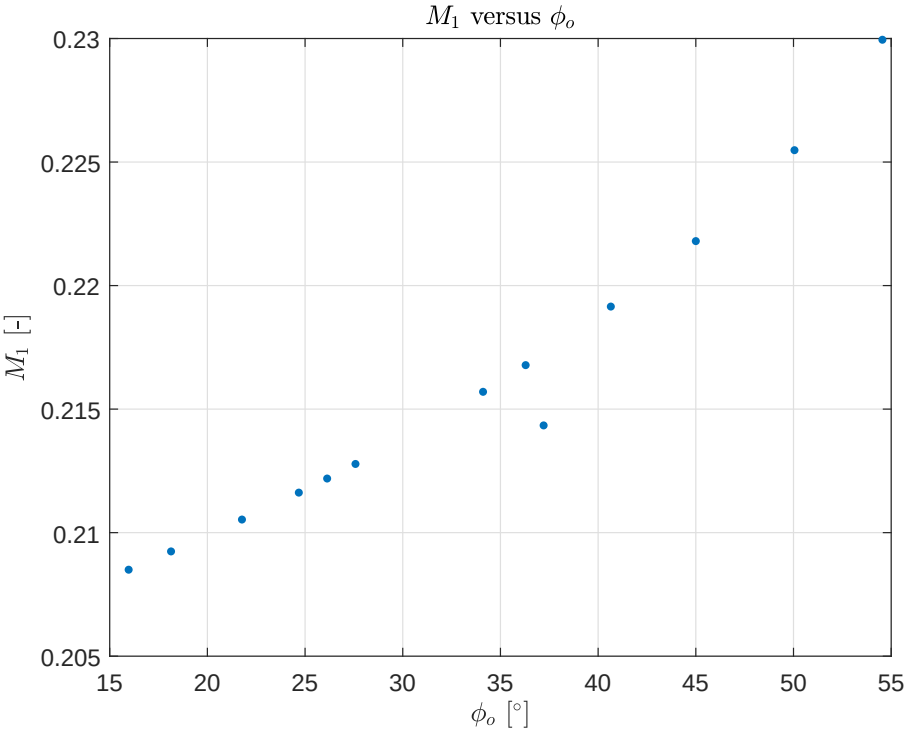

Figure 5.47: Inlet Mach Number as a function of ϕ_o

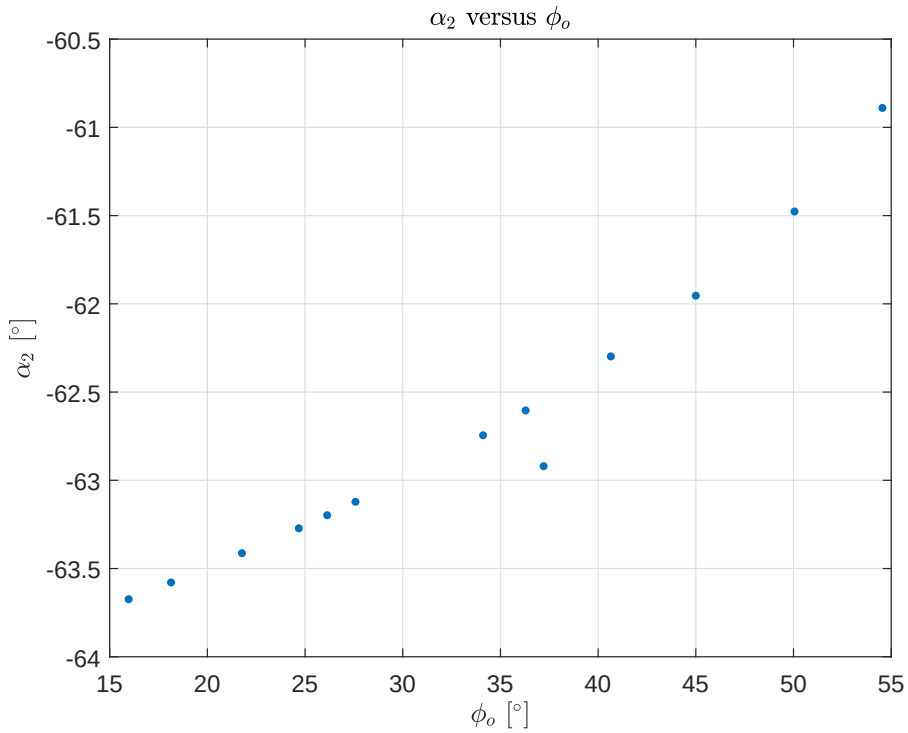

Figure 5.48: Outlet flow angle as a function of ϕ_o

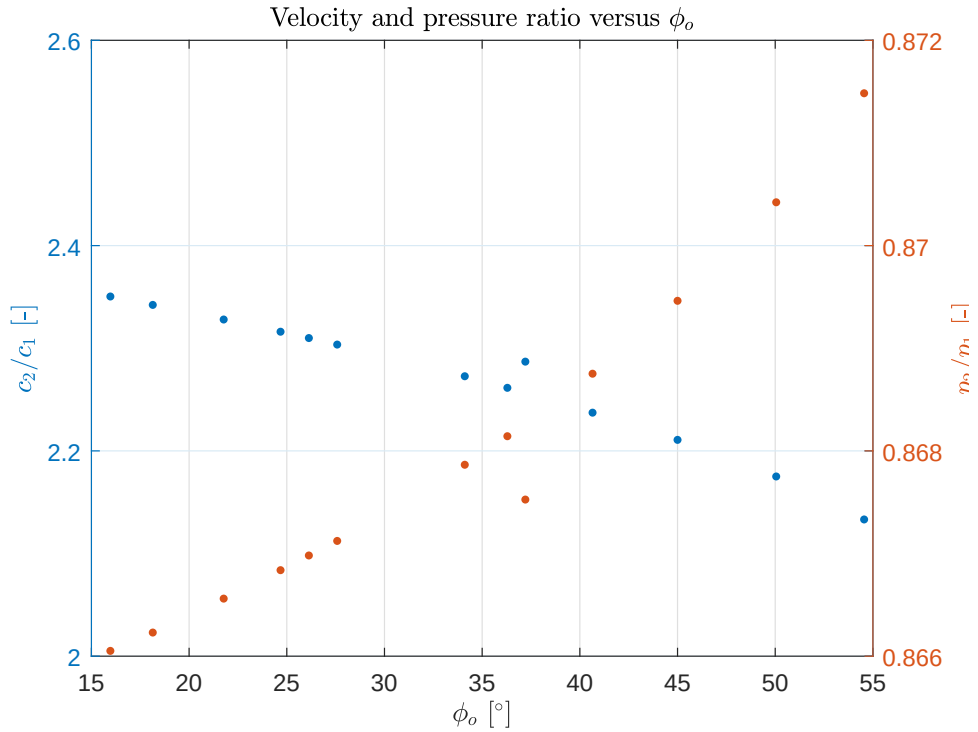

Figure 5.49: Velocity and pressure ratios as a function of ϕ_o

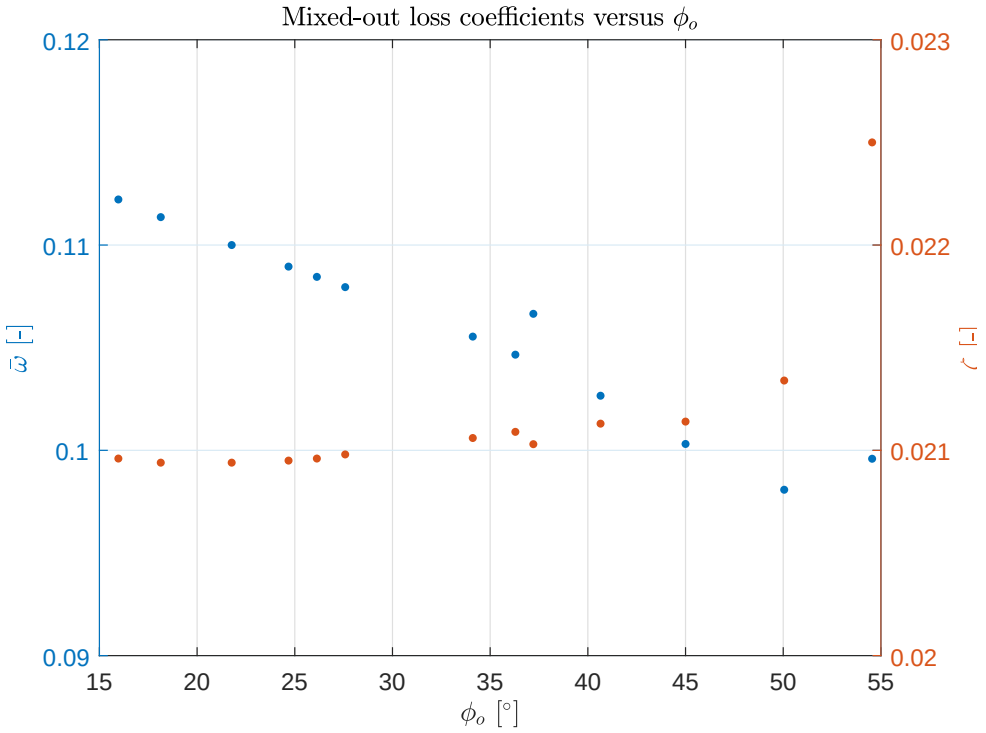

Figure 5.50: Mixed-out loss coefficients as a function of ϕ_o

From C_p curves, it is observed that the peak is translated to the left side as ϕ_o increases. Therefore, the flow separation occurs earlier. The separation point

on the pressure side is nearly constant and as the flow reaches the TE, it tries to reattach to the wall. In the next figures, it is observed that a higher inlet Mach Number is needed in order to reach the M_2 set. It is also seen that less energy is extracted from the fluid since the pressure ratio increases (note that the turning angle decreases). About losses, it has to be said that ζ is almost constant (or at least the variation is tiny). Although it is not convenient to increase this parameter because of the lower energy extraction, it may be advantageous since $\bar{\omega}$ decreases with ϕ_o. The reduction of velocity ratio can be the origin of this behaviour.

Chapter 6

Conclusion and further work

In this chapter, it is presented the conclusions of this work but also possible improvements are stated.

6.1 Further work

The possible improvements that can be done to the program is that to obtain a 3D turbomachine blade. This can be done by two ways:

1. By stacking all the blade sections upon their center of gravity, for example. Afterwards, parametric surface theories can be applied in order to obtain the final 3D blade shape

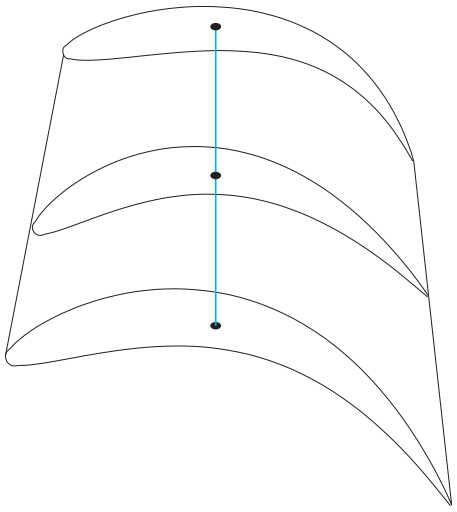

Figure 6.1: Blade sections stacked upon their centre of gravity - This is a representative sketch

2. By using three dimensional flow analysis where there is hold the condition of radial equilibrium flow. The methodology can be found in Chapter 4 of Ref [3]

As said before, this tool only works in Ubuntu. Therefore, another improvement is to make Turbomachinery Blade Designer compatible with Windows.

A 'Virtual Machine' software may be a solution.

The third improvement that can be mentioned is to have the program written in another programming language (such as Python - which is free). Currently, it needs to be opened and operated through MATLAB.

6.2 Conclusion

TURBOMACHINERY BLADE DESIGNER offers to a researcher the opportunity to design a turbine and/or compressor blade and also to compute the flow using a blade-to-blade program called MISES. This tool is user-friendly in the way that the designer can easily use the program and modify any parameter. There are two possible ways to do the design: cascade families and a high geometric parameters process. Although the drawing is 2D, in fact, it can be used to do a 3D blade just by designing several 2D blade section. Apart from that, it also includes certain setups that help users to use it (for example, help windows and the possibility of adding a new thickness family in the program) that may be useful in the research process. In other words, the design process has been optimized in terms of time.

After the problem has been analysed and solved, the work continued with the analysis of several examples (made with both designing options). Typical flow values were used in the investigation. It can be concluded that all the parameters behaved as expected. A rare peak was observed in the Leading Edge area (in the case of cascade families). The possible cause is the lack of resolution in the thickness profile.

The results of the blades designed manually were also as expected. No strange peaks were observed since Bézier parametric curve theory is employed to obtain the profile which is smooth.

In the last part of the work, two case studies were performed: one using cascade families option and changing the Stagger angle ξ; and another following the manual drawing procedure and here ϕ_o was varied. In both cases, a turbine blade was preferred. Regarding the first analysis, the final conclusion was more power is extracted from the fluid (pressure ratio decreases) as the stagger increases but the penalty is that the loss coefficients increase from certain ξ. Different results were obtained in the second investigation: pressure ratio is increasing since the turning reduction. But at the same time, improved loss coefficients are get. Therefore, a trade-off process these two facts should be done.

Finally, improvements to this work are also remarked: create 3D blade design, Windows compatibility and make it work autonomously - without using MATLAB.

Bibliography

[1] R. I. Lewis. *Turbomachinery Performance Analysis*. Elsevier Science & Technology Books, 1996.

[2] Schlichting, H., Gersten, K. *Boundary-Layer Theory*. Springer, Heidelberg, 2000.

[3] Seppo A. Korpela. *Principles of Turbomachinery*. John Wiley & Sons, Inc., Hoboken, New Jersey, 2011.

[4] S. L. Dixon and C. A. Hall. *Fluid Mechanics and Thermodynamics of Turbomachinery*. Elsevier Inc., United States of America, 2010.

[5] T. Korakianitis, I.A. Hamakhan, M.A. Rezaienia, A.P.S. Wheeler, E.J. Avital, J.J.R. Williams. *Design of high-efficiency turbomachinery blades for energy conversion devices with the three-dimensional prescribed surface curvature distribution blade design (CIRCLE) method*. In Applied Energy, Volume 89, Issue 1, Pages 215-227, ISSN 0306-2619, 2012.

[6] L. Joseph Herrig, James C. Emery, and John R. Erwin. *SYSTEMATIC TWO-DIMENSIONAL CASCADE TESTS OF NACA 65-SERIES COMPRESSOR BLADES AT LOW SPEEDS*. NATIONAL ADVISORY COMMITTEE FOR AERONAUTICS, WASHINGTON, September 14, 1951.

[7] Michael Kerho and Brian Kramer. *Enhanced Airfoil Design Incorporating Boundary Layer Mixing Devices*. 41st AIAA Aerospace Sciences Meeting & Exhibit, Reno, NV, 6-9 January 2013.

[8] Mark Drela, Harold Youngren. *A User's Guide to MISES 2.63*. MIT Aerospace Computational Design Laboratory, February 2008.

[9] A. Samson & S. Sarkar. *Effects of Free-Stream Turbulence on Transition of a Separated Boundary Layer Over the Leading-Edge of a Constant Thickness Airfoil*. ASME, Journal of Fluids Engineering, Vol. 138 / 021202-1, February 2016.

[10] R.C.W. de Koning. *Development of a Parametric 3D Turbomachinery Blade Modeler*. Delft University of Technology, Delft, 8-08-2015.

[11] Denton, J. D., & Cumpsty, N. A. *Loss mechanisms in turbomachines*. Journal of Turbomachinery. Transactions of the ASME, 115(4), 621-656, 1993.

[12] HORIZON 2020 – WORK PROGRAMME 2014-2015. *Smart, green and integrated transport*. European Commission Decision C (2015)2453, 17 April 2015.

[13] International Civil Aviation Organization (ICAO). *Environmental Protection*. Annex 16, Volume II Aircraft Engineering Emissions, July 2008.

[14] European Aviation Safety Agency (EASA). *ICAO Aircraft Engine Emissions Databank*. EASA, June 2017.

[15] H. A. Heikal, A. Abdel Hafiz, Nazih N. Bayomi & M. H. Ahmed. *Theoretical and Experimental Investigation on the Wells Turbine Performance*. Egyptian Committee of Theoretical & Applied Mechanics, 7th Conference on Theoretical & Applied Mechanics, Cairo - Egypt, March 11 and 12 2003.

[16] S, J. Andrews. *Tests Related to the Effect of Profile Shape and Camber-Line on Compressor Cascade Performance*. Reports and Memoranda No. 2743, London, October 1949.

[17] Andrew PL, Kahveci HS. *Validation of MISES 2-D Boundary Layer Code for High Pressure Turbine Aerodynamic Design*. ASME. Turbo Expo: Power for Land, Sea, and Air, Volume 6: Turbo Expo 2007, Parts A and B, Montreal, Canada, May 14–17, 2007.

[18] Airfoil tools. *Airfoil Tools*. URL: http://www.airfoiltools.com/, Accessed on August 2017.

[19] Computer Faculty Science of Helsinki. *Parametric Curves*. URL: https://www.cs.helsinki.fi/, Accessed on February 2017.

Appendix A

Project Planner

In the next page, the project planner of this work is shown. It has to be mentioned that one period corresponds to one week. The mean working hours per week are 12 hours and the first period starts on January 30th, 2017. Although the project was designated in November 2016, due to the academic workload of the following months, the starting date was postponed.

Project Planner

Select a period to highlight at right. A legend describing the charting follows. Period Highlight: 33 — Plan Duration — Actual Start — % Complete — Actual (beyond plan) — % Complete (beyond plan

ACTIVITY	PLAN START	PLAN DURATION	ACTUAL START	ACTUAL DURATION	PERCENT COMPLETE
Analysis of the project	1	1	1	1	100%
MATLAB GUI Training	2	3	2	4	100%
Cascade families geometry	5	1	5	1	100%
Cascade families layouts	6	2	6	3	100%
Manual Design Analysis	9	2	9	3	100%
Manual Design Layout	10	7	10	6	100%
Other features of the program	14	3	15	3	100%
MISES files	18	2	19	2	100%
Bugs analysis and resolution	6	24	6	26	100%
Thesis	10	22	12	23	100%
Project Presentation	34	3	34	3	0%

PERIODS 1 2 3 4 5 6 7 8 9 10 11 12 13 14 15 16 17 18 19 20 21 22 23 24 25 26 27 28 29 30 31 32 33 34 35 36

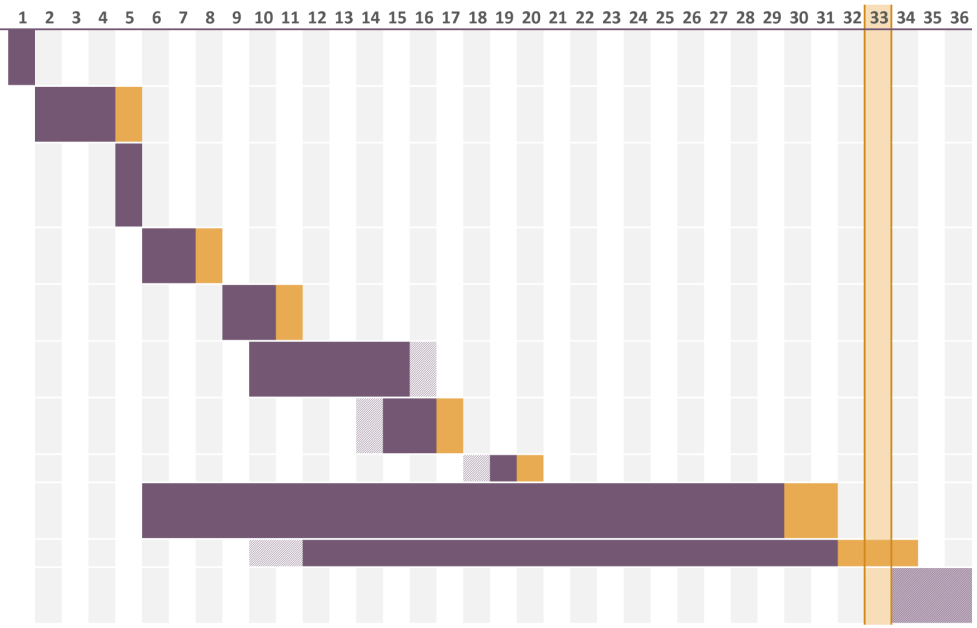

Figure A.1: Project planner of TURBOMACHINERY BLADE DESIGNER program

Appendix B

Thickness profiles

c4

$\tilde{x}_t$	0.00	1.25	2.50	5.00	7.50	10.00	15.00	20.00	30.00	40.00	50.00
$\tilde{y}_t$	0.00	1.65	2.27	3.08	3.62	4.02	4.55	4.83	5.00	4.89	4.57

$\tilde{x}_t$	60.00	70.00	80.00	90.00	95.00	100.00
$\tilde{y}_t$	4.05	3.27	2.54	1.60	1.06	0.00

NACA 0012

$\tilde{x}_t$	0.00	1.25	2.50	5.00	7.50	10.00	15.00	20.00	25.00	30.00
$\tilde{y}_t$	0.00	1.894	2.615	3.555	4.200	4.683	5.345	5.737	5.941	6.002

$\tilde{x}_t$	40.00	50.00	60.00	70.00	80.00	90.00	95.00	100.00
$\tilde{y}_t$	5.803	5.294	4.563	3.664	2.623	1.448	0.807	0.00

NACA 0015

$\tilde{x}_t$	0.00	1.25	2.50	5.00	7.50	10.00	15.00	20.00	25.00	30.00
$\tilde{y}_t$	0.000	2.367	3.268	4.443	5.250	5.853	6.682	7.172	7.427	7.502

$\tilde{x}_t$	40.00	50.00	60.00	70.00	80.00	90.00	95.00	100.00
$\tilde{y}_t$	7.254	6.617	5.704	4.580	3.273	1.810	1.008	0.000

NACA 66-010

$\tilde{x}_t$	0.00	0.50	0.75	1.25	2.50	5.00	7.50	10.00	15.00	20.00
$\tilde{y}_t$	0.000	0.759	0.913	1.141	1.516	2.087	2.536	2.917	3.530	4.001
$\tilde{x}_t$	25.00	30.00	35.00	40.00	45.00	50.00	55.00	60.00	65.00	70.00
$\tilde{y}_t$	4.363	4.636	4.832	4.953	5.000	4.971	4.865	4.665	4.302	3.787

$\tilde{x}_t$	75.00	80.00	85.00	90.00	95.00	100.0
$\tilde{y}_t$	3.176	2.494	1.773	1.054	0.408	0.000

NGTEmod

$\tilde{x}_t$	0.00	1.25	2.50	5.00	7.50	10.00	15.00	20.00	30.00	40.00
$\tilde{y}_t$	0.000	1.375	1.910	2.680	3.195	3.600	4.180	4.550	4.950	4.820
$\tilde{x}_t$	50.00	60.00	70.00	80.00	85.00	90.00	92.50	95.00	97.50	100.0
$\tilde{y}_t$	3.980	3.250	2.450	1.740	1.500	1.270	1.170	1.080	0.980	0.000

NACA 65-010

$\tilde{x}_t$	0.00	0.50	0.75	1.25	2.50	5.00	7.50	10.00	15.00	20.00
$\tilde{y}_t$	0.000	0.772	0.932	1.169	1.574	2.177	2.647	3.040	3.666	4.143
$\tilde{x}_t$	25.00	30.00	35.00	40.00	45.00	50.00	55.00	60.00	65.00	70.00
$\tilde{y}_t$	4.503	4.760	4.924	4.996	4.963	4.812	4.530	4.146	3.682	3.156

$\tilde{x}_t$	75.00	80.00	85.00	90.00	95.00	100.0
$\tilde{y}_t$	2.584	1.987	1.385	0.810	0.306	0.000

T4

$\tilde{x}_t$	0.00	1.25	2.50	5.00	7.50	10.00	15.00	20.00	30.00	40.00	50.00
$\tilde{y}_t$	0.00	1.17	1.54	1.99	2.37	2.74	3.40	3.95	4.72	5.00	4.67

$\tilde{x}_t$	60.00	70.00	80.00	90.00	95.00	100.00
$\tilde{y}_t$	3.70	2.51	1.42	0.85	0.72	0.00

A3K7

$\tilde{x}_t$	0.00	1.25	2.50	5.00	10.00	15.00	20.00	25.00	30.00	35.00
$\tilde{y}_t$	0.000	3.469	4.972	6.918	9.007	9.827	10.000	9.899	9.613	9.106

$\tilde{x}_t$	40.00	45.00	50.00	55.00	60.00	65.00	70.00	75.00	80.00
$\tilde{y}_t$	8.594	7.913	7.152	6.339	5.500	4.661	3.848	3.087	2.406

$\tilde{x}_t$	85.00	90.00	95.00	100.0
$\tilde{y}_t$	1.830	1.387	1.101	0.000

Table B.1: Prescribed thickness families

In Table B.1, $\tilde{x}_t$ is the non-dimensional axial coordinate (represented in %) and it is defined as x_t/l; similarly, $\tilde{y}_t$ is defined as y_t/l and it is represented in %. It is important to note that, according to the nomenclature of NACA profiles, the last two digits correspond to $t/l_{\max}$ but in fact TURBOMACHINERY BLADE DESIGNER has the option to change the maximum thickness of the turbomachinery blade. As a result, that NACA name is no longer prevailed.

Appendix C

MISES configuration

In the next lines, it can be found a typical ises file configuration of a turbine blade. As global variables or unknowns are set `SINL` inlet flow slope, `SLEX` grid exit slope, `SBLE` LE stagnation point, `PREX` grid exit static pressure and `MINL` inlet Mach number. About the constraints, it is set that drive inlet slope `S1` to `SINLin`, set LE Kutta condition (for all non-sharp LE blades), set TE Kutta condition (for all blades), drive inlet `P0a` to `PSTr0` ($= 1/\gamma$) and drive outlet Mach M_2 to `MOUTin`.

```
1          1 2 5 6 15
2          1 3 4 6 17
3          0.3000 0.0000 0.36397 -0.40000 | Minl P1/Po1 Sinl
              Xinl
4          0.5 0.00000 0.267949 1.40000 | MOUT P2/Po1 Sout Xout
5          0.0000 0.0000   |mfr
6          500000 -0.8 | REYin ACRIT
7          0.02  0.02 | XTR1 XTR2
8          1 0.95 +1.0 |ISMOM MCRIT MUCON
9          0.0 0. | Bvr1 Bvr2
10         0. 0.  0. 0. 0. 0. 0. 0. 0. 0. 0.
```

Compressor flow file is defined similarly to the turbine one but it does not take into account the global variable `PREX` grid exit static pressure. About the global constrain, it is stated to drive outlet Mach M_1 to `MINLin`. Note that in the turbine one of the input is the outlet Mach and in the compressor, the inlet one.

```
1          1 2 5 15
2          1 3 4 15
3          0.4 0.1000 1 -0.25 | Minl P1/Po1 Sinl Xinl
4          0.400000 0.790126628 -1.97966 1.25 | MOUT P2/Po1
              Sout Xout
5          0.0000 0.0000   |mfr
6          250000 4.500000 | REYin NCRIT
7          1.10000  1.10000 | XTR1 XTR2
8          1 0.95 +1.0 |ISMOM MCRIT MUCON
9          0.0 0. | Bvr1 Bvr
10         20. 0. 0. 0.0
```

Apart from this file and the blade one, there exists another called gridpar. It defines how the grid is displayed. In this file, which the user does not modify, appear parameters such as number of streamlines. The grid topology depends on the flow condition. By default, it is set as low speed and low turning flow.